

Protein-Metal Hybrids as Catalysts for Selective Oxidations

Seda KANBAK-AKSU

Protein-Metal Hybrids as Catalysts for Selective Oxidations

PROEFSCHRIFT

ter verkrijging van de graad van doctor
aan de Technische Universiteit Delft,
op gezag van de Rector Magnificus prof. ir. K.C.A.M. Luyben,
voorzitter van het College voor Promoties,
in het openbaar te verdedigen
op woensdag 9 juni 2010 om 10.00 uur
door

Seda KANBAK-AKSU

Master of Science in Pharmaceutical Chemistry,
Hacettepe University, Ankara, Turkije
geboren te Aksaray, Turkije

Dit proefschrift is goedgekeurd door de promotoren:

Prof. dr. R.A. Sheldon

Prof. dr. I.W.C.E. Arends

Samenstelling promotiecommissie:

Rector Magnificus, voorzitter

Prof. dr. R. A. Sheldon	Technische Universiteit Delft, promotor
Prof. dr. I. W.C.E. Arends	Technische Universiteit Delft, promotor
Prof. dr. W. R. Hagen	Technische Universiteit Delft
Prof. dr. S. de Vries	Technische Universiteit Delft
Prof. dr. V. Conte	Universita di Roma, Tor Vergata, Italy
Prof. dr. R. Wever	Universiteit van Amsterdam
Dr. M. Schreuder Goedheijt	MSD
Prof. dr. H. de Winde	Technische Universiteit Delft (reserve lid)

ISBN: 978-94-6108-055-4

The research described in this thesis was financially supported by the Netherlands Ministry of Economic Affairs and the B-Basic partner organizations (www.b-basic.nl) through B-Basic, a public-private NWO-ACTS programme (ACTS = Advanced Chemical Technologies for Sustainability).

Copyright ©2010 by Seda KANBAK.

All rights reserved. No part of the material protected by this copyright notice may be reproduced or utilized in any form or by any means, electronic or mechanical, including photocopying, recording or by any information storage and retrieval system, without written permission from the author.

Contents

Chapter 1	Introduction	1
Chapter 2	Vanadate Incorporated Phytase: Catalysis and Structure in the Presence of Organic Solvents	23
Chapter 3	Metal Replacement in Laccase	47
Chapter 4	Ferritin Cage as a Carrier for Palladium Nanoparticles	67
Chapter 5	Nano γ -Fe ₂ O ₃ in Ferritin Cage	87
Chapter 6	A New Regeneration Method for Oxidized Nicotinamide Cofactors	99
Summary		113
Samenvatting		115
Acknowledgements		117
Curriculum Vitae		121

Introduction

1. Oxidoreductases: Overview and Structural Requirements
2. Industrial Biocatalysis
 - 2.1. Oxidoreductases in Industrial Applications
3. Artificial Metalloenzymes
 - 3.1. Design of Artificial Metalloenzymes Following Covalent Approach
 - 3.2. Design of Artificial Metalloenzymes Following non-Covalent Approach
 - 3.3. Design of Bio-Hybrid Catalysts Using DNA as a Protein Template
 - 3.4. Antibodies and Artificial Proteins as Templates for Hybrid Enzymes
 - 3.5. Cage-Like Protein as Template for Redox-Active Hybrid-Catalysts
4. Scope of This Thesis
5. References

Selective oxidation reactions are important transformations for the production of fine chemicals. However, classical oxidation protocols –as annotated in organic chemistry textbooks– commonly require heavy metal containing stoichiometric chromium or manganese oxidants or toxic and hazardous reagents, such as the Swern or Dess-Martin methods. In all cases a surplus of waste is generated, which could be easily prevented by using atom-efficient oxidants activated by dedicated catalysts¹. Dioxygen and hydrogen peroxide are highly attractive oxidants, in terms of minimum waste generation. Moreover the vast repertoire of today's chemo- and biocatalysts, give researchers the opportunity to design catalysts that have the potential to carry out sustainable oxidations. Biocatalysis has many attractive features especially in the context of minimum energy use and waste generation. The power of biocatalysis originates from the demand in mild reaction conditions, and is accompanied by high chemo-, regio- and stereoselectivities in reactions of multifunctional molecules².

The focus of this thesis is on the design of oxidative enzymes that can be readily applied in fine chemical synthesis. For this purpose we will give an overview of the different types of enzymes, and their structural requirements. This will be followed by a brief overview of the most used redox enzymes in industry. A preliminary conclusion that can be drawn is that many obstacles still need to be overcome in order to make significant progress in the use of oxidoreductases. This is partly inherent to oxidation reactions: they are in essence degradation reactions that pose strict requirements on stability of the catalysts involved. Biocatalysts are in general less stable than chemical catalysts. Therefore in order to fully exploit their selectivity and their potential activity at low temperatures, stability issues need to be addressed. Much research effort has been devoted to the design of novel enzymes. The second part of this chapter will give an overview of the different hybrid-technologies that have been directed towards design of mainly oxidative enzymes.

1. Oxidoreductases: Overview and Structural Requirements

In nature, oxidation reactions are catalyzed by so-called redox enzymes which form the class of oxidoreductases (EC 1). In Figure 1, the four enzyme types that perform oxidations are denoted. Oxidases, peroxidases and oxygenases (mono- and dioxygenase) are the members of this class of enzymes that are extensively studied for industrial applications. In each of these classes, oxygen atom (as molecular oxygen or peroxide) serve as the electron acceptor,

separating them from dehydrogenases. Dehydrogenases remove hydrogen from the electron donor as but do not involve in active oxygen intermediates³.

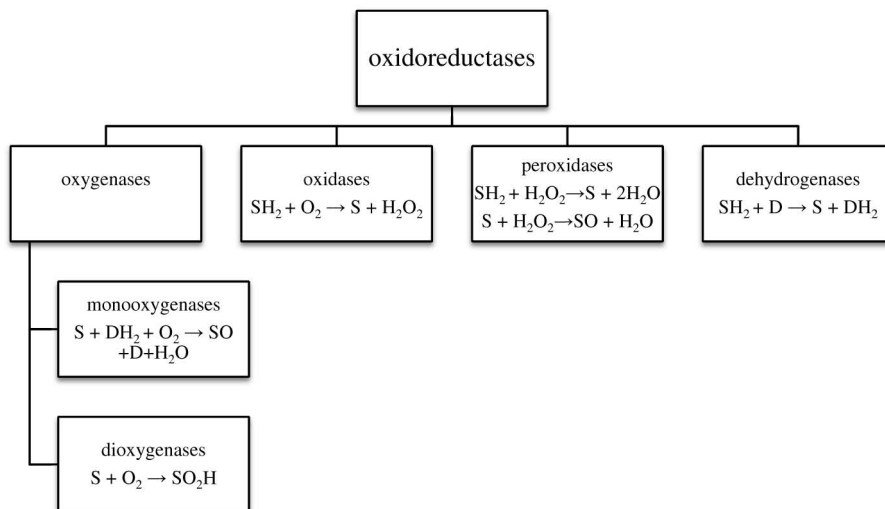


Figure 1: Classification of oxidative enzymes

Systematic classification of enzymes is based on the “donor: acceptor” concept and on the reaction products formed⁴. The substrate that is oxidized is regarded as the hydrogen or electron donor. For example, the EC 1.10 sub-class to which laccase belongs contains oxidoreductases that catalyze the oxidation of diphenols and ascorbate. Further classification is based on acceptors involved in catalysis; e.g. for EC 1.10.3: acceptor is oxygen. Oxygenases (EC 1.13) act on single or paired donors with incorporation of molecular oxygen. Monooxygenases catalyze single oxygen atom introduction into substrate. These reactions can lead to a wide range of conversions, such as hydroxylations, epoxidations, heteroatom oxygenations and oxidative dehalogenations. Dioxygenases on the other hand, are able to activate molecular oxygen and/or substrates in a way that leads to incorporation of both oxygen atoms into the final product. Similarly, for the enzymes of EC 1.11 (peroxidases) acceptor is a peroxide. Haloperoxidases are peroxidases that catalyze the oxidative halogenation in the presence of halide and hydrogen peroxide. The haloperoxidase group

comprises three structurally and mechanistically different types; heme-containing, vanadium-containing and metal-free (flavin-dependent) haloperoxidases. Alcohol dehydrogenases (EC 1.1.1.1) facilitate the interconversion between alcohol and aldehydes/ ketones with the use of nicotinamide cofactors.

Nature solves the problem of specifically activating molecular oxygen under ambient conditions by employing either a transition metal (such as iron, copper or manganese) or an organic cofactor (such as a flavin).

Table 1: Structural overview of oxidoreductases

Redox enzymes	Cofactor involved	Example
Monooxygenases	heme	cytochrome P450
	non-heme iron center	methane monooxygenase
	copper	tyrosinase
	flavin (FAD)	phenol hydroxylase
Dioxygenases	metal center	catechol dioxygenase
Oxidases	flavin (FAD)	glucose oxidase
	copper	laccase
Peroxidases	heme	horseradish peroxidase
	vanadate	chloroperoxidase
	selenium	glutathione peroxidase
Dehydrogenases	zinc	alcohol dehydrogenase
	NAD(P)H	

Despite the potential value of oxidoreductases for industrial oxidation reactions, they do not find wide application in fine chemicals industry (vide infra). The major reason underlying is the fact that some oxidoreductases, namely dehydrogenases and monooxygenases operate together with co-factors (e.g. NAD(H), NADP(H), FAD or PQQ). Although, the limited scope and requirement of cofactors would, at first sight, make dehydrogenases not very attractive for industrial applications, the current potential of this enzyme class is comparable to that of oxidases (vide infra). Advancements in cofactor regeneration methods and enzyme production methodologies assist in the progression of coupled enzymatic reactions.

Another reason is the so-called stability problem: both thermodynamic stability (which is measured as the tendency of a protein to reversibly unfold) and kinetic stability (i.e. denaturation) of enzymes need to be considered⁵. One other concern limiting the wide application of oxidoreductases is their narrow substrate scope. Thus the inherent specificity of enzymes can be of course extremely beneficial, but in the area of selective oxidation catalysis it interferes with the quest for catalysts that can operate on wide classes of substrates; examples are oxidation of aliphatic primary alcohols, epoxidation of terminal olefins, or epoxidation of allylic alcohols.

2. Industrial Biocatalysis

Fermentation processes such as in bread, cheese, wine and beer making can be considered as the typical and oldest examples of industrial biocatalysis. These processes dating back to ancient times rely on enzymes present in added compounds or spontaneously growing microorganisms. Introduction of enzymes in true industrial processes however, has started only a century ago⁶. Fermentation processes aimed specifically at selected production strains made enzyme manufacture possible. More than 100 processes are on stream for special applications⁷. The range of commercial application types of biocatalysis is very wide. The majority of currently used industrial enzymes are hydrolases, including proteases, glycosidases and esterases.

In detergent, food and textile industries enzymes are generally used as processing aids^{6,8}. Another field in which biocatalysts find a range of applications is the production of (bio)chemicals. These processes mostly originate from the fine chemicals and food industries⁹. Some significant examples include the production of high fructose corn syrup by xylose isomerise¹⁰ and synthesis of semisynthetic penicillins catalyzed by penicillin acylase¹¹. Conversion of primary feed stocks by fermentation, such as glucose to ethanol is another field where biocatalysis plays a role. Advances in enzymatic catalysis have been extended to the synthesis of specialty chemicals and polymers¹².

2.1. Oxidoreductases in Industrial Applications

In contrast to their vast natural occurrence, the application of oxidoreductases lags that of other enzymes⁷. A few oxidoreductases are in use for textile, food and other industries. Laccase, peroxidase and other enzymes are being studied for bleaching stains. Laccase catalyzed textile dye-bleaching is also useful in finishing dyed cotton fabric.

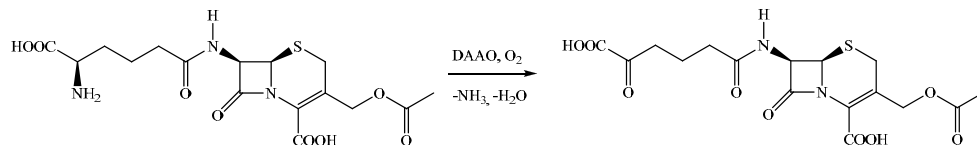
Some oxidoreductases are applied in the food industry. For example, glucose oxidase and catalase are able to improve the freshness preservation of shrimp and fish¹³. A laccase has recently been commercialized for preparing cork stoppers for wine bottles. The enzyme oxidatively removes the characteristic cork taint which is frequently imparted to the bottled wine¹⁴.

Table 2. Major commercial/ industrial oxidoreductases¹⁵

	Product name	Producer
<i>Baking, diary and other food applications</i>		
Glucose oxidase	Gluzyme	Novozymes
	OxyGo	Genencor
	Bakezyme GO	DSM
	Grindamyl	Danisco
	Hyderase	Amano
	SEBake-GO	Specialty Enzymes
Hexose oxidase	Grindamyl SUREBake	Danisco
	DairyHOX	Danisco
Catalase	Fermcolase	Genencor
	Enzeco	Enzyme Development
Laccase	Suberase	Novozymes
<i>Textile and other technical applications</i>		
Catalase	Terminox	Novozymes
	CAT-IG	Genencor
	Enzeco	Enzyme Development
Laccase	DeniLite	Novozymes
	Novozym 51003*	Novozymes
Heme peroxidase	Baylase, Guardzyme*	Novozymes

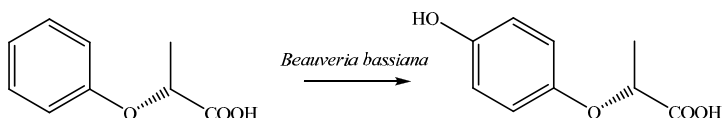
*Produced for pilot/ large-scale trials

A notable example of biocatalysis replacing classical chemical processes is the use of D-amino acid oxidase in the transformation of cephalosporin C to α -ketoadipyl-7-aminocephalosporinic acid¹⁶.



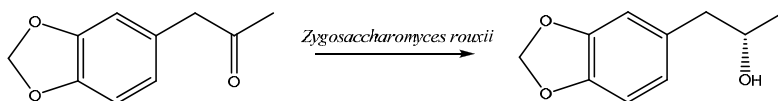
Scheme 1: D-amino acid oxidase (DAAO) catalyzed synthesis of α -ketoadipyl-7-aminocephalosporinic acid

Using isolated enzymes is generally the preferred approach in industrial biocatalysis, since much higher volumetric yields can be achieved in this way. However, still whole cell technologies involving living cells that facilitate the production and regeneration of cofactors, are worth to be considered, especially when the insertion of oxygen is concerned. A notable example is the commercialization by BASF of the regio-selective hydroxylation of (R)-2-phenoxypropionic acid to (R)-2-(4'-hydroxyphenoxy)-propionic acid (Scheme 2)¹⁷. Although no chiral center is formed here, the use of an entire microorganism was the hallmark of this process.



Scheme 2: Synthesis of (R)-2-(4'-hydroxyphenoxy)-propionic acid

Another example of a whole-cell biotransformation was developed by Lilly (U.S.A.)¹⁸ where a prochiral ketone is reduced to an optically active secondary alcohol using an NADH dependent oxidoreductase.



Scheme 3: Synthesis of (S)-(3,4-methylenedioxyphenyl)-2-propanol

3. Artificial Metalloenzymes

In order to facilitate the large scale application of enzymes as catalysts, the above-mentioned drawbacks need to be overcome. One approach is to design new (semi)synthetic biocatalysts with improved stability and comparable selectivity and activity to natural enzymes. In essence a redox active protein consists of a protein shell, surrounding a redox active centre. The most common redox centres are metals or flavins¹⁹. One role of the protein shell is to bind and position the substrate, which is the origin of (enantio) selective properties. In addition, the protein creates a nanoreactor, which is able to control the entrance and removal of substrates, products and reagents. Another important effect of the protein shell is to stabilize and coordinate the metal centre, comparable to the function of ligands in homogeneous catalysis. Therefore most efforts in designing artificial metalloenzymes involve the incorporation of a synthetic transition metal catalyst into a protein binding site. The pioneers in this area were Whitesides²⁰ and Kaiser²¹ in the late 1970's.

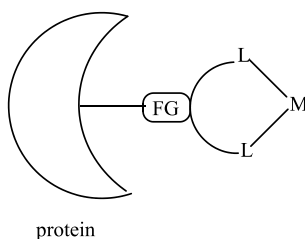
Here we would like to give a brief overview of the hybrid enzymes based on the character of the metal-protein bond. The focus of this mini-review will be the design of oxidoreductases. In order to illustrate the conceptual approaches, related examples will be presented as well in some cases.

3.1. Design of Artificial Metalloenzymes Following Covalent Approach

Kaiser's approach^{21,22} involved the covalent attachment of coenzyme analogues at or on the periphery of the active sites of hydrolytic enzymes. He proposed that if the binding of the substrate happens in close proximity to the coenzyme function, it might be possible to catalyze new reactions with modified enzymes. Inspired by Kaiser, several groups have modified proteins covalently by incorporating transition metal catalysts. Hilvert and co-workers converted subtilisin into a redox-active protein by replacing serine with

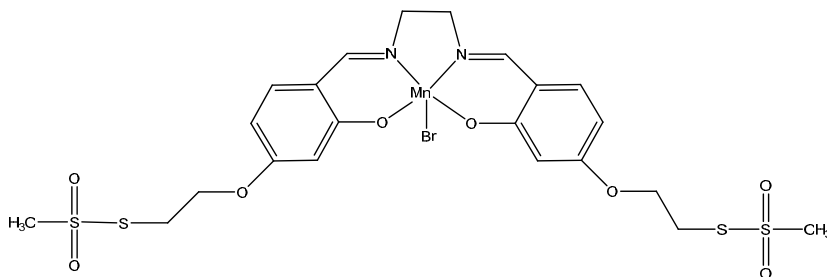
selenocysteine²³⁻²⁵. The formed protein acts as a glutathione peroxidase mimic and catalyzes the oxidation of 3-carboxy-4-nitrobenzenethiol. Recently the use of phosphonate esters and phosphonic acid derivatives as active-site directed complexes which act as serine hydrolase inhibitors has been demonstrated. These complexes have been used to introduce Pd and Pt in lipase and cutinase^{26,27}.

Another example using the covalent approach was the attachment of Mn-salen and Cu-, Pd- and Rh-complexes to papain by using a maleimide linker²⁸⁻³⁰. The aim here was to make enantioselective catalysts for either oxidation or reduction. Although the maleimide linker was very useful in linking the active site cysteine residues to the ligand, activity as well as selectivity with these hybrid catalysts was very low.



Scheme 4: Schematic representation of insertion of ligand/metal moieties into proteins. FG: functional group (such as thiol), L: ligand, M: metal

The low enantioselectivity of these single attachment examples may be due to multiple orientations of the metallocomplex. Carey *et al.*³¹ hypothesized that an improved catalyst could be engineered using a multiple attachment strategy. They followed a site-selective two-point covalent attachment strategy to introduce an achiral Mn-salen complex into apo sperm whale myoglobin (Mb). The effectiveness of the dual anchoring approach was demonstrated by the observed enantioselectivity (51 %) and better oxidation rate compared to single point covalent attachments in thioanisole oxidation.

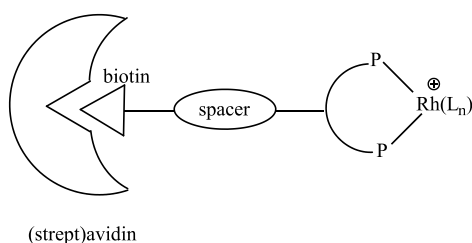


Scheme 5: Mn(salen) incorporated to apo-Mb(Y103C) by methane thiosulfonate groups with high selectivity and reactivity toward cysteines³¹

Another example of covalent strategy was given by Distefano and co-workers. They demonstrated the covalent attachment of a Cu-phenanthroline complex to a single cysteine in an adipocyte lipid binding protein, resulting in a catalyst that promotes highly enantioselective hydrolysis^{32,33}.

3.2. Design of Artificial Metalloenzymes Following non-Covalent Approach

Instead of covalently modifying the active site of an enzyme, and thereby often removing the natural enzyme activity, an alternative is to regard the protein as a chiral cavity. The cavity can be left intact, and serve as template for chiral catalysis. Whitesides²⁰ introduced the concept based on the so-called biotin-(strept)avidin approach.



Scheme 6: (Strept)avidin displays high affinity for the anchor, biotin; introduction of a spacer and variation of the ligand scaffold allow chemical optimization of enantioselectivity.

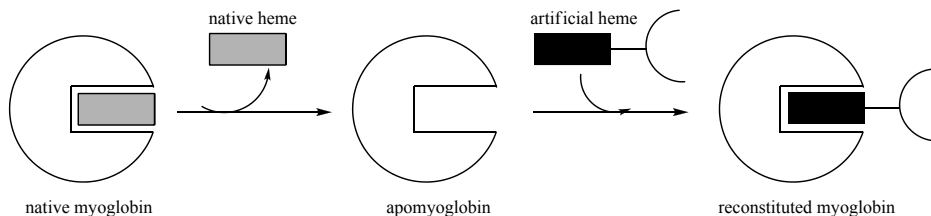
In this approach a homogeneous catalyst is anchored to biotin. The complementary (strept)avidin moiety will then complex with the homogeneous catalyst, endowing a specific

chiral environment. This approach was further exploited by using libraries of streptavidin by the Ward group³⁴⁻³⁹. The most promising catalyst is a Rh-based hybrid catalyst, which gave up to 94 % ee in the quantitative hydrogenation of acetamidoacrylate³⁸.

The V-phytase which was prepared in our laboratories in the late 1990s⁴⁰ and further studied in this thesis (see Chapter 2), can also be categorized as a non-covalent approach. Using vanadate as a substrate instead of phosphate, results in an inhibited hydrolase with a redox active cavity. This hybrid enzyme can be denoted as a semi-synthetic peroxidase, due to its ability to activate hydrogen peroxide and perform the sulfoxidation with high activity (conversions up to 100 %) and reasonable enantioselectivity (66 % ee).

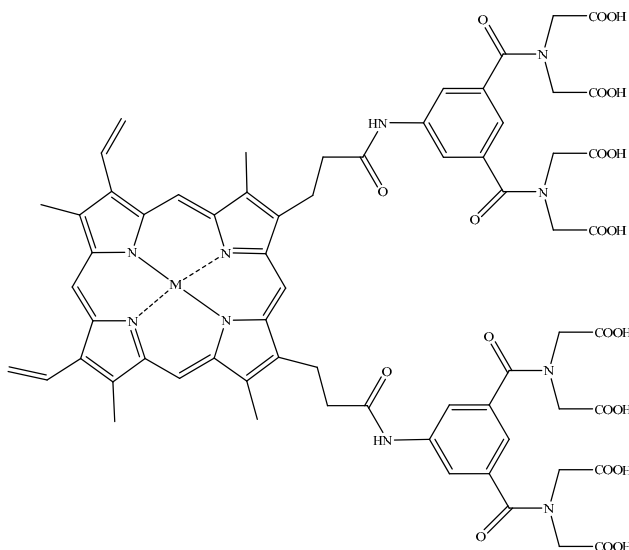
Metal replacement in enzymes has also been performed by several groups with the aim of altering the enzyme activity and/or increasing the redox potential. Yamamura and Kaiser replaced the zinc in carboxypeptidase with copper(II) with the aim of converting a hydrolytic catalyst into an oxidase⁴¹. They could perform slow air oxidation of ascorbic acid to dehydroascorbic acid with this semi-synthetic oxidase. Similarly, Bakker *et al.*⁴² replaced the zinc in thermolysin with anions such as molybdate, selenate, or tungstate. These hybrid enzymes catalyzed the oxidation of thioanisols with hydrogen peroxide, albeit with low activity and no enantioselectivity. A more recent example is the metal replacement in carbonic anhydrase by Kazlauskas⁴³. In this case, Zn^{2+} that is present in the enzyme was substituted for Mn^{2+} and by doing so the hydrolase was converted into an enantioselective peroxidase. By using stoichiometric amounts of carbonate, the authors were able to attain moderate enantioselectivities (~50 %) in the Mn-catalyzed epoxidation of styrenes.

A different approach in the history of hybrid enzymes is the use of artificial hemes. In contrast to the example above where heme-mimics were anchored to myoglobin, in this approach i.e. myoglobin is reconstituted with a chemically modified heme⁴⁴⁻⁴⁷.



Scheme 7: Reconstituted myoglobin preparation

Hayashi *et al.*⁴⁷ have shown that the myoglobin reconstituted with a modified heme, bearing a total of eight carboxylate groups on the edge of two propionate side chains of the heme-propionate enhanced the peroxidase activity of myoglobin. Thus, myoglobin was converted into a peroxidase: In the guaiacol oxidation catalyzed by reconstituted myoglobin, the k_{cat}/K_m , was approximately 14-fold higher than that of native myoglobin.

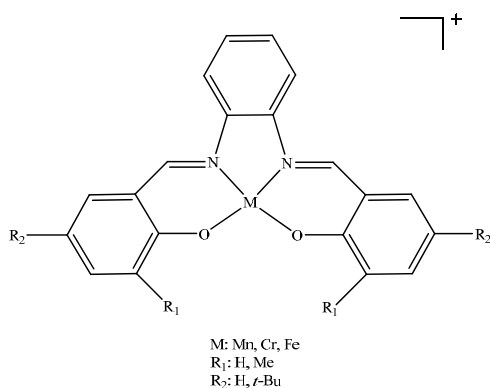


Scheme 8: Metalloporphyrins (M: Zn or Fe) prepared by Hayashi to reconstitute apo myoglobin

The group further investigated the oxygen insertion activity of the reconstituted myoglobin (Fe-porphyrin) toward the substrate oxidation in the presence of H_2O_2 ⁴⁸. The catalytic efficiency toward the thioanisole oxidation in rMb, was significantly increased compared to

that observed in the nMb. They reasoned that the artificial substrate binding site enhanced the oxygen insertion activity of myoglobin. In another approach to heme modification in myoglobins, the amino acid configuration of the heme environment was also altered. In 2004 Sato *et al.*⁴⁹ proposed a combined approach with a suitable amino acid configuration on the heme distal side and a hydrophobic substrate binding site near the heme pocket. In this way it was possible to improve K_m and k_{cat}/K_m values remarkably for the oxidation of 2-methoxyphenol.

Watanabe group has also contributed to modified myoglobin research by introducing a series of M(III)salophen-apoMb. Catalytic activity was improved by designing metal ligands on the basis of first generation crystal structures⁵⁰⁻⁵².

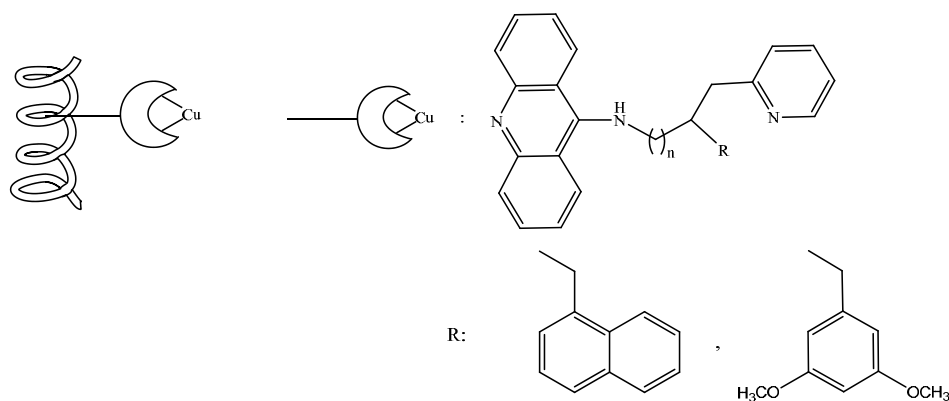


Scheme 9: $[M(\text{III})-(\text{salophen})]^+$ complexes for apomyoglobin reconstitution

The advantage of Schiff base complexes in heme substitution is that their molecular size and coordination geometry are almost identical to those of hemes, while their ligand size and hydrophobicity can be easily modified. Unfortunately these semi-synthetic metalloenzymes exhibited low reactivity and enantioselectivity in the sulfoxidation of thioanisole. The Watanabe group has also demonstrated the insertion of other Cu- and Rh-complexes^{53,54}. These results indicated that the myoglobin cavity is capable of accommodating organometallic compounds totally different from the heme in its molecular shape and the arrangement in the cavity. However the resulting hybrids were not always catalytically active.

3.3. Design of Bio-Hybrid Catalysts Using DNA as a Protein Template

Choice of the protein scaffolds in covalent or non-covalent approaches are relatively limited (e.g. avidin, streptavidin, bovine serum albumin, and apo-myoglobin). This is partly due to the need for a large pocket to bind the active catalyst moiety. It has also been shown that biomolecular scaffolds that do not contain an existing active site, such as DNA, can also supply a chiral environment. Roelfes *et al.* have introduced a novel DNA-based asymmetric catalysis concept based on the modular assembly of a DNA-based catalyst, using a copper complex of a non chiral ligand that can bind to DNA⁵⁵⁻⁵⁷.



Scheme 10: Schematic representation of DNA-bound copper complexes⁵⁵

The chirality of the DNA double helix could be transferred directly to a metal-catalyzed reaction, by positioning a non chiral or racemic catalyst in the intimate contact with DNA. A successful example of this approach was reported by Coquiere *et al.*⁵⁸ on enantioselective Michael reactions in water (ee's up to 99 % could be obtained). The results presented demonstrate that the DNA is the source of chirality in these reactions and that the close contact between DNA and the copper complex allows for direct transfer of this chirality to the catalyzed reaction. It would be worthwhile to investigate whether this approach could also be applied for oxidation reactions as well.

3.4. Antibodies and Artificial Proteins as Templates for Hybrid Enzymes

Other protein scaffolds that found considerable interest for creating metal sites are the antibodies. The advantage of using antibodies as templates is their ability to tolerate large changes in their variable regions. Several reports have shown that they are able to bind metals and metal-ligand complexes productively, and both redox and hydrolytic reactions have been reported^{59,60}. An example of using genetic engineering techniques to build the coordination complexes into the antibody molecule was reported by Wade *et al.*⁶¹. Later on, other groups have also reported on antibodies together with transition metal-ligand systems. An antibody-metalloporphyrin assembly that catalyzes the enantioselective oxidation of aromatic sulfides to sulfoxides was presented in 1999⁶². This catalytic assembly represents a close model of natural heme-dependent oxidation enzymes. It exhibits enzyme characteristics, such as predetermined oxidant and substrate selectivity, enantioselective delivery of oxygen to the substrate, and Michaelis-Menten saturation kinetics. However, these catalytic antibodies with a metalloporphyrin cofactor were not as efficient as their natural hemoprotein counterparts. In 2004, Ricoux claimed that the relatively low efficiency of these porphyrin-antibody complexes could be the result of the fact that no proximal ligand of the iron has been induced in these antibodies and he introduced an antibody-microperoxidase Fe(II) system⁶³. Oxidation of thioanisole with this catalyst in the presence of 5 % *tert*-butanol gave 49 % yield with 45 % ee. The modest yields were attributed to the oxidative degradation of the catalyst.

In an ultimate approach to design catalytically active proteins, a *de novo* design of proteins could be probed. This first proof of principle thereof was demonstrated by Regan *et al.* in 1990. They described a protein consisting of four identical, 16-residue helices connected by three identical loops⁶⁴, which resembled the Zn²⁺-binding site in carbonic anhydrase⁶⁵. In addition, the group has computationally designed a four-helix bundle protein that selectively binds a non-biological metalloporphyrin cofactor⁶⁶. Successful incorporation of a non-biological cofactor indicates the robustness of the design methodology and may be extended beyond purely natural systems.

Recently, Koshiyama *et al.*⁶⁷ have investigated a heteroprotein assembly as a catalytic reaction space. This cage is formed by a trimer of gene product 27 and gene product 5, (gp27-gp5)₃ from bacteriophage T4 with an internal diameter and height of 3 nm and 6 nm

respectively. The cysteinyl thiols inside this heteroprotein space of (gp27-gp5)₃ were covalently linked with metal-porphyrin complexes. The sulfoxidation catalyzed by these composites proceeded however without enantiomeric selectivity (<2 %). Overall, the oxidation reactivity of these composites was 1.3–7 times lower than that of other oxidation catalysts such as catalytic antibodies, artificial metalloenzymes with metalloporphyrins⁶³ and Schiff-base complexes⁵².

3.5. Cage-Like Protein as Template for Redox-Active Hybrid-Catalysts

The earliest reports on occluding metals inside protein cages date from 1991, when Mann and co-workers⁶⁸ began to explore the use of ferritin as a nanometer sized bioreactor for producing monodisperse metal particles from metal ions other than the natural hydrated iron(III) oxide. Horse spleen apoferritin (HsFn) was used as a nanocontainer to generate iron sulfide particles, as well as manganese oxide and uranyl oxohydroxide crystals. Other examples of clusters such as monodisperse FeS and Prussian blue are reported by Mann⁶⁹ and Dominguez-Vera⁷⁰, respectively. Parker *et al.* published a study on the use of *Pyrococcus furiosus* ferritin (PfFn) in the biomimetic synthesis of maghemite (γ -Fe₂O₃) nanoparticles at elevated temperatures for the potential application in MR imaging and cancer treatment⁷¹. Medical applications were also considered using ferritin cage as a carrier^{72,73}. Examples of incorporation of organic guest molecules inside ferritin have also been reported⁷⁴⁻⁷⁶.

Ueno *et al.* were the first to report on the use of ferritin cage as a catalyst carrier. They described a size-selective hydrogenation hybrid catalyst, consisting of Pd nanoclusters in the *Horse spleen* apoferritin cavity⁷⁷. These results are highly promising and warranted the further exploitation of this material as a basis for oxidation catalysis (see below). Besides nanoclusters, the cysteine residues in ferritin can also be modified with simple organometallic compounds. Watanabe *et al.*⁷⁸ thus introduced organometallic Pd-complexes at distinct sites in the cage.

4. Scope of This Thesis

The scope of this thesis, as referred to above, is to design redox-active proteins that can be applied for industrial biocatalytic oxidations. For this reason, a number of approaches were

investigated that combine the advantages of biocatalysis, with the activity and versatility of chemo-catalysts. This brought us to the approach of designing protein-metal hybrids that can act as either oxidases or peroxidases.

Incorporation of vanadate in the active site of phytase which *in vivo* mediates the hydrolysis of phosphate esters, leads to the formation of a semi-synthetic peroxidase, as discussed in Chapter 2. V-phytase has the potential to act as peroxidase, as previously demonstrated in sulfide oxidations⁴⁰. Moreover, it is more stable compared to the heme-containing peroxidases that suffer from oxidative degradation. Our goal was to extend the substrate scope of V-phytase and apply this semi-synthetic catalyst in reactions other than sulfoxidations; notably alcohol oxidations and epoxidations.

In Chapter 3, the multi-copper oxidase enzyme, laccase, was studied as template enzyme. Replacement of the Cu by Co has been previously demonstrated, and our aim was to study the redox activity of the thus modified laccase. A higher redox potential would endow this enzyme with the possibility to oxidize a wider range of substrates, without the need for a mediator.

The approach using ferritin as a catalyst template is described in Chapters 4 and 5. Ferritin is an iron-storage protein and does not catalyze a specific reaction in nature. By forming either palladium or iron oxide nanoclusters in the protein cavity, it was possible to create a novel protein-metal hybrid catalyst.

In chapter 6, we give a brief overview of the potential use of alcohol dehydrogenases as oxidation catalysts for alcohol oxidation. Their application is generally hampered by the so-called cofactor regeneration problem. In this chapter we introduce a method to circumvent the need for additional co-oxidants, by introducing laccase as enzyme for regeneration with molecular oxygen. Thus a new regeneration method to facilitate the large scale application of these enzymes was introduced.

The work described in this thesis was financially supported by B-Basic, a Dutch research consortium, operating as an independent programme of NWO-ACTS. It is an extension of

existing cooperations between TU Delft (coordination), University of Groningen, Leiden University, Wageningen University, TNO and Agrotechnology and Food Sciences group, as well as a consortium of large and small industries including DSM, AkzoNobel, Shell Global Solutions, Paques and Schering-Plough, which have proved to be successful and well advanced in the Netherlands. B-Basic focuses on the development of new bio-based production methods for the chemical (and energy) industry which are rooted in the current explosive increase in fundamental insights in molecular biology through the genomics revolution combined with advanced bioprocess technology and existing chemical knowledge.

5. References

1. Backvall, J. E., Ed. *Modern Oxidation Methods*; Wiley, 2004.
2. Sheldon, R. A. *Green Chem.* 2007, 9, 1273-1283.
3. Burton, S. G. *Trends Biotechnol.* 2003, 21, 543-549.
4. <http://expasy.org> Swiss Institute of Bioinformatics.
5. Polizzi, K. M.; Bommarius, A. S.; Broering, J. M.; Chaparro-Riggers, J. F. *Curr. Opin. Chem. Biol.* 2007, 11, 220-225.
6. Bornscheuer, U. T.; Buchholz, K. *Eng. Life Sci.* 2005, 5, 309-323.
7. Straathof, A. J. J.; Panke, S.; Schmid, A. *Curr. Opin. Biotech.* 2002, 13, 548-556.
8. Kirk, O.; Borchert, T. V.; Fuglsang, C. C. *Curr. Opin. Biotech.* 2002, 13, 345-351.
9. Straathof, A. J. J.; Adlercreutz, P., Eds. *Applied Biocatalysis*, 2nd edition ed.; Harwood Academic: Amsterdam, 2000.
10. Jensen, V. J.; Rugh, S. *Method Enzymol.* 1987, 136, 356-370.
11. Boesten, W. H. J.; van Doorent, J. G. M.; Smeets, J. C. M.; Chemferm VoF: The Netherlands, 1996, WO9623897-A.
12. Xu, P.; Singh, A.; Kaplan, D. L. In *Enzyme-Catalyzed Synthesis of Polymers*; Springer-Verlag Berlin: Berlin, 2006; pp. 69-94.
13. Dondredo, M.; Egana, W.; Tarky, W.; Cifuentes, A.; Torres, J. A. *J. Food Sci.* 1993, 58, 774-779.

14. Minussi, R. C.; Pastore, G. M.; Duran, N. *Trends Food Sci. Technol.* 2002, *13*, 205-216.
15. Xu, F. *Ind. Biotechnol.* 2005, *1*, 38-50.
16. Wandrey, C.; Liese, A.; Kihumbu, D. *Org. Process Res. Dev.* 2000, *4*, 286-290.
17. Ladner, W.; Staudenmaier, H. R.; Hauer, B.; Mueller, U.; Pressler, U.; Meyer, J.; Siegel, H.; BASF AG, 1992; WO9313214-A1.
18. Anderson, B.; Hansen, M.; Harkness, A.; Henry, C.; Vinzenzi, J.; Zmijewski, M. *J. Am. Chem. Soc.* 1995, *117*, 12358-12359.
19. Albrecht, M. In *Highlights in Bioorganic Chemistry*; Schmuck, C.; Wennemers, H. Eds.; Wiley-VCH Verlag GmbH & Co. KGaA: Weinheim, Germany 2004; pp. 46-47.
20. Wilson, M. E.; Whitesides, G. M. *J. Am. Chem. Soc.* 1978, *100*, 306-307.
21. Levine, H. L.; Kaiser, E. T. *J. Am. Chem. Soc.* 1978, *100*, 7670-7677.
22. Kaiser, E. T.; Lawrence, D. S. *Science* 1984, *226*, 505-511.
23. Wu, Z. P.; Hilvert, D. *J. Am. Chem. Soc.* 1990, *112*, 5647-5648.
24. Bell, I. M.; Fisher, M. L.; Wu, Z. P.; Hilvert, D. *Biochemistry* 1993, *32*, 3754-3762.
25. Bell, I. M.; Hilvert, D. *Biochemistry* 1993, *32*, 13969-13973.
26. Kruithof, C. A.; Casado, M. A.; Guillena, G.; Egmond, M. R.; Hoof, A. v. d. K.-v.; Heck, A. J. R.; Gebbink, R. J. M. K.; Koten, G. v. *Chem. Eur. J.* 2005, *11*, 6869-6877.
27. Kruithof, C. A.; Dijkstra, H. P.; Lutz, M.; Spek, A. L.; Egmond, M. R.; Gebbink, R.; van Koten, G. *Eur. J. Inorg. Chem.* 2008, 4425-4432.
28. Reetz, M. T.; Rentzsch, M.; Pletsch, A.; Maywald, M. *Chimia* 2002, *56*, 721-723.
29. Lavinia Panella; Jaap Broos; Jianfeng Jin; Marco W. Fraaije; Dick B. Janssen; Margot Jeronimus-Stratingh; Ben L. Feringa; Minnaard, A. J.; Vries, J. G. d. *Chem. Commun.* 2005, 5656-5658.
30. Pierre Haquette; Salmain, M.; Svedlung, K.; Martel, A.; Rudolf, B.; Zakrzewski, J.; Cordier, S.; Roisnel, T.; Fosse, C.; Jaouen, G. *ChemBioChem* 2007, *8*, 224-231.
31. Carey, J. R.; Ma, S. K.; Pfister, T. D.; Garner, D. K.; Kim, H. K.; Abramite, J. A.; Wang, Z.; Guo, Z.; Lu, Y. *J. Am. Chem. Soc.* 2004, *126*, 10812-10813.

32. Davies, R. R.; Distefano, M. D. *J. Am. Chem. Soc.* 1997, *119*, 11643-11652.
33. Qi, D.; Tann, C.-M.; Haring, D.; Distefano, M. D. *Chem. Rev.* 2001, *101*, 3081-3112.
34. Lin, C.-C.; Lin, C.-W.; Chan, A. S. C. *Tetrahedron: Asymmetry* 1999, *10*, 1887-1893.
35. Collot, J.; Gradinaru, J.; Humbert, N.; Skander, M.; Zocchi, A.; Ward, T. R. *J. Am. Chem. Soc.* 2003, *125*, 9030-9031.
36. Skander, M.; Humbert, N.; Collot, J.; Gradinaru, J.; Klein, G.; Loosli, A.; Sauser, J.; Zocchi, A.; Gilardoni, F.; Ward, T. R. *J. Am. Chem. Soc.* 2004, *126*, 14411-14418.
37. Collot, J.; Humbert, N.; Skander, M.; Klein, G.; Ward, T. R. *J. Organomet. Chem.* 2004, *689*, 4868-4871.
38. Ward, T. R. *Chem. Eur. J.* 2005, *11*, 3798-3804.
39. Skander, M.; Malan, C.; Ivanova, A.; Ward, T. R. *Chem. Commun.* 2005, 4815 - 4817.
40. van de Velde, F.; Könemann, L.; van Rantwijk, F.; Sheldon, R. A. *Biotechnol. Bioeng.* 2000, *67*, 87-96.
41. Yamamura, K.; Kaiser, E. T. *Chem. Commun.* 1976, 830-831.
42. Bakker, M.; van Rantwijk, F.; Sheldon, R. A. *Can. J. Chem.* 2002, *80*, 622-625.
43. Okrasa, K.; Kazlauskas, R. J. *Chem. Eur. J.* 2006, *12*, 1587-1596.
44. Hayashi, T.; Ogoshi, H. *Chem. Soc. Rev.* 1997, *26*, 355-364.
45. Hayashi, T.; Hitomi, Y.; Takimura, T.; Tomokuni, A.; Mizutani, T.; Hisaeda, Y.; Ogoshi, H. *Coordin. Chem. Rev.* 1999, *190-192*, 961-974.
46. Hamachi, I.; Shinkai, S. *Eur. J. Org. Chem.* 1999, *1999*, 539-549.
47. Hayashi, T.; Hitomi, Y.; Ando, T.; Mizutani, T.; Hisaeda, Y.; Kitagawa, S.; Ogoshi, H. *J. Am. Chem. Soc.* 1999, *121*, 7747-7750.
48. Hayashi, T.; Matsuda, T.; Hisaeda, Y. *Chem. Lett.* 2003, *32*, 496-497.
49. Sato, H.; Hayashi, T.; Ando, T.; Hisaeda, Y.; Ueno, T.; Watanabe, Y. *J. Am. Chem. Soc.* 2004, *126*, 436-437.
50. Ohashi, M.; Koshiyama, T.; Ueno, T.; Yanase, M.; Fujii, H.; Watanabe, Y. *Angew. Chem. Int. Ed.* 2003, *42*, 1005-1008.

51. Ueno, T.; Ohashi, M.; Kono, M.; Kondo, K.; Suzuki, A.; Yamane, T.; Watanabe, Y. *Inorg. Chem.* 2004, *43*, 2852-2858.
52. Ueno, T.; Koshiyama, T.; Ohashi, M.; Kondo, K.; Kono, M.; Suzuki, A.; Yamane, T.; Watanabe, Y. *J. Am. Chem. Soc.* 2005, *127*, 6556-6562.
53. Abe, S.; Ueno, T.; Reddy, P. A. N.; Okazaki, S.; Hikage, T.; Suzuki, A.; Yamane, T.; Nakajima, H.; Watanabe, Y. *Inorg. Chem.* 2007, *46*, 5137-5139.
54. Satake, Y.; Abe, S.; Okazaki, S.; Ban, N.; Hikage, T.; Ueno, T.; Nakajima, H.; Suzuki, A.; Yamane, T.; Nishiyama, H.; Watanabe, Y. *Organometallics* 2007, *26*, 4904-4908.
55. Roelfes, G.; Feringa, B. L. *Angew. Chem. Int. Ed.* 2005, *44*, 3230-3232.
56. Roelfes, G.; Boersma, A. J.; Feringa, B. L. *Chem. Commun.* 2006, 635-637.
57. Roelfes, G. *Mol. Biosyst.* 2007, *3*, 126-135.
58. Coquiere, D.; Feringa, B. L.; Roelfes, G. *Angew. Chem. Int. Ed.* 2007, *46*, 9308-9311.
59. Iverson, B. L.; Lerner, R. A. *Science* 1989, *243*, 1184-1188.
60. Cochran, A. G.; Schultz, P. G. *J. Am. Chem. Soc.* 1990, *112*, 9414-9415.
61. Wade, W. S.; Koh, J. S.; Han, N.; Hoekstra, D. M.; Lerner, R. A. *J. Am. Chem. Soc.* 1993, *115*, 4449-4456.
62. Nimri, S.; Keinan, E. *J. Am. Chem. Soc.* 1999, *121*, 8978-8982.
63. Ricoux, R.; Lukowska, E.; Pezzotti, F.; Mahy, J.-P. *Eur. J. Biochem.* 2004, *271*, 1277-1283.
64. Regan, L.; Clarke, N. D. *Biochemistry* 1990, *29*, 10878-10883.
65. Handel, T.; DeGrado, W. F. *J. Am. Chem. Soc.* 1990, *112*, 6710-6711.
66. Cochran, F. V.; Wu, S. P.; Wang, W.; Nanda, V.; Saven, J. G.; Therien, M. J.; DeGrado, W. F. *J. Am. Chem. Soc.* 2005, *127*, 1346-1347.
67. Koshiyama, T.; Yokoi, N.; Ueno, T.; Kanamaru, S.; Nagano, S.; Shiro, Y.; Arisaka, F.; Watanabe, Y. *Small* 2008, *4*, 50-54.
68. Meldrum, F. C.; Wade, V. J.; Nimmo, D. L.; Heywood, B. R.; Mann, S. *Nature* 1991, *349*, 684-687.

69. Mackle, P.; Charnock, J. M.; Garner, C. D.; Meldrum, F. C.; Mann, S. *J. Am. Chem. Soc.* 1993, *115*, 8471-8472.
70. Dominguez-Vera, J. M.; Colacio, E. *Inorg. Chem.* 2003, *42*, 6983-6985.
71. Parker, M. J.; Allen, M. A.; Ramsey, B.; Klem, M. T.; Young, M.; Douglas, T. *Chem. Mater.* 2008, *20*, 1541-1547.
72. Liu, R. Y.; Loll, P. J.; Eckenhoﬀ, R. G. *Faseb J.* 2005, *19*, 567-576.
73. Yang, Z.; Wang, X.; Diao, H.; Zhang, J.; Li, H.; Sun, H.; Guo, Z. *Chem. Commun.* 2007, 3453-3455.
74. Webb, B.; Frame, J.; Zhao, Z.; Lee, M. L.; Watt, G. D. *Arch. Biochem. Biophys.* 1994, *309*, 178-183.
75. Yang, D. W.; Nagayama, K. *Biochem. J.* 1995, *307*, 253-256.
76. Aime, S.; Frullano, L.; Crich, S. G. *Angew. Chem. Int. Ed.* 2002, *41*, 1017-1019.
77. Ueno, T.; Suzuki, M.; Goto, T.; Matsumoto, T.; Nagayama, K.; Watanabe, Y. *Angew. Chem. Int. Ed.* 2004, *43*, 2527-2530.
78. Niemeyer, J.; Abe, S.; Hikage, T.; Ueno, T.; Erker, G.; Watanabe, Y. *Chem. Commun.* 2008, 6519-6521.

Vanadate Incorporated Phytase: Catalysis and Structure in the Presence of Organic Solvents

1. Introduction
2. Catalytic Studies
3. Materials and Methods
 - 3.1. Enzyme Activity
 - 3.2. Catalytic Oxidations
 - 3.3. Qualitative Determination of Bromination Activity
 - 3.4. Haloperoxidase Activity
 - 3.5. Halohydrin Formation with V-Phytase
 - 3.6. Synthesis of 1-(3-hydroxypropyl)-3-methyl imidazolium glycolate
 - 3.7. CLEA Preparation
 - 3.8. CD Spectroscopy
4. Results and Discussion
 - 4.1. Phytase Activity in the Presence of Organic Solvents
 - 4.2. Activity of V-Phytase in the Presence of Organic Solvents
 - 4.3. V-Phytase Activity in Co-solvent Mixtures
 - 4.4. Stability of V-Phytase CLEA
 - 4.5. Characterization
 - 4.6. Scope of V-Phytase Oxidation Catalysis in Aqueous Solutions
5. Conclusions
6. References

1. Introduction

There is a definite need for stable and active redox enzymes, that can perform selective oxidations using hydrogen peroxide or oxygen as oxidants. The class of peroxidases have been investigated for this purpose. Heme-peroxidases, namely chloroperoxidases (CPO) became popular in the last few decades, because of their ability to catalyze a variety of synthetically useful selective oxidations with hydrogen peroxide without the need for cofactors¹⁻⁴. Especially CPO from *Caldariomyces fumago* shows a wide reaction scope, including sulfide oxidations, alcohol oxidations and epoxidations^{5,6}. Although much research effort has been devoted towards the use of (heme)-peroxidases in industrial oxidative processes, examples are scarce. The major shortcoming of all heme-dependent peroxidases, including CPO, is their low operational stability, resulting from facile oxidative degradation of the porphyrin ring⁷. Vanadium haloperoxidases (VHPOs), such as vanadium chloroperoxidase (V-CPO) differ from heme-containing peroxidases by their active site architecture and reaction mechanism. Instead of an iron-porphyrin complex, their active sites contain a vanadate ion, which makes them more stable against oxidative degradation⁸. Unfortunately, the active site of vanadium-dependent haloperoxidases can only accommodate very small substrates^{9,10}.

In the last decade Wever *et al.* found that V-CPO was structurally related to acid phosphatases and the apo enzyme was shown to exhibit phosphatase like activity¹¹⁻¹³. Moreover vanadate and other transition metal oxoanions are known to be potent inhibitors of acid phosphatases and related phytases and sulfatases. Therefore, incorporation of vanadate ion in the active site of phytase, which *in vivo* mediates the hydrolysis of phosphate esters, would lead to the formation of a semi-synthetic peroxidase that can catalyze the enantioselective oxidation reactions with hydrogen peroxide. Since phosphate and vanadate show many similar physico-chemical properties, vanadate is able to behave as a transition state analogue, forming a trigonal bipyramidal complex with the nucleophilic histidine present in the active site of acid phosphatases^{14,15}.

In this study we focus on the use of phytase as a template enzyme for oxygen transfer reactions. Phytase (myo-inositol hexakisphosphate phosphohydrolase) belongs to the group of phosphoric monoester hydrolases. It catalyzes the hydrolysis of phytic acid (myo-inositol

hexaphosphate) to inorganic monophosphate and lower phosphoric esters of myo-inositol, or in some cases to free myo-inositol. Two types of phytases can be distinguished; 3-phytase (EC 3.1.3.8) and 6-phytase (EC 3.1.3.26)¹⁶. This classification is based on the first phosphate group attacked by the enzyme. The 3-phytase and 6-phytase, although they are produced by the same *phyA* gene, are different enzymes and show different characteristics¹⁷.

The incorporation of vanadate in the active site of phytase was studied by ⁵¹V NMR¹⁸. It turned out that in both 3- and 6-phytase, selective binding of vanadate to the active site took place, in line with the fact that vanadate is a potent inhibitor of phosphatases. However, upon reaction with hydrogen peroxide, major differences are observed. Upon addition of H₂O₂ two mono-peroxovanadate-phytase complexes are formed at pH 5.0 in the case of 3-phytase. For the 6-phytase however, no such peroxide-vanadate-phytase complexes are observed. In addition, with both enzymes diperoxovanadate species (vide infra) were observed, which could be due to the elevated concentrations required to visualize V-enzymes in the ⁵¹V-NMR experiments. These studies supported us in conducting a study towards the further possibilities of oxygen transfer by this vanadate-phytase apart from sulfide oxidation^{19,20}.

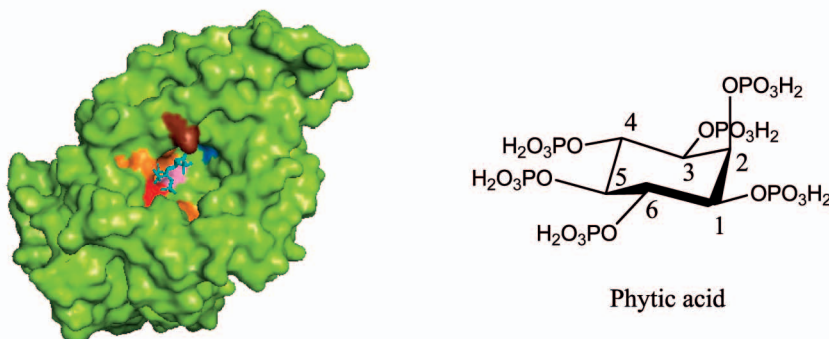
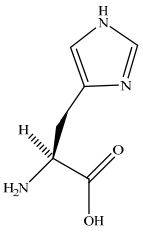
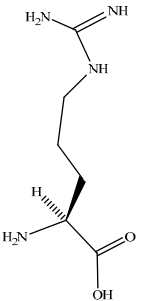
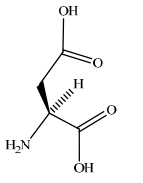
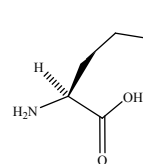
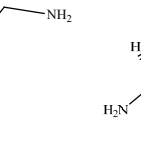
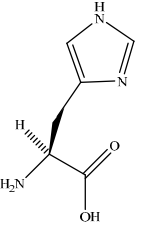
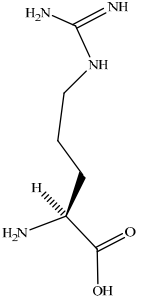
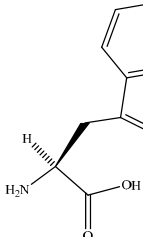
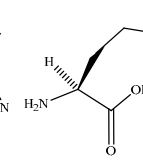
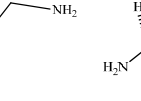
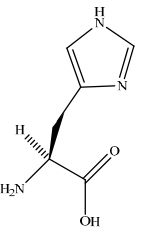
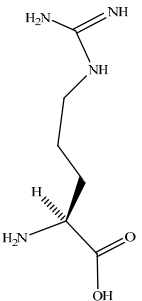
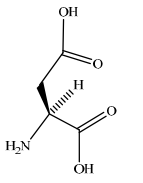


Figure 1: Phytase structure prepared with PyMol programme Swiss PDB ID: 1dkp, color codes: His303: red, lys24: brown, ser215:blue, arg92, 20, 16, 267: orange, Asp304: pink, phytic acid (C₆H₁₈O₂₄P₆): cyan

The active site of the phytase shows remarkable homology to the active site residue of a particular class of acid phosphatase named “histidine phosphatase”²¹.

Table 1: Comparison of the amino acids present in the active sites of phytase, V-CPO and V-BPO (based on model structures prepared with PyMoL, Swiss PDB IDs, phytase: 1dkb, V-CPO: 1ldq, V-BPO: 1qi9)

Phytase	 histidine	 arginine	 aspartate	 lysine	 threonine
V-CPO	 histidine	 arginine	 tryptophane	 lysine	 alanine
V-BPO	 histidine	 arginine	 aspartate		

In Table 1, the structure of phytase is compared to that of V-CPO and V-BPO. The amino acids present at the active sites of the three enzymes show remarkable similarity. The histidine covalently binds to the vanadate in vanadium haloperoxidases (Figure 2). Arginine and lysine compensate the negative charge by hydrogen bonding. Aspartate plays a role as acid-base group in catalysis^{13,22,23}.

2. Catalytic Studies

Previously in our group it was shown that vanadate-phytase was very active in selective oxidation of sulfide to sulfoxide^{19,20}. Our goal was to extend the substrate scope of V-phytase and apply this semi-synthetic catalyst in reactions other than sulfoxidations, notably alcohol oxidations and epoxidations. Initial experiments however, indicated that benzyl alcohol oxidation does not take place under the standard reaction environment used for sulfoxidation (see experimental). For interpretation of these data it is useful to shortly describe the chemical oxidation catalysis, commonly performed by vanadium.

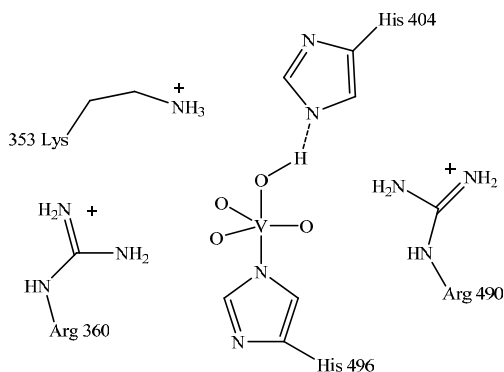


Figure 2: Active site of V-CPO from *C. inaequalis*¹³

In general for vanadium catalysis with HOOH, two V(V) species can be discerned: a monoperoxo and a diperoxo complex (Figure 3). For sulfide oxidations in organic solvents, both monoperoxo and diperoxovanadium(V) complexes are present in the solution²⁴ and are reacting with the sulfide^{25,26}. The presence of the latter achiral species would however decrease the enantioselectivity²⁷.

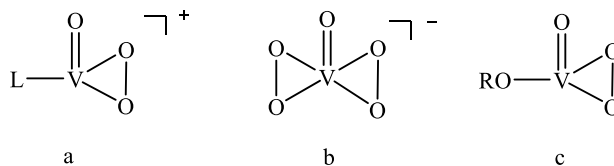


Figure 3: Vanadium mono- and diperoxo species, a) ligand bound vanadium-oxoperoxo species b) oxodiperoxo complex c) alkoxo oxomonoperoxo species reactive in alcohol oxidation

Literature data suggest that alcohol oxidation catalyzed by vanadium is a radical process^{28,29}. The active species is the alkoxo monoperoxovanadium complex (Figure 3c). A simplified mechanistic description of the process involves hydrogen abstraction from an alkoxy molecule bound to the monoperoxo complex to form a carbon centered radical, which may then escape from the coordination sphere of the metal and react with dioxygen to produce ketone and hydrogen peroxide^{30,31}.

Also in the natural haloperoxidase systems the active peroxidic intermediate is shown to be monoperoxo-vanadate stabilized by a histidine residue in the active site^{32,33}.

In order to explain the observed lack of reactivity of alcohols, we considered that binding of alcohol to the vanadium - which is required for catalytic activity - might be hampered in the active site of the enzyme. It was shown that at pH 5.5 there is a very stable water molecule in the active site with hydrogen bond interactions to another water molecule and two histidines, that may prevent the substrate from binding³⁴. Therefore, we reasoned that lowering the concentration of water from the enzyme active site and exclusion of water from the reaction environment, could improve the binding of the alcohol and by doing so the reaction could be stimulated.

A second class of substrates which is prone to undergo oxidation by vanadium-peroxo species is that of allylic alcohols. Alcohols readily coordinate to vanadium and in this way the neighbouring double bond is well positioned to react with the electrophilic monoperoxovanadium species. This reactivity is well documented and was intensively studied by

Sharpless in the 1980s to develop an enantioselective epoxidation of a wide variety of allylic alcohols³⁵⁻³⁷.

In this chapter we report on our efforts to lower the water concentration in vanadate-phytase catalyzed reactions, by performing the reaction in organic media. Especially immobilization of the enzyme is a key step, because it can highly improve the stability of the enzyme in organic solvents. Cross Linked Enzyme Aggregates (CLEA) of phytase were prepared, and provided a straightforward and robust approach towards its immobilization³⁸. In general, CLEAs are characterized by increased operational stability and recyclability.

3. Materials and Methods

All the chemicals used were purchased from commercial suppliers in the highest purity available. Commercial phytase preparations; Natuphos[®], from *Aspergillus niger* (3-phytase) and Ronozyme[®], from *Peniophora lycii* (6-phytase) were generously donated by BASF and Novozymes, respectively and used without further purification.

3.1. Enzyme Activity

The enzymatic activity and the protein content were monitored on a Varian Cary 3 Bio, equipped with a Cary temperature controller. Instead of the standard phytase activity protocol we employed an activity test commonly used for acid phosphatases which is more suitable for organic solvents: The activity was measured in a mixture containing 0.5 ml of *p*-nitrophenyl phosphate (15.2 mM), 0.5 ml of acetate buffer (100 mM, pH 5.5) and 0.1 ml of the enzyme (conveniently diluted). After 10 min of incubation at 37°C the reaction was stopped by addition of 4 ml 0.1 M NaOH. The formation of *p*-nitrophenol was monitored by UV-Vis spectroscopy at 410 nm (18.3 mM⁻¹cm⁻¹). One unit of phytase is defined as 1 μmol of inorganic phosphate produced per minute at pH 5.5 at 37°C. The protein concentration was determined by the Bradford method³⁹ using Bovine Serum Albumin (BSA) as the standard protein.

3.2. Catalytic Oxidations

As a general procedure, 140 U (200 μ l, 24 mg protein) phytase was incubated with 15 μ M vanadium in 100 mM acetate buffer, pH 5.0, for 1 hour. Then 5 mM substrate, dissolved in organic solvent, was added. The reaction was initiated by the addition of 5.5 mM H₂O₂ (final concentration). Usually the oxidant was added at 5 μ l/min with a Metrohm Dosimat[®]. The typical total reaction time was 2 hours. At the end of the reaction organic compounds were extracted with ethyl acetate. The solutions were centrifuged; the organic phases dried over MgSO₄ and samples for chiral HPLC were taken. The reaction mixtures were analyzed on chiral HPLC using a Chiralcel OD column (Daicel Chemical Industries, Ltd., 250 \times 4.6 mm) equipped with Waters 486 tunable absorbance detector (set to 215 nm). *n*-Hexane: isopropanol (75:25) mixture was used as eluent, flow rate of 0.5 ml min⁻¹.

3.3. Qualitative Determination of Bromination Activity

The brominating activity of V-phytase was measured qualitatively by the bromination of 40 μ M phenol red in 100 mM acetate buffer pH 5, containing 2 mM H₂O₂ and 100 mM KBr. By bromination of phenol red to bromophenol blue, large color changes can be observed and can easily be detected visually⁴⁰.

3.4. Haloperoxidase Activity

The haloperoxidase activity of V-phytase was measured with monochlorodimedon (MCD) as substrate at pH 5, 100 mM acetate buffer. 0.1 ml MCD (1.25 mM stock solution), 0.2 ml KBr (12.5 mM), 0.2 ml H₂O₂ (12.5 mM) and 5 μ l enzyme was mixed in a total volume of 2.5 ml in UV cuvette. The change in absorbance in the 390-190 nm range was recorded every 3 minutes (repeated 10 times).

3.5. Halohydrin Formation with V-Phytase

Halohydrin formation with V-phytase was investigated using a reported procedure⁴¹ with 2,3-dimethyl-2-butene and allyl bromide as substrate. 200 μ l phytase is pre-incubated with 25 μ M vanadate in acetate buffer pH 5.0 (100 mM). Then 25 mg olefin, 50 mg KBr and H₂O₂ 5 mg/5

ml added to the mixture and stirred for 5 hours. The reaction mixture was then extracted with diethyl ether and analyzed with GC for products.

3.6. Synthesis of 1-(3-hydroxypropyl)-3-methylimidazolium glycolate

As a first step 3-chloropropanol was distilled under vacuum and then mixed with 3-methyl imidazol (mol ratio 3:2). The mixture was stirred under N₂ for 4 days. At the end of 4 days, the product was washed with ethyl acetate in order to remove the excess of 3-chloropropanol from the mixture. A resin ion exchange column was prepared and saturated with NaCl. 1 M glycolic acid solution was prepared and the pH was brought to 6.5 and applied in the column. Consequently, the column was washed with water until no more chloride ion was eluted. The synthesized 1-(3-hydroxypropyl)-3-methylimidazolium salt was then added to the column. 1-(3-hydroxypropyl)-3-methylimidazolium glycolate was eluted with water and then water was removed. The dried ionic liquid (IL) kept in a vacuum desiccator until use.

3.7. CLEA Preparation

As a general procedure the free enzyme was dissolved in 100 mM acetate buffer pH 5.5 and added dropwise to a saturated (NH₄)₂SO₄ solution or to (–)-ethyl-L-lactate for precipitation. Then, for the cross-linking step, glutaraldehyde (25 % w/v in water) was added to the mixture, which was stirred at room temperature for 3 hours to allow the cross-linking. After centrifugation, the supernatant was decanted and the residue was washed 3 times with acetate buffer (100 mM, pH 5.5), centrifuged and decanted. The final enzyme preparation was kept in pH 5.5 acetate buffer.

3.8. CD Spectroscopy

The CD spectra were measured using a cylindrical 1 mm Hellma Quartz Suprasil cuvette, on a Jasco J-720 Spectropolarimeter in the wavelength range 185–260 nm (whenever possible) at room temperature (except for the temperature dependent studies). The measuring conditions were: band width, 0.5 nm; response, 4 s; data pitch, 0.2 nm; scanning speed, 50 nm/min; number of accumulations, 5. The baseline obtained with the buffer was subtracted from the sample spectra. Molar ellipticities (in deg cm² dmole⁻¹) were plotted against wavelength. The

samples were prepared in acetate buffer (10 mM, pH 4.5). The protein concentrations in the samples were 0.12 and 0.10 mg/ml, for the 3- and 6-phytase, respectively. Samples were incubated with different vanadate concentrations for 30 min at 25°C before their spectra were measured. For the temperature dependence studies the samples were incubated for 30 min at 40°C, 60°C or 80°C. Subsequently, either the CD spectra were measured directly at the same temperature using a thermostated sample compartment, with rectangular 1 mm quartz cuvettes, or the samples were first allowed to renature for 30 minutes at 25°C and then the CD spectra were measured at 25°C. Temperature was controlled with a Haake DC10 thermostat. The analysis of the circular dichroism spectra for the determination of protein secondary structure was carried out using the CDPro suite of programs⁴². The calculations were made using the three programs included in this software: SELCON3, CONTINLL and CDSSTR. Different bases for the reference set of proteins were used and the best results (lower rmsd values) were obtained using the set based on 43 soluble proteins (with λ between 190-240nm).

4. Results and Discussion

4.1. Phytase Activity in the Presence of Organic Solvents

The aim of the research was to employ V-phytase in oxidation reactions other than sulfoxidations. Initial experiments on the oxidation of benzylic alcohols in buffer yielded no product. We reasoned that the water bound to the active site of the phytase could be competing with the alcohol molecule and thereby prevent its interaction with the active site³⁴. One possible solution to this problem could be the removal of water from the enzyme environment and also from the reaction medium. In an initial approach to study the activity of phytase in the presence of organic solvents, we tested the natural phosphatase activity of phytase.

Table 2 shows a comparison of phosphatase activity of phytase under various conditions.

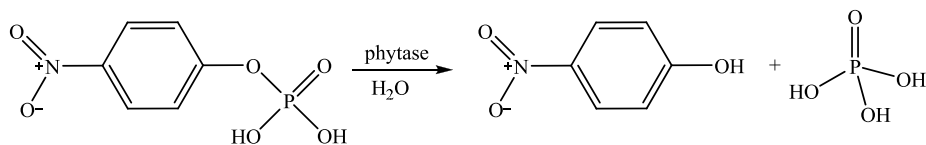


Table 2: Comparison of phytase activity with buffer and organic solvents (for conditions, see experimental part)

Entry	Solvent	Temperature	Activity
1	pH 5.5 buffer	20°C	922 U/ml
2	pH 5.5 buffer	37°C	937 U/ml
3	DME	37°C	1121 U/ml
4	1-(3-hydroxypropyl)-3-methylimidazolium	37°C	1044 U/ml

It can be seen that the hydrolytic activity of phytase at 37°C is similar to that at room temperature. In entries 3 and 4, the substrate is dissolved in DME and in an ionic liquid, respectively, and then the enzyme preparation was added in order to calculate the relative activities with respect to the activity in buffer. Ionic liquids (IL) have recently been reported as attractive media for enzyme reactions. 1-(3-hydroxypropyl)-3-methylimidazolium glycolate was chosen since it is known to dissolve most enzymes due to its hydrophilic character^{43,44}. Apparently phytase activity is not effected by replacement of buffer with organic solvent. After incubation for 15 hours in DME, the activity did not decrease. In addition, we studied hydrolysis with phytase in an ionic liquid. Also in this experiment, excellent phytase activity could be observed. It should be mentioned that the reactions reported here are not completely water-free: a small amount of water was introduced in the reaction mixture that is present in the commercial enzyme preparation.

4.2. Activity of V-Phytase in the Presence of Organic Solvents

Encouraged by these results, we performed thioanisole oxidation in organic solvents. We replaced the buffer with different solvents, such as DME, isopropanol, *tert*-butanol, 1-octanol, glycerol and also with 1-(3-hydroxypropyl)-3-methylimidazolium glycolate. However, in all

cases the oxidation of thioanisole yielded < 2 % of the desired sulfoxide product. In addition *tert*-butyl hydroperoxide (TBHP) was tested as oxidant, first in buffer and then in organic media (in DME and in 1-(3-hydroxypropyl)-3-methylimidazolium glycolate at room temperature). Also in these experiments we could not detect any sulfoxidation product.

Besides sulfides, allylic alcohols, such as 1-phenyl ethanol and cinnamylalcohol were studied as substrates for oxidation by V-phytase in the organic media (in DME and in glycerol, at room temperature, overnight experiments) with H₂O₂ as oxidant. Also with these alcohols we did not observe any product formation.

4.3. V-Phytase Activity in Co-solvent Mixtures

At this point, we decided that we needed a better understanding of the effects that organic solvents have on the activity of V-phytase. For this the catalyst performance of V-phytase in thioanisole oxidation was chosen as model reaction. For this series of experiments, we used free enzyme as well as immobilised enzyme in the form of CLEA. In the case of free enzyme, the best results were obtained using 10 % DME as co-solvent to solubilize the substrate, resulting in high conversion and 37 % ee (Table 3). Increasing the temperature clearly decreased the enantioselectivity. At 80°C, nearly all enantioselectivity had disappeared (ee 3%). The best results were obtained when a H₂O₂ solution was continuously and slowly added (5 µl/min, 5.5 mM final concentration, see experimental).

In experiments employing CLEA-phytase, the CLEA-phytase was incubated for 1 hour at 37°C with vanadate solution, and then mixed with the substrate. CLEA-phytase showed similar efficiency and selectivity to the free enzyme in the presence of 10 % DME (see entries 1 and 6, Table 3). In the presence of organic solvent, a slight decrease in enantioselectivity (from 46 % to 41 %) was observed. Overall the activity is similar to that of free enzyme.

Table 4 presents the results obtained with the CLEA-phytase with different organic solvents and different pH. As can be seen from the table, CLEA-phytase is quite active and not very sensitive to most of the experimental conditions such as pH and V⁵⁺ concentration. In the vanadate concentration range studied, the conversion does not seem to be effected by the

increase of vanadate concentration (entries 12-15). However the selectivity decreases slightly upon increase of vanadate concentration; 15 μM is a good compromise between high conversion and selectivity.

Table 3: Parameters and results obtained in the oxidation of thioanisole with the 3-phytase

Free enzyme						
Entry	T ($^{\circ}\text{C}$)	t (h)	V^{5+} (μM)	% DME	Conv (%)	ee (%)
1	25	2	15	10	96	37
2	40	2	15	10	99	28
3	60	2	15	10	89	7
4	80	2	15	10	92	3
CLEA						
5	25	3	20	0	35	46
6	25	3	20	10	99	41

Conditions: acetate buffer (100 mM, pH 5.0), 3-phytase: 50 U, thioanisole: 5 mM, H_2O_2 : 5.5 mM.

Organic solvents substantially deactivate the immobilized enzyme (see entries 8-11, Table 4), and acetonitrile has the strongest effect, almost completely inactivating the CLEA. However with 10 % of dimethoxyethane (DME) the enzyme is still very active and the substrate is soluble in the reaction media. The formation of over-oxidation products, like sulfone, was negligible (<1 %). The maximum enantiomeric excess obtained was 62 % (for the S-sulfoxide, entry 5). This is probably due to the inherent selectivity of the enzyme, but we have also tested if free vanadate is catalyzing the non-enzymatic reaction: some assays were conducted in which the CLEA was incubated with vanadate for 1 h at 37 $^{\circ}\text{C}$, after which the supernatant was removed and replaced by an equivalent amount of buffer (entries 18-19). Comparison of entries 16 and 18 (or 17 and 19) show that there is no influence of the free vanadium since the ee is 40 % in both assays. Therefore we conclude that only enzyme-bound vanadate activates the peroxide in our reaction.

Table 4: Conditions and results obtained in the oxidation of thioanisole with V-3-phytase-CLEA

Entry	CLEA (ml) ^a	V ⁵⁺ (μM)	t (h)	% DME	Conv (%)	ee (%)
1	1	15	2	10	98	56
2	1	15	2	30	86	42
3	1	15	2	40	25	28
pH						
4	1	15	4.5	3.6	96	60
5	1	15	4.5	4.2	93	62
6	1	15	4.5	5	92	57
7	1	15	4.5	5.6	98	57
30 % solvent						
8	1	15	3.5	MeOH	58	19
9	1	15	3.5	EtOH	55	22
10	1	15	3.5	MeCN	3	1
11	1	15	3.5	DME	86	42
V⁵⁺ (μM)						
12	1	10.5	3.5		92	57
13	1	21	3.5		93	48
14	1	42	3.5		96	50
15	1	84	3.5		89	45
16	1	15	3		85	40
17	0.5	15	3		69	40
18	1	15	3	a	70	40
19	0.5	15	3	a	52	42

Conditions: acetate buffer (100 mM pH 5.0) with 10 % DME, 5.5 mM H₂O₂ and 5 mM thioanisole, T: 25°C; 3-phytase-CLEA : 90U. ^a After incubating the CLEA 1h at 40°C with vanadate supernatant was removed and replaced by buffer.

4.4. Stability of V-Phytase CLEA

All data in Table 4 were collected in co-solvent mixtures with maximum 30 % of co-solvent. The reason for this is that when we completely removed water from the reaction environment, no reaction occurred (data not shown). This is similar to the results obtained with free enzyme in the sulfoxidation of thioanisole (vide supra). In other words, stabilisation of enzyme by means of immobilisation did not enable the vanadium centered catalysis in the active site. When we collected the CLEA after the reaction in organic solvent, and re-dissolved it in buffer, the thioanisole oxidation in buffer took place. This indicates that any structural

changes which might have occurred in the phytase upon adding organic solvents, and which might effect vanadium binding, are however reversible.

One of the advantages of the CLEA is the possibility of recycling after use. To test this parameter, after the first catalytic cycle the CLEA was centrifuged and washed twice with water. Acetate buffer and vanadate were then added to the CLEA, and left overnight at 37°C and reused. This procedure was done twice. Figure 4 shows that the CLEA does not lose activity or selectivity even after being used three times.

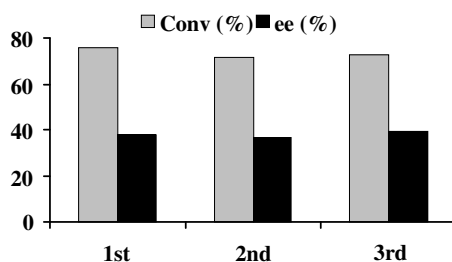


Figure 4: Conversion of thioanisole and ee of sulfoxide product with 1, 2, and 3 times recycled CLEA-V-phytase

Conditions: acetate buffer (100 mM pH 5.0) with 10 % DME, 5.5 mM H₂O₂ and 5 mM thioanisole, T: 25°C; 3-phytase-CLEA : 90 U

4.5. Characterization

To study the behaviour of phytase in organic solvents more closely, we embarked on characterization of the structure of phytase in different solvents. Circular Dichroism (CD) is a spectroscopic tool that may be used to study the conformation of biomolecules such as proteins^{42,45}. Different secondary structures give characteristic CD spectra, and it is considered that the spectrum is a sum of the spectra of the individual secondary structures (α -helices, β -sheets and turns) present in the protein. We used the CD-technique to study the stability of the enzyme as a function of solvent, especially because the negative effect of the solvent could not be avoided by using a CLEA-phytase. Most catalytic experiments were done with 10 % DME to allow the dissolution of the substrate. We also observed that when a

higher percentage of an organic solvent was used, in some cases, the activity sharply decreased. Therefore, we measured the CD spectra of both phytases in the presence of 10 % DME and 30 % DME, ethanol, methanol, and acetonitrile (Figure 5).

A rough estimate of the α -helical content can be obtained from the mean residue ellipticity⁴⁶. It is quite clear from Figure 5 and Table 5 that in the presence of 30 % ethanol and 30 % DME the α -helical content of the enzymes had increased. In particular, the band at 208 nm has higher intensity. Acetonitrile, on the other hand, has a very strong effect on the secondary structure by decreasing the α -helical content in both enzymes.

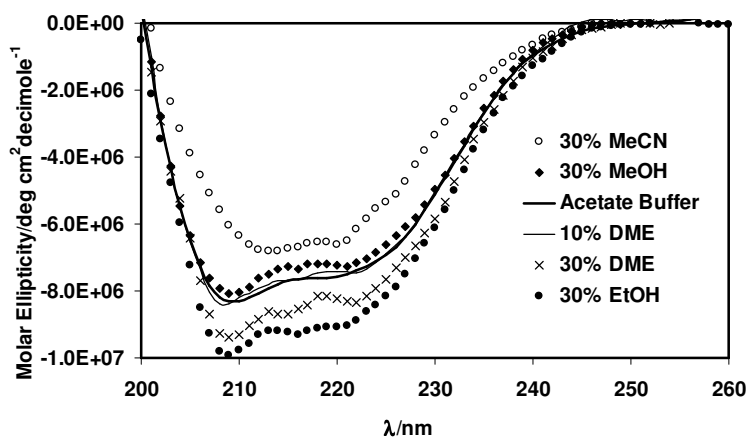


Figure 5: CD spectra recorded in buffer and in the presence of organic solvents

If we compare this to the almost complete loss of enantiomeric excess in the catalytic experiments done with 30 % acetonitrile (Table 4, entry 10), we can conclude that a loss in α -helical content is detrimental for the vanadium catalysis. Admittedly, experiments in Table 4 were performed with CLEA-phytase and not with free phytase as in the CD-experiments. However, in view of the similar catalytic results, we feel that a qualitative comparison is justified.

Table 5: α -Helical content of 3-phytase with different percentages of organic solvents

3-phytase	
Solvent	
Buffer pH=4.5	59.0
10% DME	59.5
30% DME	65.4
30% MeOH	57.5
30% EtOH	69.2
30% MeCN	50.8

Conditions; 25°C, and pH 4.5. [Estimated with the expression: fraction of α -helix = $-([\theta]_{222} + 3000) / 33000$ ⁴⁶].

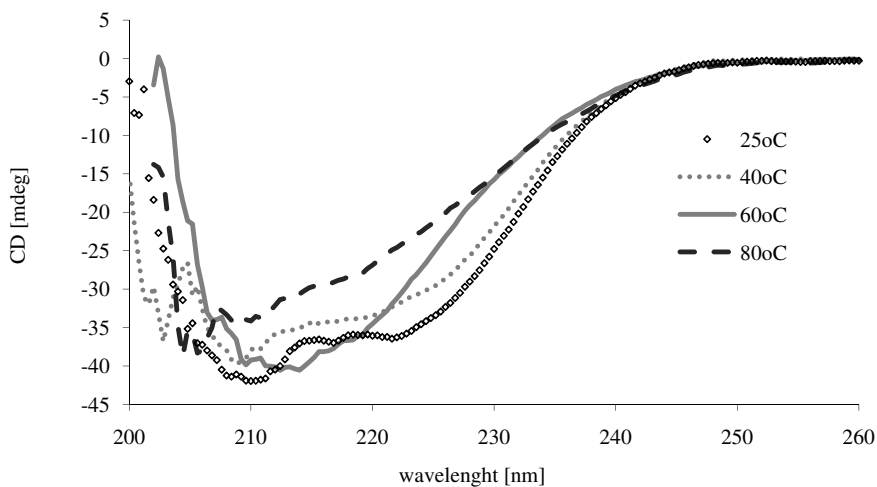


Figure 6: CD spectra recorded in buffer and 10 % DME at different temperatures.

Thermostability is an important criterium for the industrial applicability of enzymes. Especially during pelletizing of enzyme preparations, enzymes should be able to withstand high temperatures for several minutes⁴⁷. CD-spectroscopy is convenient and valuable

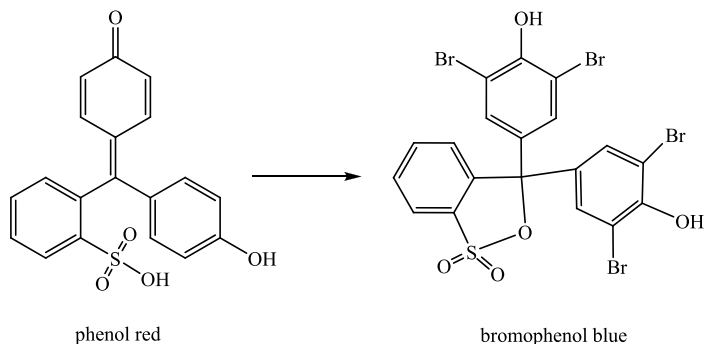
technique to study the temperature dependence (Figure 6 and Table 6). The samples were incubated at 25°C, 40°C, 60°C and 80°C respectively for 30 minutes and then the CD spectra were measured. The data indicate that the enzyme structure has altered upon increasing the temperature. The α -helical content decreased at higher temperature while β -sheet and unordered secondary structure elements increased. In other words, the phytase structure collapses at higher temperatures in 30 minutes (a process commonly denoted as denaturation), which also explains the decrease in enantioselectivity of sulfoxide formation in oxidation at elevated temperatures (see Table 3). Table 6 contains the results obtained from the CDPro suite of programs⁴².

Table 6: Secondary structure content of 3-phytase at pH:4.5 determined by CD spectroscopy with the CDPro suite of programs

	α -helix	β -sheet	Turns	Unordered
3-phytase				
T=25°C	61.3	11.3	9.1	18.3
T=40°C	49.1	9.1	18.2	23.1
T=60°C	23.9	30.0	23.4	22.4

4.6. Scope of V-Phytase Oxidation Catalysis in Aqueous Solutions

In an attempt to extend the reactivity of vanadium-peroxidase to other reactions, we went back to the starting point: namely the resemblance between V-phytase and vanadium dependent haloperoxidases. Thus, the semi-synthetic peroxidase would be able to perform halogenation reactions. The brominating activity of V-phytase was measured qualitatively by the bromination of phenol red in 100 mM acetate buffer pH 5, containing 2 mM H₂O₂ and 100 mM KBr. By bromination of phenol red to bromophenol blue, large color changes can be observed which can be visually detected⁴⁰. However, when we tested the activity of V-3-phytase and V-6-phytase, in neither reaction could bromination activity be observed.



Monochlorodimedon (MCD) is a standard substrate for the haloperoxidase activity assay. V-phytase was also tested in the bromination of MCD. No change in MCD absorbance was however observed (monitored by UV). As third possibility we searched for halohydrin formation with V-phytase, using a reported procedure⁴¹ with 2,3-dimethyl-2-butene and allyl bromide as substrate. Also in this reaction, no product formation was observed. At this point we have to conclude, that V-phytase is not able to induce HOCl, or HOBr formation. This is unexpected, and leaves us to conclude that the vanadium-peroxo complexes formed in the presence of H₂O₂ are different for V-phytase and VHPOs. It can be claimed that other residues further away from the active site play an important role in binding of vanadate and in tuning the activity and specificity of these enzymes.

5. Conclusions

In previous reports it was shown that binding of vanadate by 3-phytase results in a semi-synthetic enzyme, that can activate HOOH, and thus catalyze oxygen transfer to sulfides to produce the corresponding sulfoxides selectively, resulting in ee's up to 60 %. ⁵¹V-NMR studies revealed the presence of monoperoxovanadium species. This is in-line with chemocatalytic data, where these species are good oxidants not only for sulfoxidation but also for the oxidation of alcohols and epoxidation of allylic alcohols in polar non-coordinating solvents. In order to extend the potential of V-phytase the latter reactions were probed in organic media. However, attempts to perform oxidation reactions with V-phytase in organic media were unsuccessful. Also the immobilisation of phytase as cross-linked-enzyme aggregates, CLEA-phytase, was not able to stabilize V-phytase in such a way that oxygen transfer in organic media could be observed. It turned out that the presence of already 30 %

co-solvent led to large disturbances in the enzyme's secondary structure. These structural changes could be conveniently monitored using CD spectroscopy. Another parameter to enhance the activity of V-phytase, namely the temperature, could also not be used. CD spectroscopy indicated that denaturation of the enzyme took place at temperatures of 40°C or higher at longer incubation times. Although it is not clear at this moment whether vanadate binding still occurs in the presence of organic solvents, it is reasonable to assume that the major structural changes that occur in the protein, are connected with the lack of reactivity.

Finally we conclude that CLEA-phytase was equally efficient in the binding of vanadate as the free enzyme. CLEA-V-phytase was a robust, stable and easy to use catalyst for the sulfoxidation of thioanisole. Recycling of CLEA-V-phytase was demonstrated, and high activity and enantioselectivity could be demonstrated for three cycles.

6. References

1. Seelbach, K.; van Deurzen, M. P. J.; van Rantwijk, F.; Sheldon, R. A. *Biotechnol. Bioeng.* **1997**, *55*, 283-288.
2. van Deurzen, M. P. J.; Remkes, I. J.; van Rantwijk, F.; Sheldon, R. A. *J. Mol. Catal. A-Chem.* **1997**, *117*, 329-337.
3. Colonna, S.; Gaggero, N.; Carrea, G.; Pasta, P. *Chem. Commun.* **1997**, 439-440.
4. Kiljunen, E.; Kanerva, L. T. *J. Mol. Catal. B-Enzym.* **2000**, *9*, 163-172.
5. van Rantwijk, F.; Sheldon, R. A. *Curr. Opin. Biotech.* **2000**, *11*, 554-564.
6. Dembitsky, V. M. *Tetrahedron* **2003**, *59*, 4701-4720.
7. Andersson, M.; Andersson, M. A.; Adlercreutz, P. *Biocatal. Biotransfor.* **2000**, *18*, 457-469.
8. Messerschmidt, A.; Wever, R. *Inorg. Chim. Acta* **1998**, *273*, 160-166.
9. ten Brink, H. B.; Tuynman, A.; Dekker, H. L.; Hemrika, W.; Izumi, Y.; Wever, R. *Inorg. Chem.* **1998**, *37*, 6780-6784.
10. ten Brink, H. B.; Holland, H. L.; Schoemaker, H. E.; van Lingen, H.; Wever, R. *Tetrahedron: Asymmetry* **1999**, *10*, 4563-4572.

11. Hemrika, W.; Renirie, R.; Dekker, H. L.; Barnett, P.; Wever, R. *Proc. Natl. Acad. Sci. USA* **1997**, *94*, 2145-2149.
12. Hemrika, W.; Renirie, R.; Dekker, H.; Wever, R. *Vanadate-containing haloperoxidases and acid phosphatases: the conserved active site*; ACS, 1998; Vol. 711.
13. Renirie, R.; Hemrika, W.; Wever, R. *J. Biol. Chem.* **2000**, *275*, 11650-11657.
14. Plass, W. *Angew. Chem. Int. Edit.* **1999**, *38*, 909-912.
15. Davies, D. R.; Hol, W. G. J. *FEBS Lett.* **2004**, *577*, 315-321.
16. Mullaney, E. J.; Daly, C. B.; Ullah, A. H. J. *Adv. Appl. Microbiol.* **2000**, *47*, 157-199.
17. Ullah, A. H. J.; Sethumadhavan, K. *Biochem. Biophys. Res. Commun.* **2003**, *303*, 463-468.
18. Correia, I.; Aksu, S.; Adao, P.; Costa-Pessoa, J.; Sheldon, R. A.; Arends, I. *J. Inorg. Biochem.* **2008**, *102*, 318-329.
19. van de Velde, F.; Konemann, L.; van Rantwijk, F.; Sheldon, R. A. *Biotechnol. Bioeng.* **2000**, *67*, 87-96.
20. van de Velde, F.; Arends, I. W. C. E.; Sheldon, R. A. *Top. Catal.* **2000**, *13*, 259-265.
21. Kostrewa, D.; Wyss, M.; Allan, D. A.; Loon, A. P. G. M. *J. Mol. Biol.* **1999**, *288*, 965-974.
22. Pecoraro, V. L.; Slebodnick, C.; Hamstra, B. In *ACS Symposium Series 711; Vanadium Compounds; Chemistry, Biochemistry, and Therapeutic Applications* Tracey, A. S.; Crans, D. C. Eds.; ACS, 1998.
23. Weyand, M.; Hecht, H.-J.; Kiess, M.; Liaud, M.-F.; Vilter, H.; Schomburg, D. *J. Mol. Biol.* **1999**, *293*, 595-611.
24. Bortolini, O.; Di Furia, F.; Modena, G. *J. Mol. Catal.* **1982**, *16*, 61-68.
25. Bortolini, O.; Di Furia, F.; Scrimin, P.; Modena, G. *J. Mol. Catal.* **1980**, *7*, 59-74.
26. Bonchio, M.; Conte, V.; Di Furia, F.; Modena, G.; Padovani, C.; Sivak, M. *Res. Chem. Intermed.* **1989**, *12*, 111-124.
27. Karpyshev, N. N.; Yakovleva, O. D.; Talsi, E. P.; Bryliakov, K. P.; Tolstikova, O. V.; Tolstikov, A. G. *J. Mol. Catal. A-Chem.* **2000**, *157*, 91-95.

28. Mimoun, H.; Saussine, L.; Daire, E.; Postel, M.; Fischer, J.; Weiss, R. *J. Am. Chem. Soc.* **1983**, *105*, 3101-3110.
29. Conte, V.; Di Furia, F.; Licini, G. *Appl. Catal. A-Gen.* **1997**, *157*, 335-361.
30. Conte, V.; Di Furia, F.; Modena, G. *J. Org. Chem.* **1988**, *53*, 1665-1669.
31. Bonchio, M.; Bortolini, O.; Conte, V.; Primon, S. *J. Chem. Soc.-Perkin Trans. 2* **2001**, 763-765.
32. Messerschmidt, A.; Wever, R. *Proc. Natl. Acad. Sci. USA* **1996**, *93*, 392-396.
33. Messerschmidt, A.; Prade, L.; Wever, R. *Biol.Chem.* **1997**, *378*, 309-315.
34. Liu, Q.; Huang, Q.; Lei, X. G.; Hao, Q. *Structure* **2004**, *12*, 1575-1583.
35. Rossiter, B. E.; Verhoeven, T. R.; Sharpless, K. B. *Tetrahedron Lett.* **1979**, *49*, 4733-4736.
36. Sharpless, K. B.; Verhoeven, T. R. *Aldrichim. Acta* **1979**, *12*, 63-74.
37. Arends, I. W. C. E.; Vos, M.; Sheldon, R. A. In *ACS Symposium Series 711; Vanadium Compounds; Chemistry, Biochemistry and Therapeutic Applications*; Tracey, A. S.; Crans, D. C. Eds., 1998.
38. Schoevaart, R.; Wolbers, M. W.; Golubovic, M.; van Rantwijk, F.; Sheldon, R. A. *Biotechnol. Bioeng.* **2004**, *87*, 754-762.
39. Bradford, M. M. *Anal. Biochem.* **1976**, *72*, 248-254.
40. de Boer, E.; Plat, H.; Tromp, M. G. M.; Wever, R.; Franssen, M. C. R.; Vanderplas, H. C.; Meijer, E. M.; Schoemaker, H. E. *Biotechnol. Bioeng.* **1987**, *30*, 607-610.
41. Neidleman, S. L.; Amon, W. F.; Geigert, J.; Cetus Corp (Cetu); US 4,247,641-A, Jan 1981.
42. Sreerama, N.; Woody, R. W. *J. Mol. Biol.* **1994**, *242*, 497-507.
43. van Rantwijk, F.; Sheldon, R. A. *Chem. Rev.* **2007**, *107*, 2757-2785.
44. Bermejo, M. D.; Kotlewska, A. J.; Florusse, L. J.; Cocero, M. J.; van Rantwijk, F.; Peters, C. J. *Green Chem.* **2008**, *10*, 1049-1054.
45. Pelton, J. T.; McLean, L. R. *Anal. Biochem.* **2000**, *277*, 167-176.

46. Morriset, J. D.; David, J. S. K.; Pownall, H. J.; Gotto, A. M. *Biochemistry* **1973**, *12*, 1290-1299.
47. Wyss, M.; Pasamontes, L.; Friedlein, A.; Remy, R.; Tessier, M.; van Loon, A. P. G. M. *Appl. Environ. Microb.* **1999**, *65*, 359-366.

Metal Replacement in Laccase

3

1. Introduction
2. Materials and Methods
 - 2.1. Enzyme Purification
 - 2.2. SDS Gel Assay
 - 2.3. Determination of Protein Concentration
 - 2.4. Laccase Activity Assay
 - 2.5. Dialysis
 - 2.6. Enzymatic Oxidation Reactions
3. Results and Discussion
 - 3.1. Purification and Characterization of Laccase by Spectroscopy
 - 3.2. Primary Alcohol Oxidations
 - 3.3. Oxidation of Secondary Alcohols
4. Conclusions and Future Work
5. References

1. Introduction

Laccase belongs to the multicopper oxidase family, which includes among others ascorbic acid oxidase and ceruloplasmin. This group of enzymes couples the four-electron reduction of dioxygen to water with the one electron oxidation of the substrate¹. Copper centers in these enzymes have historically been divided into three classes: type 1 (T1) or blue copper, type 2 (T2), and type 3 (T3) or coupled binuclear copper centers. Multicopper oxidases usually contain a T1 copper site and a T2/T3 trinuclear cluster as the minimal functional unit (with the exception of ceruloplasmin which possesses more copper centers). The overall structure of the copper centers is depicted in Figure 1:

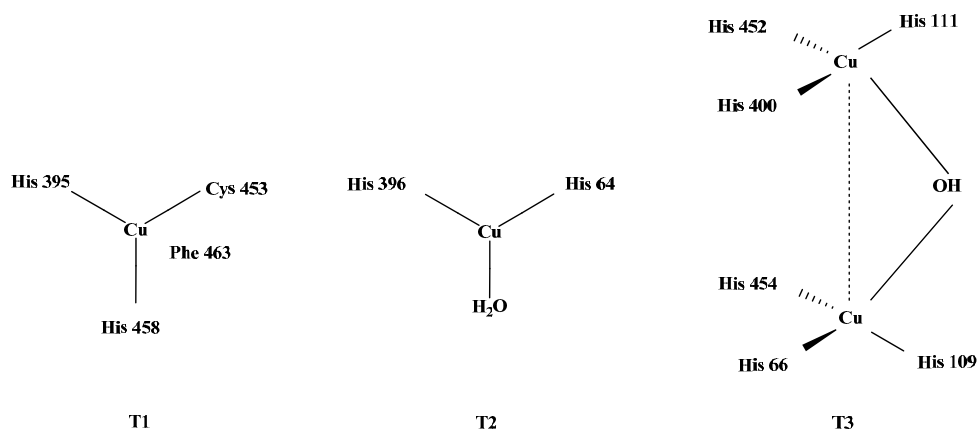


Figure 1: Geometry of copper centers in *Trametes versicolor* laccase

In vivo, laccase catalyzes the initial polymerization of monolignols to oligolignols in higher plants, as well as lignin depolymerization, as suggested by the great abundance of this enzyme in wood-rotting fungi². The interactions with substrates may change depending on the source of enzyme. The plant and fungal laccases are usually defined as enzymes with narrow substrate specificity. They can oxidize diphenols, aryl diamines, and aminophenols¹. The range of substrates that can be oxidized is limited either by size or because they have a particularly high redox potential. The oxidation of non-natural substrates is promoted by metabolites or fragments of lignin present in its natural environment. These metabolites are usually phenolic compounds and they act like mediators^{3,4}. In general, a mediator is a low-

molecular weight compound that acts as an “electron shuttle”. After being oxidized by the enzyme, it diffuses away from the active site to oxidize any substrate that could not react with laccase directly⁵. However, in order to effectuate the oxidation of non-natural substrates, a large excess of these mediators is often required. This could be due to the fact that phenolic mediators are, themselves, good substrates for laccase, leading to non-catalytic, undesired routes, such as radical coupling or fragmentation⁶. A stoichiometric amount of a mediator is economically and environmentally not attractive. For this reason, artificial mediators have been developed. The first artificial mediator to be used for pulp delignification in a laccase-mediator system was ABTS (2,2'-azino-bis (3-ethylbenzothiazoline-6-sulfonic acid))⁷. Subsequently, more than a hundred other compounds have been tested for their ability to oxidize lignin through the selective oxidation of its benzylic hydroxyl groups⁸. The most suitable compounds for this purpose proved to be the N-heterocycles bearing N-OH groups, such as HBT (N-hydroxybenzotriazole), NHPI (N-hydroxyphthalimide), VLA (violuric acid, 2,4,5,6(1*H*,3*H*)-pyrimidinetrone 5-oxime), and stable N-oxy radicals such as TEMPO (2,2,6,6-tetramethylpiperidine-1-oxy). It has been suggested that, depending on their chemical structure, mediators follow different mechanisms of oxidation^{5,9}.

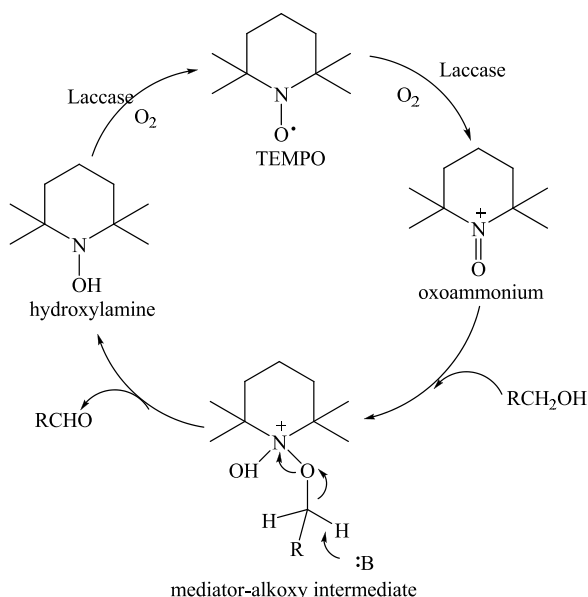


Figure 2: Alcohol oxidation via TEMPO radical

An electron-transfer mechanism can be envisaged for the mediator ABTS¹⁰, while a radical hydrogen atom transfer route may operate with N-OH-type mediators¹¹. N-oxy radicals such as TEMPO undergo one-electron oxidation to the corresponding oxoammonium cations which are the active oxidants (Figure 2).

The oxoammonium cation and the alcohol substrate form a mediator-alkoxy intermediate which subsequently decomposes to aldehyde and hydroxylamine via proton abstraction³. The oxidation of primary alcohols proceeds smoothly with the laccase/TEMPO system. Oxidation of secondary alcohols however, is not effective under the same conditions, probably due to the steric hindrance in binding to the oxoammonium. Recently, Ishii and coworkers^{12,13} demonstrated the highly efficient oxidation of 2-octanol with molecular oxygen in the presence of catalytic amounts of NHPI and (Co(OAc)₂) (Figure 3).

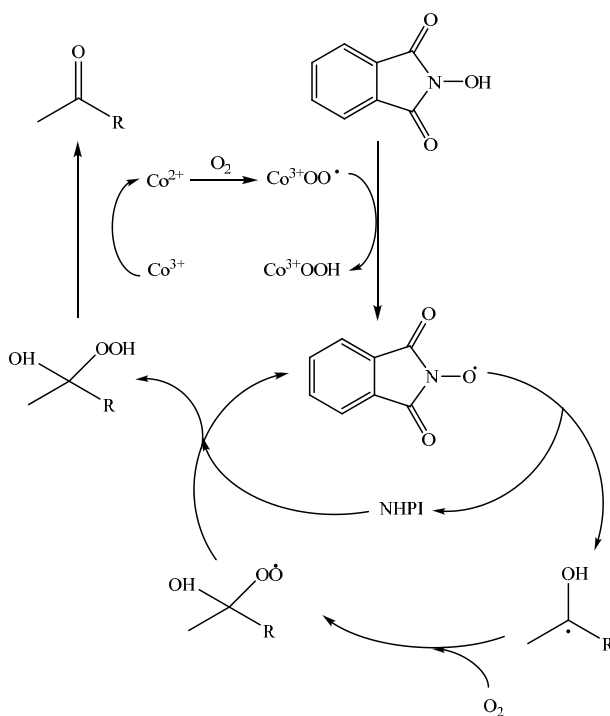


Figure 3: Alcohol oxidation catalyzed by Co(II) and NHPI

In this scheme the cobalt has two functions: it acts as an initiator in generating PINO radicals and it catalyzes the decomposition of intermediate hydroperoxides into products. While secondary alcohols could be efficiently oxidized to the corresponding ketones with this method, the oxidation of primary alcohols yielded carboxylic acids. Presumably hydrogen atom abstraction from aldehydes to form acyl radicals occurs readily, leading to overoxidation. In general a range of metal salts can be used in this radical oxidation system, but it is not clear how the rate and selectivity is influenced by the solvent, temperature and metal used¹⁴.

The suggested mechanism involves the formation of a Co(III)-dioxygen complex by Co(II) species and O₂ which then assists the generation of the phthalimide *N*-oxyl radical (PINO). This is the same active species as in laccase-mediator systems with NHPI. In order to combine the catalytic properties of Co(II)/NHPI system and the natural ability of laccase in alcohol oxidations, a laccase derivative with Co(II) in T1 site was envisaged, that could improve the catalytic efficiency and specificity of laccase in alcohol oxidation. The high standard redox potential of Co(III)/ Co(II) couple (1.82 V¹⁵), also suggests that the replacement of Cu in the laccase active site with Co, should produce a highly redox active enzyme. In the replacement or removal of a specific metal center, many factors have to be taken in account. First of all, these procedures may cause loss of enzymatic activity. Another possible concern is that structural changes within the active site caused by metal removal or replacement could influence the catalytic efficiency and the stability of the enzyme¹⁶. However evidence suggests that the changes are minimal when the metal is an integral part of the active site. In the case of azurin, Shepard *et al.* reported that the crystal structures of apo-azurin and holo-azurin show minimal differences in the active site¹⁷. Another example on the structural similarity of apo- and the holo-enzyme is reported for plastocyanin¹⁸. It was shown that the Hg substituted plastocyanin preserved the active site conformation¹⁹. The flexibility that permits the radial movement of the ligands is an intrinsic property of the metal-binding site. Similarly, structural data available for depleted and metal substituted laccases revealed only minimal structural changes, almost certainly because the protein is able to control the ligand disposition; moreover the structures of derivatives probably reveal the geometry that the protein favors. Greater structural variability is expected for T2 and T3 coppers, because they bind various diatomic and monoatomic intermediates and products when dioxygen is reduced to water²⁰⁻²³.

2. Materials and Methods

The chemicals used in this project were from commercial sources and of the highest purity available. Laccase was from *Trametes versicolor* (Fluka, 21.7 U/mg). The N-hydroxy phthalimide derivatives; 6-hydroxy-5H-pyrrolo[3,4-*b*]pyridine-5,7(6*H*)-dione, 4,5,6,7-tetrachloro-2-hydroxyisindoline-1,3-dione and 2-hydroxy-5-methylisindoline-1,3-dione were synthesized according to literature procedures²⁴⁻²⁶ and purities were checked by NMR.

2.1. Enzyme Purification

Two different columns were used in a two-step protein purification: ion-exchange on Q-Sepharose column followed by size exclusion on a prep-grade Superdex-75, 26/60 HiLoad column. The Q-Sepharose column had a volume of 210 ml and was composed of a cross-linked spherical agarose derivatized with the quaternary ammonium cation, $\text{CH}_2\text{N}^+(\text{CH}_3)_3$, as the functional group. Before use, it was equilibrated with 10 mM Tris-HCl buffer pH 7.5 (flow rate 10 ml/min). 1 g of crude laccase was dissolved in 10 ml Tris-HCl buffer pH 7.5 and injected in the column and eluted with a linear gradient of 0-1 M NaCl in Tris-HCl at flow rate of 10 ml/min. Laccase containing fractions were collected and the most active fractions were concentrated to 10 ml by use of centrifugal filters (Centriprep® Centrifugal Filter Units 50.000 kDa, Millipore) in an IEC Centra GP8R centrifuge. The concentrated and filtered enzyme solution was then injected on the gel filtration column, pre-equilibrated with 50 mM MES (2-(N-morpholino)ethanesulfonic acid) buffer pH 6.0, at room temperature at a flow rate of 3 ml/min. Superdex 75 column has a total volume of 360 ml and is composed of a gel with a composite matrix of dextran and highly cross-linked agarose. 50 mM MES-buffer (pH 6.0 with NaOH) was used for elution.

2.2. SDS Gel Assay

After purification, the purity of the enzyme was checked by SDS gel and compared with the batchwise and the enzyme solution after Q-Sepharose column. 5 μl of sample were mixed with 5 μl of denaturation solution, boiled for 5 minutes, and centrifuged. 5 μl of denatured enzyme solution was put on a Phast Gel SDS gradient 4-15 and run in a Pharmacia-Phast SystemTM together with a marker (low molecular weight calibration kit). After the run, the gel

was stained in Coomassie Blue for 30 minutes (0.025% Coomassie Brilliant Blue R250, 40 % methanol, 7 % acetic acid) and de-stained for 30 minutes.

2.3. Determination of Protein Concentration

The protein concentration was determined using the BC Assay protein quantification kit (Uptima). The color intensity of the standards and the samples were measured at 562 nm on a UV-VIS Hewlett-Packard 8452A Diode Array Spectrophotometer.

2.4. Laccase Activity Assay

Laccase activity was checked spectroscopically before and after dialysis and before each oxidation reaction. 4-Methylaminophenol sulfate (metol) was used as the assay substrate. The substrate solution was prepared right before use and kept out of light to avoid its rapid oxidation. 100 mM acetate buffer pH 5 was used to maintain a slightly acidic pH. The reaction mixture contained 30 mM metol and 50 μ l enzyme solution. The absorbance was measured at 542 nm (ϵ_{540} : 2000 M⁻¹ cm⁻¹) on a UV-VIS Hewlett-Packard 8452A Diode Array Spectrophotometer. The absorbance change was recorded for a total time of 300 seconds. 1 U of laccase is defined as 1 μ mol metol oxidized per 1 minute.

2.5. Dialysis

The original protocol²¹ was improved and adapted according to analysis results. The anaerobic dialysis was carried out using Slide-A-Lyzer 10 kDa dialysis cassettes (Pierce), volume 0.5-3 ml, in 1 L glass beaker in ice bath, degassed by bubbling N₂. The range of protein concentration was 1-6 mg/ml. A four step dialysis procedure was applied for Cu removal; the first step was dialysis against 20 mM NaCN and 50 mM ascorbic acid, under N₂, in an ice bath for 2 hours. This step was then followed by a washing step for 2 hours. In the third step, the enzyme was dialyzed against 2 mM cobalt chloride solution overnight. Another washing step was performed, in order to remove the unbound cobalt ions, as the fourth step. In all four steps, 25 mM Tris HCl buffer pH 7.4 was used.

Before and after dialysis, the sample was analyzed by graphite furnace atomic absorption (AAS) for both copper and cobalt in order to determine their relative amounts in the sample (mg/L). Because of the insufficient literature about cobalt and copper content in cobalt laccase derivatives, the results analysis was carried out by comparing the amount of copper removed to the amount of cobalt that has been inserted and by comparing the relative amount of both copper and cobalt in the dialyzed sample. Since the atomic weight of Cu (63.5 g/mol) does not differ so much from Co (58.9 g/mol), it was not strictly necessary to convert the results (mg/L) in molar amount.

In order to improve the efficiency of the dialysis method, direct addition of cyanide in the protein solution was used for Cu removal. For this approach, a literature method was adopted and simplified²⁷. According to this method, a mixture of sodium cyanide and ascorbic acid was prepared and made anoxic under vacuum-Argon. The laccase solution was treated the same way and then added to the cyanide –ascorbic acid solution. The mixture was kept under argon for another 15 minutes and then incubated at room temperature for 1.5 hours. At the end of incubation, the mixture was passed over a PD-10 column. The protein fractions and the washing fractions were collected in order to make the Cu quantification test. To each fraction collected, the bichinconinic acid test mixture was added and checked for absorbance at 355 and 562 nm. The protein fraction was also checked for A_{280/614} ratio.

2.6. Enzymatic Oxidation Reactions

A 10 Place Omni-Reactor Station (Prosense), which allows heating control, magnetic stirring and cooling, was used for the set up. The 10 ml reaction mixture (in 100 mM phosphate buffer, pH 4.4) contained 1.6 mmol of substrate, 0.15 mmol mediator, 0-100 U enzyme. The reactions were carried out at 30°C, over 4-7 hours of reaction time. In order to maintain sufficient aeration, air was bubbled through the reaction mixture. When the oxidation reactions were terminated, the reaction mixtures were extracted with organic solvent. After extraction, the external standard was added in the organic phase and samples taken, dried with sodium sulphate and analyzed by gas chromatography (Varian Star 3400 CX gas chromatograph equipped with Varian CP-8200 autosampler and CP-Wax 52 CB column (50m x 0.53mm) with a FID detector).

3. Results and Discussion

3.1. Purification and Characterization of Laccase by Spectroscopy

As a first step, the commercial sample of crude laccase was purified according to the procedure described in the Experimental section. The purification was necessary in order to eliminate the possibility of non-specific cobalt binding to the impurities during the exchange. Purified enzyme was also required for subsequent EPR measurements. Figure 4 shows the changes in enzyme color during the purification. The collected fractions after each step were tested for activity, concentrated, and protein concentration was determined (Table 1).

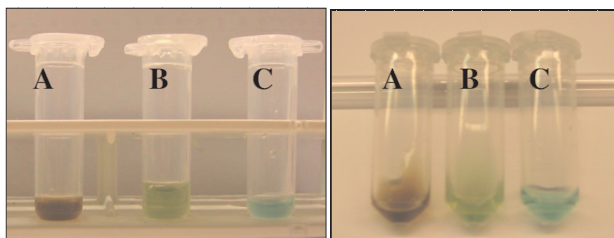


Figure 4: Changes in enzyme color during the purification A) crude extract injected in the first column (batchwise); B) sample after the first column; C) pure enzyme

According to the SDS-gel (Figure 5), *T. versicolor* laccase has a mass equal to 67 kDa, in accordance with the reported literature.

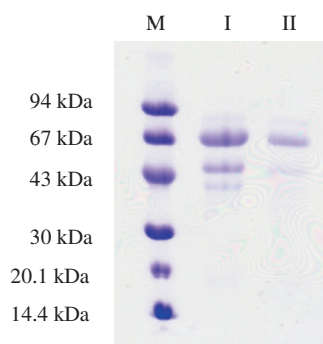


Figure 5: SDS-Gel of laccase, M: marker; I: after Q-Sepharose; II: after Superdex-75

Table 1: Purification table

	Volume	Activity		Protein Conc.		Specific Activity	Yield	Purification Factor
	ml	U/ml	U	mg/ml	mg	U/mg	%	
Batchwise	14	984	13776	21	294	46.9	100.0	1.0
Q-Sepharose	10	930	9300	9.3	93	100.0	67.5	2.1
Superdex-75	10	707	7070	6	60	117.8	51.3	2.5

After exchange of Cu by Co according to the procedure described in the Experimental section, the Cu and Co content of the enzyme solution was measured by Atomic Absorption Spectroscopy (AAS) (Table 2).

Table 2: Co and Cu content of laccase (mg/l), before and after the exchange procedure

	Copper	Cobalt
Laccase	3.28	<0.005
Co-Laccase	2.00	3.08

According to these results, 60 % of the overall Cu content of the enzyme is still present after the dialysis procedure. In addition, Co could be introduced in comparable amounts to Cu. Overall, around 2 mg/l of metal in excess was present in the enzyme preparation. This suggests the non-selective binding of Co, even after the extensive washing step during the dialysis procedure. EPR and UV spectra of the native, apo and Co-laccase were recorded (Figure 6) to provide additional information. In particular the T1 Cu site could be followed, since it is both EPR and UV active.

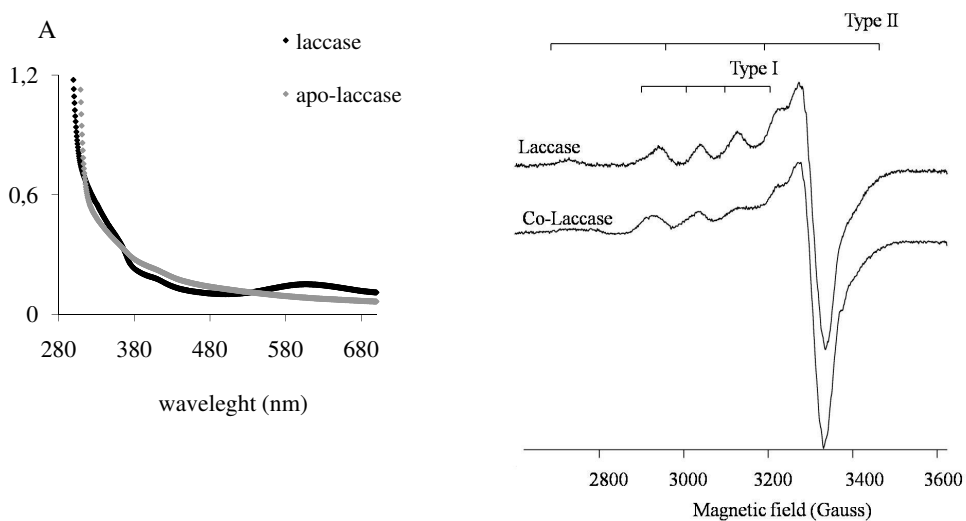


Figure 6: UV and EPR spectra of laccase before and after the exchange procedure

In the UV-VIS spectrum of laccase, the typical signals are at 600 nm for T1 copper and 330 nm for T3; no signals are present for T2. From the comparison, a reduction of absorbance is evident at 600 nm in the UV spectrum. The EPR spectrum was recorded only for Cu in both samples: in Co-laccase copper signals, although reduced, are still present. A total reduction of 40 % was calculated in T1 and T2 sites. This value also fits with the AAS analysis and UV spectra, where Cu in the dialyzed sample was reduced by 40 %.

In order to improve the Cu removal from the laccase, a second method was used in which the cyanide was directly added to the laccase solution. By comparing the $A_{280/614}$ it was possible to see that the reduction in the T1 copper content was ~50 % (Table 3).

Table 3: Absorbance at 280 nm and 614 nm for laccase before and after the cyanide addition, $A_{280/614}$ ratio changes after the treatment

sample	A (280 nm)	A (614 nm)	$A_{280/614}$
Before CN	3.31100	0.25951	12.75900
After CN (0.8ml)	2.87840	0.11957	24.07400

As explained in the Introduction to this chapter, there are several factors effecting the metal removal and metal replacement. Although the history of copper removal from laccase goes back more than three decades, a standard procedure which can be applied to laccases from different sources has not been established yet. Hauenstein and McMillin demonstrated an efficient dialysis method for copper removal in tree laccase²⁸. They also showed that the reconstitution was successful upon treatment with copper(I) under a nitrogen atmosphere. In contrast to tree laccase, fungal laccase does not release its copper very readily. For example, in the case of the enzyme from *Polyporus versicolor*, Hanna *et al.*²⁹ found that copper removal was incomplete following the reported procedure²⁸ even after 48 hours. They succeeded in removing the copper at a higher pH, but they failed to reconstitute the apoprotein. The apoprotein took up the copper(I) but neither the 610 nm absorbance, nor the EPR signal of T1 copper reappeared. The T1 copper site may not have such strong binding ability for Co(II) as that of simple blue copper proteins because of a delicate difference in local structure²². Alternatively, the low affinity for Co(II) binding may be a reflection of poor conformational flexibility within the protein²³.

Although the exchange procedure was not optimum, we reasoned that it could be possible to see an effect of copper removal and cobalt insertion by catalytic experiments.

3.2. Primary Alcohol Oxidations

The initial experiments were done using 4-methoxybenzyl alcohol as substrate which is a lignin type compound. The conditions were determined by following the previous protocols applied in our group³⁰. The effect of the amount of enzyme, using NHPI as mediator, was determined and these results were compared with replicates where crude laccase was the catalyst. In addition, other mediators have been tested in 4-methoxybenzyl alcohol oxidation, including substituted-NHPI derivatives. Finally, these optimized conditions were applied for the oxidation of secondary alcohols.

Effect of the amount of enzyme and time-dependence

For laccase catalyzed 4-methoxy benzylalcohol oxidations, NHPI as the mediator, conversions up to 60 % were reached in 4 hours. We compared the activity of crude laccase to

Co-treated laccase, in order to investigate the effect of substitution. The amount of enzyme required for the highest conversion is depicted in Figure 7.

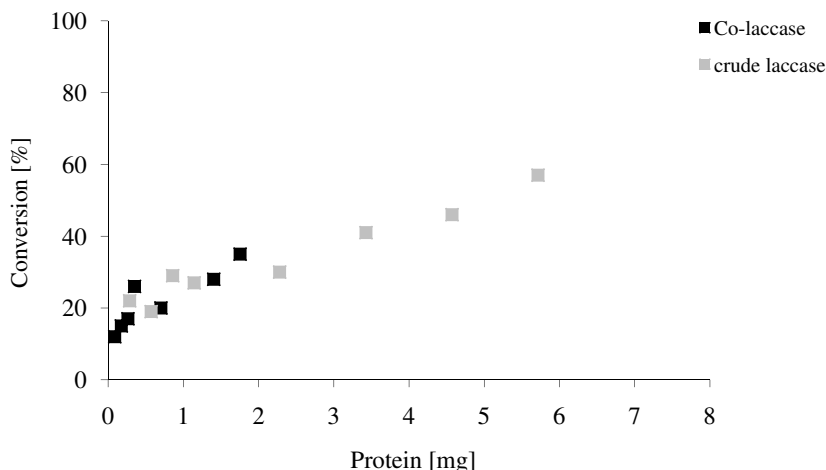


Figure 7: Influence of the amount of the enzyme on the oxidation of 4-methoxybenzyl alcohol

Conditions: 1.6 mmol 4-methoxybenzyl alcohol, 0.15 mmol NHPI, 30°C, 4 h

Obviously, increasing the amount of enzyme leads to higher substrate conversion. We observed a linear trend in the range that we scanned. Considering the low availability of Co-laccase, in further experiments 0.7 mg (40 U, 468 μ l) of the Co-treated enzyme was used. Duplicates with crude laccase gave comparable conversions. These results indicate that the Co-laccase is not more active per active gram of protein than the crude laccase (estimation based on purification factor). The time dependence of the 4-methoxybenzyl alcohol oxidation by Co-laccase (40 U, 0.7 mg) with NHPI as mediator was followed in time (Figure 8). As expected, a gradual increase of the conversion is observed: the reaction slows down after the first hour.

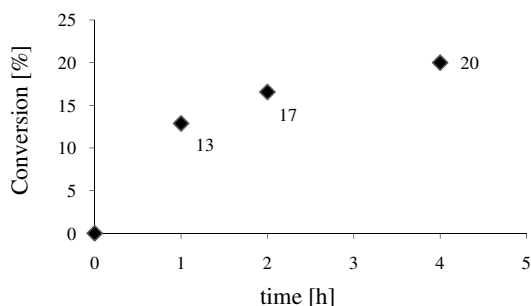


Figure 8: Time-dependence of the oxidation of 4-methoxybenzyl alcohol by Co-laccase

Conditions: 40 U Co-laccase, 1.6 mmol 4-methoxybenzyl alcohol, 0.15 mmol NHPI, 30°C, 4 h

Effect of different mediators

For Co-laccase catalysis, different mediators have been tested and compared. We envisaged that Co(II) in T1 site would be particularly active in oxidizing N-OH mediators by hydrogen abstraction. Thus it would be interesting to see if Co-laccase is more effective with N-OH type mediators such as NHPI, HBT and VLA compared to TEMPO, which is oxidized by electron transfer (Table 4).

Table 4: Effect of different mediators in the oxidation of 4-methoxybenzyl alcohol

Mediator	Conversion [%]	
	Co-Laccase	Crude laccase
NHPI	20	30
VLA	46	48
HBT	31	48
TEMPO	65	83

Conditions: 1.2 mg Co- or crude laccase, 1.6 mmol 4-methoxybenzyl alcohol, 30°C, 4 h

We observed that the activity difference in all the cases is rather small. From this set of data not a clear trend is observed. The hypothesis that Co-laccase is relatively more effective in activating N-OH mediators compared to TEMPO is not supported by the data. Strikingly, Co-laccase was equally effective as crude laccase in employing VLA as mediator.

Substituted-NHPI derivatives

It was demonstrated that the presence of substituents on the aromatic ring of NHPI, in particular electron donor groups, can affect the performances of NHPI as mediator in laccase oxidations³¹. Thus, three NHPI derivatives have been tested under the same reaction conditions, namely; 6-hydroxy-5H-pyrrolo[3,4-*b*]pyridine-5,7(6*H*)-dione, tetrachloro-NHPI, and methyl NHPI (Figure 9).

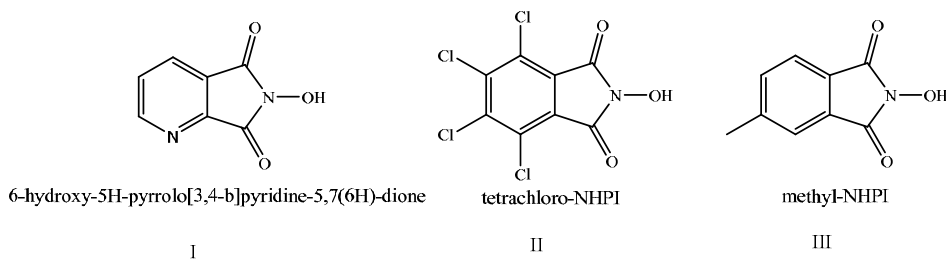


Figure 9: NHPI derivatives

Among these three NHPI derivatives, 6-hydroxy-5H-pyrrolo[3,4-*b*]pyridine-5,7(6*H*)-dione resulted in the highest conversion of 4-methoxy benzyl alcohol (Table 5). This could be explained by the electron poor character of the compound. In a recent study Annunziatini *et al.* showed that the electron donating substituents on the aryl group of NHPI increased the reactivity of this mediator and improved the yields of the oxidation products of non-phenolic lignin model compounds by laccase³². However, it is known from earlier literature that the efficiency of the mediator is not only dependent on the substitution, but also the substrate that will be oxidized³¹. For example Nolte reported that electron withdrawing substituents increased the rate and K/A ratio in the case of arylacetic ester oxidation with Co/NHPI

system²⁶. In our experiments, tetrachloro- and methyl- substituted NHPI gave comparable results, therefore it is not possible to make a substantial conclusion.

Table 5: Effect of different NHPI derivatives in the oxidation of 4-methoxybenzyl alcohol

	NHPI	I	II	III
Conversion [%]	20	41	21	23

Conditions: 40U Co-laccase, 1.6 mmol 4-methoxybenzyl alcohol, 30°C, 4 h

3.3. Oxidation of Secondary Alcohols

The oxidation of 4-methoxybenzyl alcohol, as primary alcohol is best performed with TEMPO. Secondary alcohols, however, are not very good substrates with TEMPO and laccase. This is probably due to the mechanism of alcohol oxidation, where binding of secondary alcohol to the oxoammonium is unfavorable due to the steric hindrance. A way to deal with this, is to introduce NHPI as mediator which operates via hydrogen abstraction. As known from the chemical Co/NHPI system, the conversion of primary and secondary alcohols takes place at comparable rates (see Figure 3).

For this purpose, 1-phenyl ethanol, cyclohexanol and 2-octanol was selected as substrates and oxidations were performed with 40 U (1.3 mg) and 60 U (1.9 mg) Co-laccase and TEMPO, NHPI, and VLA as mediator (Table 6).

Table 6: Influence of different mediators on the oxidation of secondary alcohols by Co-laccase

Mediator	1-Phenyl ethanol		Cyclohexanol	
	Conversion (%) (1.3 mg)	Conversion (%) (1.9 mg)	Conversion (%) (1.3 mg)	Conversion (%) (1.9 mg)
TEMPO	55	51	29	42
VLA	29	23	16	n.d.
NHPI	13	21	19	n.d.

Conditions: 1.6 mmol substrate, 0.15 mmol mediator, 30°C, 4 h

For 1-phenyl ethanol oxidation, in the case of TEMPO and VLA as the mediator, the conversion does not seem to be effected by the increase in the amount of enzyme. But when NHPI is used as mediator, although the overall conversion is less than the other two examples, the increase in the amount of enzyme, increases the conversion by a factor of two. For the oxidation of cyclohexanol, when we compare the influence of different mediators, TEMPO seems to be the most effective mediator and with more enzyme conversion is increasing. 2-octanol oxidation was carried out under the same reaction conditions with 40U (1.3 mg) of Co-laccase, but very little product was detected on the GC spectra. Therefore, no other experiments were performed with 2-octanol.

4. Conclusions and Future Work

Using both the dialysis procedure and the direct incubation approach, we could observe a decrease in the copper concentration (AAS results). However, according to the EPR spectrum, the T1 copper is still present and only a 40 % decrease was estimated. Therefore, despite the high concentration of cobalt detected in the enzyme sample, it is not possible to conclude that the Cu/ Co exchange was completed. The fact that cobalt is present in high concentrations in the enzyme sample can be due to the unspecific binding of the metal to the surface of the enzyme. This hypothesis could also explain why Co-laccase catalysis did not give the expected results in alcohol oxidation with NHPI as the mediator. In fact, most of the experiments show that the efficiency of Co-laccase is still lower than laccase.

TEMPO seemed to be the best mediator almost all experiments that we performed and NHPI did not give the expected good conversion. Although this could partly be due to the poor solubility of NHPI in water, it is more likely to be due to the partial presence of copper in T1 site. Another point to be taken into account for replacement is the similarity between ligand geometry for Cu(I) and Co(II). In laccase, the T1 Cu(I) site symmetry is believed to be trigonal planar, but it has been previously shown that Co(II) alters the native geometry to the least distortion from tetrahedral symmetry²¹. This could be the reason for the low activity of the Co enzyme after dialysis, which was shown to decrease the enzymatic activity by 50 %.

It is difficult to make a conclusion on whether or not the replacement took place based on our findings. More effort has to be devoted in order to demonstrate a reproducible procedure. For

the improvement of the dialysis stronger conditions could be applied. While doing so, one must bear in mind that the more severe the conditions, the more damage or even denaturation will be caused to the enzyme. It has been demonstrated that chelators, such as EDTA (ethylenediamine tetraacetic acid) or neocuproine can increase the rate of copper removal from the enzyme³³. The T1 copper is the most outer cluster of all three copper sites in laccase. It can be presumed that, a selective copper complexing compound, could take up only the T1 copper.

One other approach could be the completely demetallated enzyme²³. Cobalt can be inserted in the whole cluster, regenerating a fully substituted enzyme.

5. References

1. Solomon, E. I.; Sundaram, U. M.; Machonkin, T. E. *Chem. Rev.* 1996, 96, 2563-2605.
2. Gianfreda, L.; Xu, F.; Bollag, J. M. *Bioremed. J.* 1999, 3, 1-25.
3. d'Acunzo, F.; Baiocco, P.; Fabbrini, M.; Galli, C.; Gentili, P. *Eur. J. Org. Chem.* 2002, 4195-4201.
4. Galli, C.; Gentili, P. *J. Phys. Org. Chem.* 2004, 17, 973-977.
5. Barreca, A. M.; Sjogren, B.; Fabbrini, M.; Galli, C.; Gentili, P. *Biocatal. Biotransform.* 2004, 22, 105-112.
6. d'Acunzo, F.; Galli, C. *Eur. J. Biochem.* 2003, 270, 3634-3640.
7. Bourbonnais, R.; Paice, M. G. *FEBS Lett.* 1990, 267, 99-102.
8. Riva, S. *Trends Biotechnol.* 2006, 24, 219-226.
9. Baiocco, P.; Barreca, A. M.; Fabbrini, M.; Galli, C.; Gentili, P. *Org. Biomol. Chem.* 2003, 1, 191-197.
10. Xu, F.; Deussen, H. J. W.; Lopez, B.; Lam, L.; Li, K. C. *Eur. J. Biochem.* 2001, 268, 4169-4176.
11. Crestini, C.; Jurasek, L.; Argyropoulos, D. S. *Chem. Eur. J.* 2003, 9, 5371-5378.
12. Iwahama, T.; Yoshino, Y.; Keitoku, T.; Sakaguchi, S.; Ishii, Y. *J. Org. Chem.* 2000, 65, 6502-6507.

13. Ishii, Y.; Sakaguchi, S.; Iwahama, T. *Adv. Synth. Catal.* 2001, *343*, 393-427.
14. Baucherel, X.; Gonsalvi, L.; Arends, I.; Ellwood, S.; Sheldon, R. A. *Adv. Synth. Catal.* 2004, *346*, 286-296.
15. In *CRC Handbook of Chemistry and Physics, 89th Ed (Internet version 2009)*; Lide, D. R. Ed.; CRC Press/Taylor and Francis, Boca Raton, FL, 2009.
16. McMillin, D. R.; Eggleston, M. K. In *Multicopper oxidases*; Messerschmidt, A. Ed.; World Scientific: Singapore, 1997; pp. 129-166.
17. Shepard, W. E. B.; Kingston, R. L.; Anderson, B. F.; Baker, E. N. *Acta Crystallogr. D* 1993, *49*, 331-343.
18. Garrett, T. P. J.; Clingeffer, D. J.; Guss, J. M.; Rogers, S. J.; Freeman, H. C. *J. Biol. Chem.* 1984, *259*, 2822-2825.
19. Church, W. B.; Guss, J. M.; Potter, J. J.; Freeman, H. C. *J. Biol. Chem.* 1986, *261*, 234-237.
20. McMillin, D. R.; Holwerda, R. A.; Gray, H. B., 1974; pp. 1339-1341.
21. Larrabee, J. A.; Spiro, T. G. *Biochem. Biophys. Res. Commun.* 1979, *88*, 753-760.
22. Sakurai, T.; Suzuki, S.; Fujita, M. *Inorg. Chim. Acta-Bioinor.* 1988, *152*, 139-143.
23. Li, J. B.; McMillin, D. R. *Inorg. Chim. Acta* 1990, *167*, 119-122.
24. Vitry, C.; Bedat, J.; Prigent, J.; Levacher, V.; Dupas, G.; Salliot, I.; Queguiner, G.; Bourguignon, J. *Tetrahedron* 2001, *57*, 9101-9108.
25. Li, J. *Acta Crystallogr. E* 2007, *63*, o3333.
26. Wentzel, B. B.; Donners, M. P. J.; Alsters, P. L.; Feiters, M. C.; Nolte, R. J. M. *Tetrahedron* 2000, *56*, 7797-7803.
27. Brenner, A. J.; Harris, E. D. *Anal. Biochem.* 1995, *226*, 80-84.
28. Hauenstein, B. L.; McMillin, D. R. *Biochem. Biophys. Res. Commun.* 1978, *85*, 505-510.
29. Hanna, P. M.; McMillin, D. R.; Pasenkiewicz-gierula, M.; Antholine, W. E.; Reinhammar, B. *Biochem. J.* 1988, *253*, 561-568.
30. Matijosyte, I., PhD Thesis, Delft University of Technology, 2008.

31. Gorgy, K.; Lepretre, J. C.; Saint-Aman, E.; Einhorn, C.; Einhorn, J.; Marcadal, C.; Pierre, J. L. *Electrochim. Acta* 1998, 44, 385-393.
32. Annunziatini, C.; Baiocco, P.; Gerini, M. F.; Lanzaunga, O.; Sjogren, B. *J. Mol. Catal. B-Enzym.* 2005, 32, 89-96.
33. Eggleston, M. K.; Pecoraro, C.; McMillin, D. R. *Arch. Biochem. Biophys.* 1995, 320, 276-279.

Ferritin Cage as a Carrier for Palladium Nanoparticles

1. Introduction
2. Results
 - 2.1. Catalyst Preparation
 - 2.2. Characterization
 - 2.3. Catalytic Activity
3. Discussion
4. Materials and Methods
5. References

1. Introduction

Proteins are considered as attractive building components for the construction of self-assembled cage structures¹⁻⁴. Cavities formed by proteins can be utilized as the reaction chamber and protein shells can serve as a template. They are monodispersed and easily form a close-packed structure with remarkable homogeneity. Ferritins are such a family of proteins found in all domains of life, which function primarily to store and sequester iron. These proteins are composed of 24 subunits that self-assemble to form a cage of 12 nm diameter in which hydrated ferric oxide (or phosphate) is formed⁵⁻⁷ (Figure 1).



Figure 1: Ferritin subunits and cross-section

There are pores in ferritin, forming so-called channels at the junctions of threefold and fourfold subunits which control the access of molecules to the 8 nm inner cavity (Figure 2). The threefold channels are proposed to be involved in iron entry into the protein core⁸. The pores are almost closed in native proteins when examined in crystals. Nevertheless, molecules larger than the pore size in the protein crystals reach the protein cavity in solution, which suggests that the pores are flexible or can “open”⁷. In our laboratories we recently

characterized and crystallized the native ferritin from *Pyrococcus furiosus*^{9,10}. This ferritin shows high resemblance to the well known horse spleen ferritin¹¹. *P. furiosus* ferritin is stable up to 100°C which offers significant advantages for its purification and application.

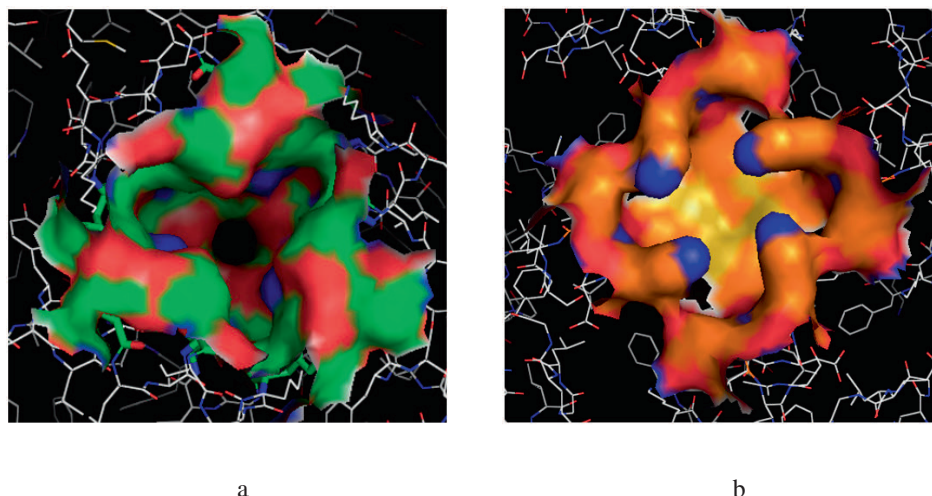
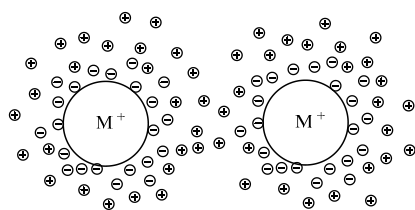


Figure 2: The funnel like structure of *Pyrococcus furiosus* ferritin a) 3-fold channel viewed from outside and b) 4-fold channel of viewed from the inside. Pictures were prepared with PyMol program

The use of ferritin as a nanometer sized bioreactor for producing monodisperse metal particles from metal ions has been studied with great interest over the years. It is known that ferritin can form cores of other metals than Fe, as well as metallic nanoparticles such as Pd¹², Ag¹³ and CoPt¹⁴. Nanoparticles are defined as having 1-50 nm diameters, a size range in which metals can exhibit size-dependent properties. The smaller the cluster of atoms, the higher the percentage of atoms present on the surface, rendering nanoparticles highly promising for catalysis¹⁵. The transition from microparticles to nanoparticles can lead to a number of changes in physical properties that effect both the properties of the isolated particle and its interaction with other materials¹⁶. Smaller nanoparticles having tens of atoms should be more like conventional molecules with defined orbital levels, while the states of larger nanoparticles with thousands of atoms should be better described as bands. Unfortunately, these metallic nanoparticles are unstable with respect to agglomeration to the bulk. In most cases, this aggregation leads to the loss of the properties associated with the colloidal state of

these metallic particles. Thus stabilization of metallic nanoparticles is a crucial aspect to consider during their synthesis¹⁷. Stabilization is usually maintained by two general procedures: (a) charge stabilization and (b) steric stabilization. The electrostatic stabilization is based upon the double electric layer formed when ions of the same sign are adsorbed at the nanoparticle surface. Ionic compounds such as halides, carboxylates, or polyoxoanions, dissolved in (generally aqueous) solution are used to attain the electrostatic stabilization. Steric stabilization is achieved by employing macromolecules such as polymers, cyclodextrins or dendrimers that are sterically bulky. These molecules are adsorbed on the metal surface, thereby providing a steric barrier and increasing the interparticle distance (Figure 3). Stabilization of nanoparticles by protein cages serves as a combined approach of the two methods.

a)



b)

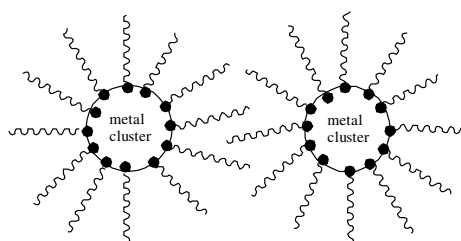


Figure 3: Schematic representation of nanocluster stabilization a) electrostatic b) steric

In the past few decades an extensive study has been devoted to the development of more efficient and selective palladium catalyst systems for oxidation reactions¹⁸⁻²³. A novel, water soluble Pd-catalyst was designed in our labs in the beginning of the present decade. Palladium-bathophenanthroline reached high turnover frequencies in aerobic oxidations in water with a wide range of substrates²⁴. Among the applications of palladium, nanoclusters are emerging as key players²⁵⁻²⁹. The pioneering work of Moiseev *et al.* on giant palladium nanoclusters is the first example of isolable nanoclusters that did catalysis while dispersed in solution^{30,31}. The current interest in nano-sized materials has given a strong impulse to the

development of such materials. Size and shape controlled metal nanoparticles are expected to exhibit superior catalytic performance over randomly sized and shaped materials.

We were inspired by the concept of generating a nanocatalyst in a protein cage which offers the unique opportunity of bringing reactant components together in a well defined chiral environment. Controlled entrance and departure of small molecules combined with the enclosure and the stabilization of the metal-based particles may lead to the concept of nanoreactor. Our interest lies in the use of palladium nanoparticles as catalysts, in particular for alcohol oxidation. Within the area of selective oxidation there still is a need for selective and stable catalysts that can operate in water³²⁻³⁴. In a recent publication Ueno *et al.*¹² described selective olefin hydrogenation by palladium nanoclusters in apoferritin cage. This indicates that the nanocompartments within ferritin have the unique possibility to induce selectivity. We wanted to extend this concept to much more demanding oxidative conditions at high temperatures. By introduction of Pd atoms inside the ferritin cavity, it is possible to prepare an artificial oxidase, which utilizes molecular oxygen as the terminal oxidant. If such a catalyst can successfully perform selective alcohol oxidations, it could offer the possibility of tuning the catalytic properties by changing the parameters in metal loading.

The work in this chapter deals with the preparation of a novel, stable and recyclable palladium catalyst using apoferritin from *Pyrococcus furiosus* as a template for the clusters. Results of the application of this catalyst in the oxidation of alcohols will also be presented.

2. Results

2.1. Catalyst Preparation

Ferritin was produced and purified as described earlier⁹. The composites were generated by mixing a solution of apoferritin at pH 8 with a 250 fold excess of palladium (as K_2PdCl_4), followed by size exclusion chromatography in order to ensure the removal of any non-incorporated palladium atoms. Consequently palladium was reduced by bubbling H_2 into the solution (Figure 4). In this way up to 200 Pd per cage could be bound.

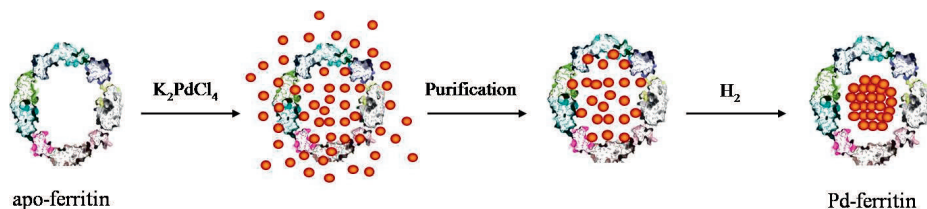


Figure 4: Preparation of the Pd nanoclusters in apoferritin cavity

2.2. Characterization

The selective synthesis of Pd nanoparticles within the *Pyrococcus furiosus* protein cage architecture is supported by multiple lines of evidence. In the presence of purified ferritin, a coffee colored solution formed with no visible precipitation, whereas in protein-free control reactions there was immediate formation of the bulk precipitate. The exact number of incorporated Pd in each batch of catalyst was determined by Inductively Coupled Plasma-Optical Emission Spectrometry (ICP-OES).

Transmission Electron Microscopy (TEM)

Transmission Electron Microscopy (TEM) is a microscopy technique whereby a beam of electrons is transmitted through a specimen. Depending on the density of the material present, some of the electrons are scattered and disappear from the beam. At the bottom of the microscope the unscattered electrons hit a fluorescent screen, which gives rise to a "shadow image" of the specimen with its different parts displayed in varied darkness according to their density. TEMs are capable of imaging at a significantly higher resolution than light microscopes, owing to the small de Broglie wavelength of electrons. This enables the instrument to be able to examine fine detail. Metal atoms scatter the electrons better than carbon atoms, therefore, they improve the contrast of the image.

The TEM images of the freshly prepared catalyst samples revealed homogeneously distributed palladium particles of ~5nm (Figure 5). Staining with uranium slightly improved the protein imaging.

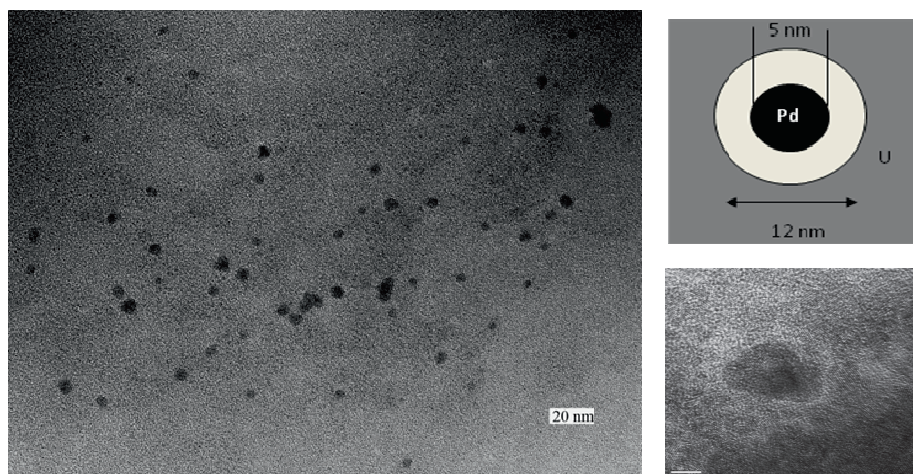


Figure 5: TEM image of Pd nanoparticles in apoferritin

Dynamic Light Scattering (DLS)

Dynamic Light Scattering, also known as Quasi Elastic Light Scattering (Quels) and Photon Correlation Spectroscopy (PCS), measures the laser light that is scattered from dissolved macromolecules or suspended particles. Due to the Brownian motion of the molecules and particles in solution, fluctuations of the scattering intensity can be observed. The diameter that is measured in Dynamic Light Scattering is called the *hydrodynamic diameter* and refers to how a particle diffuses within a fluid. The diameter obtained by this technique is that of a sphere that has the same translational diffusion coefficient as the particle being measured. The translational diffusion coefficient will depend not only on the size of the particle “core”, but also on any surface structure, as well as the concentration and type of ions in the medium. This means that the size can be larger than measured by electron microscopy, for example, where the particle is removed from its native environment.

The apparent size of the apo-protein from *Pyrococcus furiosus* and the nanocomposite Pd-ferritin containing 100 Pd per 24mer is depicted in Figure 6. The average size of the apoferritin did not change dramatically upon loading with palladium, although in general the size measured with DLS was slightly larger than the size measured with TEM.

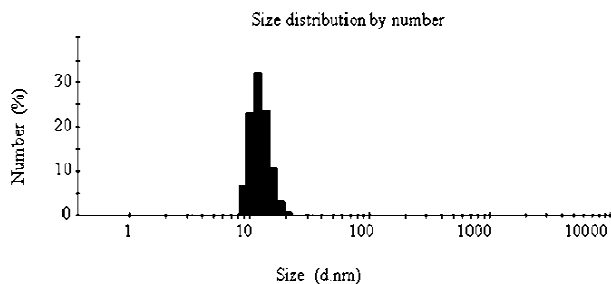


Figure 6: Particle size distribution of Pd-ferritin

Zeta Potential

Most particles dispersed in an aqueous system acquire a surface charge, principally either by ionization of surface groups, or adsorption of charged species. These surface charges modify the distribution of the surrounding ions, resulting in a layer around the particle that is different from the bulk solution. If the particle moves, under Brownian motion for example, this layer moves as part of the particle. The zeta potential is the potential at the point in this layer where it moves past the bulk solution. This is usually called the slipping plane. The charge at this plane will be very sensitive to the concentration and type of ions in solution. Zeta potential is one of the main forces that mediate interparticle interactions. Particles with a high zeta potential of the same charge sign, either positive or negative, will repel each other. Conventionally a high zeta potential can be high in a positive or negative sense, i.e. $< -30\text{mV}$ and $> +30\text{mV}$ would both be considered as high zeta potentials.

The zeta potential of the prepared catalyst was measured to be -31 mV , which is an indication of a good stability of nanoparticles.

X-Ray Photoelectron Spectroscopy (XPS)

X-Ray Photoelectron Spectroscopy (XPS) utilizes photo-ionization and energy-dispersive analysis of the emitted photoelectrons to study the composition and electronic state of the surface region of a sample. The kinetic energy distribution of the emitted photoelectrons can be measured using an electron energy analyser and a photoelectron spectrum can thus be

recorded. For each element, there is a characteristic binding energy associated with each core atomic orbital, i.e. each element will give rise to a characteristic set of peaks in the photoelectron spectrum at kinetic energies determined by the photon energy and the respective binding energies. The presence of peaks at particular energies therefore indicates the presence of a specific element in the sample under study; furthermore, the intensity of the peaks is related to the concentration of the element within the sampled region.

We performed XPS measurements of the prepared Pd-catalyst. The Pd 3d-peaks were measured for several Pd-Ferritin samples and the peaks were positioned at 335.0 and 335.1 eV, which is in agreement with the palladium metal binding energy reported in NIST XPS database³⁵.

2.3. Catalytic Activity

Reaction Conditions

In order to evaluate the activity of the catalyst in aerobic oxidation reactions, we performed a set of experiments, where we used 4-methoxybenzyl alcohol as a model substrate. Initially, the effect of temperature on the oxidation rate and catalyst stability was investigated.

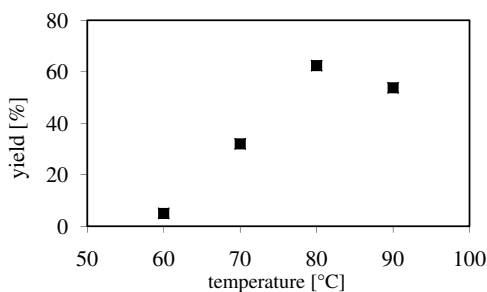


Figure 7: Oxidation of 4-methoxy benzylalcohol at different temperatures

Conditions: 50 mM substrate concentration, cat/ subs ratio; 0.48 %, final reaction volume 2 ml, 15 h, 30 bar, 8 % O₂/N₂ mixture gas, stirring at 800 rpm

At ambient temperature and below 60°C, the oxidation rate was very slow while, on the other hand, at temperatures above 80°C we observed a slight decrease in the rate (Figure 7). Therefore we performed oxidations at 80°C, unless stated otherwise.

Course of Reaction

Interestingly, during the oxidation of 4-methoxy benzyl alcohol, we observed a biphasic reaction course; after a fast initial rate, the course of the reaction levelled off (Figure 8). However, we could reach complete conversions in longer reaction times.

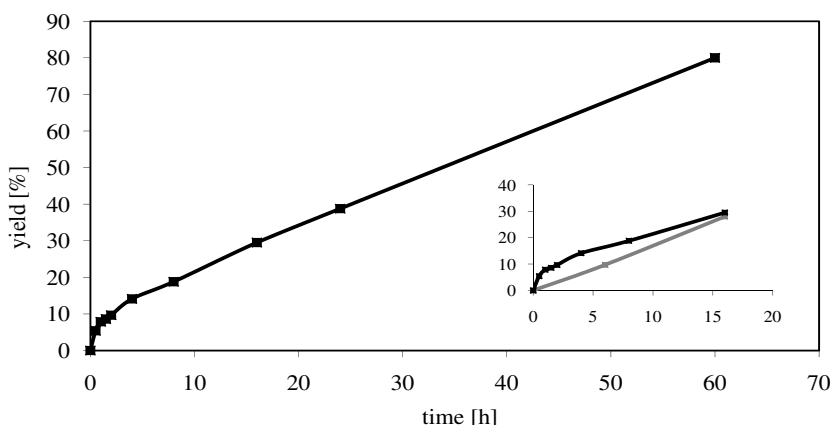


Figure 8: Oxidation of 4-methoxy benzylalcohol in time

Conditions: 40 mM substrate concentration, cat/ subs ratio; 0.28 %, final reaction volume 2 ml, 30 bar, 8 % O₂/N₂ mixture gas, stirring at 800 rpm. Insert: Oxidation of 4-methoxy benzylalcohol in time with and without a second aldehyde (black squares: oxidation under standard conditions, gray squares: oxidation in the presence of benzaldehyde).

Although the mechanism is not clear we attributed this decrease in rate to the competition between the substrate and the product towards the catalyst. In order to demonstrate this phenomenon we compared the oxidation of 4-methoxybenzyl alcohol under standard

conditions, to the reactions where we used a second aldehyde (benzaldehyde, in equal concentrations to the alcohol) present in the reaction mixture when the reaction started. It is clear that the initial rates of these two conditions are different from each other; in fact the reaction slows down more than 4 times when there is aldehyde in the reaction mixture.

Catalyst Recycling

We were able to collect the catalyst after the reaction, wash it several times with diethyl ether and reuse it in a consequent oxidation reaction (Table 1).

Table 1: Oxidation of 4-methoxy benzylalcohol with recycled catalyst

Cycle	Yield [%]
1	74
2	73
3	40

Reaction conditions: 0.8 mmol 4-methoxybenzyl alcohol, cat/ subs ratio; 1.09 % , 2 hours, 30 bar 8 % O₂/N₂ gas mixture, 80°C, stirring 800 rpm.

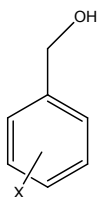
The first cycle was successful although after the second round of catalyst recycle we observed a decrease in conversion. The reasons for the lower turnovers after the second cycle are not completely clear, but it is perhaps due to the protein instability under the conditions used for recovery. It is known that the Pd nanoparticles tend to agglomerate in the presence of organic solvent.

Substituent Effects on the Oxidation Rate

In order to gain insight into the reaction mechanism we investigated the effect of substituents in the phenyl ring in the oxidation of substituted benzyl alcohols. A selection of *meta*- and *para*- substituted benzyl alcohols were oxidized and conversions were calculated at single time point (15 h). From the results of these oxidations, it was clear that electron donating groups had a significant effect on the oxidation rate. By constructing a Hammett plot from these results we could derive a ρ -value from the Hammett equation:

$$\log (k_X/k_H) = \rho^*\sigma_X$$

where the ρ -value is a measure of the influence of substituent groups on the rate constant (or equilibrium constant) of a particular organic reaction involving a family of related substrates. σ_X is a constant characteristic of the electronic properties of substituent X and of its position in the reactant molecule.



The substituents investigated ranged from the highly electron-withdrawing trifluoromethyl group ($\sigma_p = 0.54$) to the electron-donating methoxy group ($\sigma_p = -0.27$). A linear free energy relationship could be observed with a calculated ρ -value of -1.65 (Figure 9).

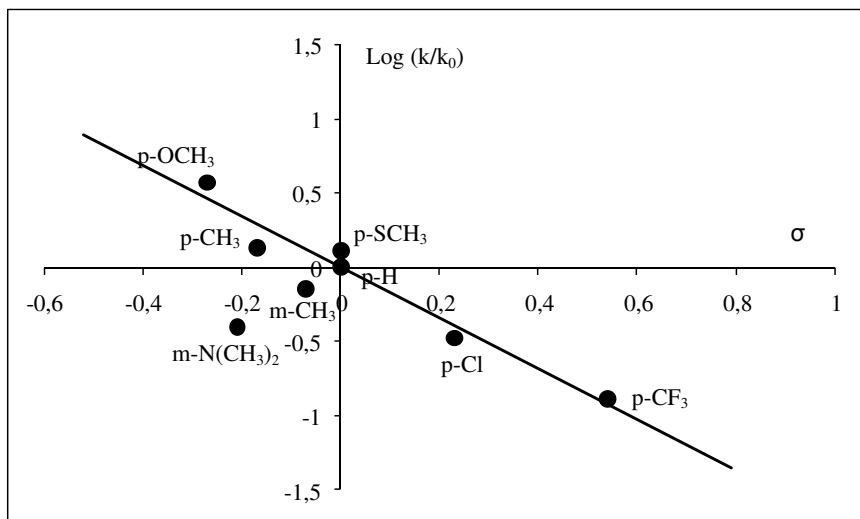


Figure 9: Hammett-plot for the substituent effects on the oxidation of benzylalcohol derivatives

The reactions were performed in the presence of 20 % v/v DMSO in order to obtain homogeneous solutions. Separate experiments were performed to evaluate how such high DMSO concentrations effected the reaction rate. In fact, in the absence of DMSO, the reaction rates turned out to be faster (almost 10 times).

Oxidation of Other Alcohols

In order to further evaluate the substrate scope of our catalyst, a range of primary and secondary, benzylic, aliphatic and allylic alcohols were selected. The oxidation of these alcohols under similar conditions to that of 4-methoxy benzylalcohol was studied.

Table 2: Oxidation of alcohols

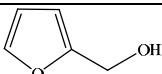
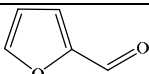
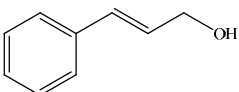
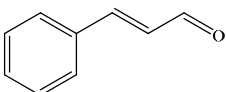
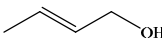
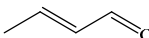
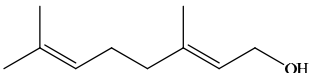
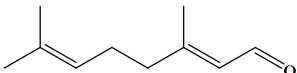
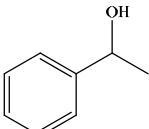
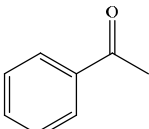
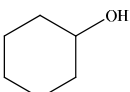
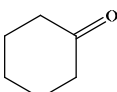
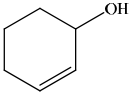
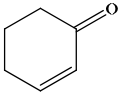
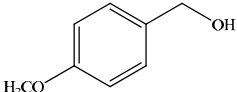
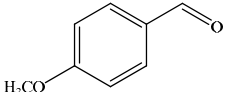
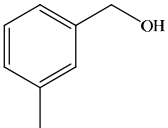
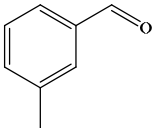
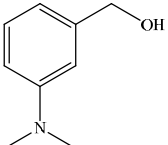
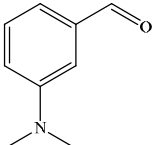
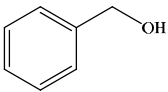
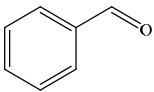
Substrate	Product	TON
		12
		197
		36
		-
		3
		3

Table 2 continued from page 79

Substrate	Product	TON
		101 ^[a]
		138 ^[a]
		48 ^[a]
		19 ^[a]
		37 ^[a]

Conditions: 40 mM substrate concentration, cat/ subs ratio; 0.34 %, selectivity 100 %, final reaction volume 2 ml, 24 h, 30 bar, 8 % O₂/N₂ mixture gas, stirring at 800 rpm. [a] cat/ subs ratio; 0.44 %; TON calculated as mmol product produced/mmol Pd present in the reaction

In general, the highest activity is found for activated alcohols, such as cinnamyl alcohol, allylic alcohols, and benzylalcohols. Aliphatic alcohols gave very low activity as shown for cyclohexanol (TON of 3) and 1-hexanol (no activity, not shown in the table). Secondary benzylic alcohols are hardly oxidized (see for 1-phenylethanol), but 3-cyclohexenol on the other hand gave very high activity. Another striking result is the observation that geraniol is not oxidized while 2-butenol, another allylic alcohol, is oxidized with a TON of 36. We attribute this to the presence of the additional double bond in geraniol.

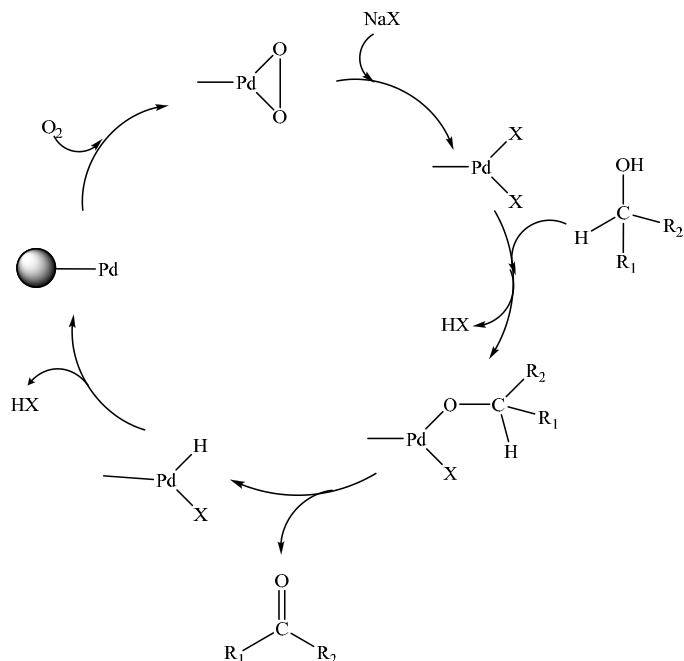
3. Discussion

A novel hybrid oxidation catalyst has been prepared by using the apoferritin cage as a template for the formation of palladium nanoclusters. The nanoparticles had a diameter of ~5 nm and a narrow size distribution and are homogeneously dispersed in the solution. In some cases we observed formation of larger particles, although we applied the same concentrations of palladium and protein. It is known from the literature that the reduction step plays a crucial role in the nanoparticle synthesis³⁶. Employing strong reducing agents may result in formation of smaller particles. This outcome can be controlled by the selection of reducing agent and varying the reduction time. The activity of the nanoclusters, in some cases, is dependent on the particle size. It is known that the catalysts with smaller mean size of Pd clusters show higher activities per surface Pd atom³⁷.

The palladium-ferritin nanoparticles were successfully used in the catalytic aerobic oxidation of alcohols. Although, a competition between the alcohol and the product has been observed, no catalyst inhibition was detected. It was possible to recycle Pd-ferritin and re-use in a subsequent reaction without loss in the activity, at least two times. The reduced reactivity after two cycles was attributed to the agglomeration of the particles due to the instability of protein against organic solvents and to physical effects, like centrifugation.

Results of oxidations of substituted benzyl alcohols and other alcohols showed that electronic effects have a large influence on the reaction rate. Even though we do not have sufficient data to claim a certain reaction pathway, the general observations on the substrate effects suggest that a β -hydride elimination taking place. The negative ρ -value signifies a positive charge build up in the transition state, implying (rate-limiting) β -hydride elimination.

The reaction between Pd(0) and dioxygen generates a peroxo-Pd(II) species which subsequently reacts with two equivalents of a Brønsted acid to generate hydrogen peroxide. Association of the alcohol to the resulting Pd(II) species followed by β -hydride elimination regenerates the Pd(0) and oxidizes the alcohol to the corresponding aldehyde or ketone^{24,38,39}.



4. Materials and Methods

All the chemicals and reagents used were of the highest purity available.

Ferritin and apoferritin production was carried out according to the previously described procedures^{9,40}. 0.5-2.5 mg apoferritin is dispersed in a buffer solution of pH 8 (100 mM EPPS, containing 10 mM NaCl) and heated up to 60°C. Then aliquots of K_2PdCl_4 stock solution (40 mM) added and incubated for 30 minutes, after which the unbound palladium was removed by size exclusion chromatography. Subsequently the palladium was reduced by bubbling H_2 in the solution (Figure 4).

TEM measurements were performed by V.C.L. Butselaar from DCT/NCHREM in Delft University of Technology using a FEI TECNAI TF20 monochromator electron microscope with a FEG as source of electrons, operated at 200 kV and a Philips CM30T electron microscope with a LaB6 filament as the source of electrons, operated at 300 kV. Samples were mounted on Quantifoil® microgrid carbon polymer supported on a copper grid by

placing a few droplets of a suspension of ground sample in water, followed by drying at ambient conditions.

DLS and ZP were measured in Zetasizer Nano ZS (Malvern Instruments) in disposable PMMO cuvettes with 1 ml sample solutions, diluted accordingly.

XPS analysis were carried out in a Quantera SXMTM from Ulvac-PHI (Q1) using monochromatic AlK α -radiation in High Power mode. The samples were stored at 4°C prior to the measurements.

Oxidation of 4-methoxybenzyl alcohol

Oxidation reactions were performed under O₂ pressure (O₂/N₂ 8 % mixture gas, 30 bars) at 80°C, by stirring at 800 rpm for a time range of 1-24 hours in a polyblock reaction platform (Hastelloy C steel mini autoclaves, 16 ml capacity, manufactured by Hel Group). After the given reaction time the reactor was cooled to 20°C and depressurized. The reaction mixtures were extracted with diethyl ether containing the internal standard and results were analyzed by GC (Varian Star 3400Cx equipped with CP wax 52CB column).

Oxidation of benzyl alcohol derivatives (Hammett Plot)

Oxidation reactions were performed under O₂ pressure (O₂/N₂ 8 % mixture gas, 30 bars) at 80°C, by stirring at 800 rpm for 15 hours in a polyblock reaction platform (Hastelloy C steel mini autoclaves, 16 ml capacity, manufactured by Hel Group). The stock solutions for each alcohol were prepared in DMSO, and final substrate concentrations inside the reactor adjusted to 40 mM with water.

Oxidation of other alcohols

The oxidation conditions were the same as 4-methoxybenzyl alcohol oxidations. The stock solutions for geraniol and cinnamyl alcohol were prepared in DMSO, and final substrate concentrations inside the reactor adjusted to 40 mM with water; cat/substrate ratio: 0.34 %.

The products were confirmed with GC/MS and the results were analyzed by GC (Varian Star 3400Cx equipped with CP wax 52CB column).

5. References

1. Douglas, T.; Dickson, D. P. E.; Betteridge, S.; Charnock, J.; Garner, D. C.; Mann, S. *Science* **1995**, 54-57.
2. Aime, S.; Frullano, L.; Crich, S. G. *Angew. Chem. Int. Edit.* **2002**, 41, 1017-1019.
3. Wang, Q.; Lin, T. W.; Tang, L.; Johnson, J. E.; Finn, M. G. *Angew. Chem. Int. Edit.* **2002**, 41, 459-462.
4. Ishii, D.; Kinbara, K.; Ishida, Y.; Ishii, N.; Okochi, M.; Yohda, M.; Aida, T. *Nature* **2003**, 423, 628-632.
5. Lawson, D. M.; Artymiuk, P. J.; Yewdall, S. J.; Smith, J. M. A.; Livingstone, J. C.; Treffry, A.; Luzzago, A.; Levi, S.; Arosio, P.; Cesareni, G.; Thomas, C. D.; Shaw, W. V.; Harrison, P. M. *Nature* **1991**, 349, 541-544.
6. Harrison, P. M.; Arosio, P. *Biochim. Biophys. Acta-Bioenerg.* **1996**, 1275, 161-203.
7. Chasteen, N. D.; Harrison, P. M. *J. Struct. Biol.* **1999**, 126, 182-194.
8. Cutler, C.; Bravo, A.; Ray, A. D.; Watt, R. K. *J. Inorg. Biochem.* **2005**, 99, 2270-2275.
9. Tatur, J.; Hagedoorn, P. L.; Overeijnder, M. L.; Hagen, W. R. *Extremophiles* **2006**, 10, 139-148.
10. Tatur, J.; Hagen, W. R.; Matias, P. M. *J. Biol. Inorg. Chem.* **2007**, 12, 615-630.
11. Carrondo, M. A. *EMBO J.* **2003**, 22, 1959-1968.
12. Ueno, T.; Suzuki, M.; Goto, T.; Matsumoto, T.; Nagayama, K.; Watanabe, Y. *Angew. Chem. Int. Edit.* **2004**, 43, 2527-2530.
13. Kramer, R. M.; Li, C.; Carter, D. C.; Stone, M. O.; Naik, R. R. *J. Am. Chem. Soc.* **2004**, 126, 13282-13286.
14. Warne, B.; Kasyutich, O. I.; Mayes, E. L.; Wiggins, J. A. L.; Wong, K. K. W. "Self assembled nanoparticulate Co : Pt for data storage applications"; International Magnetism Conference (INTERMAG 2000), 2000, Toronto, Canada.

15. Moreno-Manas, M.; Pleixats, R. *Acc. Chem. Res.* **2003**, *36*, 638-643.
16. Weller, H. *Angew. Chem. Int. Edit.* **1996**, *35*, 1079-1081.
17. Aiken, J. D.; Finke, R. G. *J. Mol. Catal. A-Chem.* **1999**, *145*, 1-44.
18. Blackburn, T. F.; Schwartz, J. J. *Chem. Soc.-Chem. Commun.* **1977**, 157-158.
19. Peterson, K. P.; Larock, R. C. *J. Org. Chem.* **1998**, *63*, 3185-3189.
20. Nishimura, T.; Kakiuchi, N.; Inoue, M.; Uemura, S. *Chem. Commun.* **2000**, 1245-1246.
21. Stahl, S. S.; Thorman, J. L.; Nelson, R. C.; Kozee, M. A. *J. Am. Chem. Soc.* **2001**, *123*, 7188-7189.
22. Steinhoff, B. A.; Fix, S. R.; Stahl, S. S. *J. Am. Chem. Soc.* **2002**, *124*, 766-767.
23. Arends, I. W. C. E.; ten Brink, G.-J.; Sheldon, R. A. *J. Mol. Catal. A-Chem.* **2006**, *251*, 246-254.
24. ten Brink, G.-J.; Arends, I. W. C. E.; Sheldon, R. A. *Science* **2000**, *287*, 1636-1639.
25. Kaneda, K.; Fujii, M.; Morioka, K. *J. Org. Chem.* **1996**, *61*, 4502-4503.
26. Uozumi, Y.; Nakao, R. *Angew. Chem. Int. Edit.* **2003**, *42*, 194-197.
27. Mori, K.; Hara, T.; Miguzaki, T.; Ebitani, K.; Kaneda, K. *J. Am. Chem. Soc.* **2004**, *126*, 10657-10666.
28. Biffis, A.; Minati, L. *J. Catal.* **2005**, *236*, 405-409.
29. Hou, Z. S.; Theyssen, N.; Leitner, W. *Green Chem.* **2007**, *9*, 127-132.
30. Vargaftik, M. N.; Zagorodnikov, V. P.; Stolyarov, I. P.; Moiseev, I. I.; Likholobov, V. A.; Kochubey, D. I.; Chuvilin, A. L.; Zaikovski, V. I.; Zamaraev, K. I.; Timofeeva, G. I. *J. Chem. Soc.-Chem. Commun.* **1985**, *14*, 937-939.
31. Vargaftik, M. N.; Zagorodnikov, V. P.; Stolyarov, I. P.; Moiseev, I. I.; Kochubey, D. I.; Likholobov, V. A.; Chuvilin, A. L.; Zamaraev, K. I. *J. Mol. Catal.* **1989**, *53*, 315-348.
32. Muzart, J. *Tetrahedron* **2003**, *59*, 5789-5816.
33. Arends, I. W. C. E.; Sheldon, R. A. In *Modern Oxidation Methods*; Backvall, J. E. Ed.; Wiley-VCH, 2004; pp. 83-118.
34. Stahl, S. S. *Science* **2005**, *309*, 1824-1826.

35. NIST X-ray Photoelectron Spectroscopy Database, Gaithersburg, 2003;
<http://srdata.nist.gov/xps/>
36. Watzky, M. A.; Finney, E. E.; Finke, R. G. *J. Am. Chem. Soc.* **2008**, *130*, 11959-11969.
37. Li, F.; Zhang, Q. H.; Wang, Y. *Appl. Catal. A-Gen.* **2008**, *334*, 217-226.
38. Mueller, J. A.; Goller, C. P.; Sigman, M. S. *J. Am. Chem. Soc.* **2004**, *126*, 9724-9734.
39. Stahl, S. S. *Angew. Chem. Int. Edit.* **2004**, *43*, 3400-3420.
40. Matias, P. M.; Tatur, J.; Carrondo, M. A.; Hagen, W. R. *Acta Crystallogr. F* **2005**, *61*, 503-506.

Nano γ -Fe₂O₃ in Ferritin Cage

5

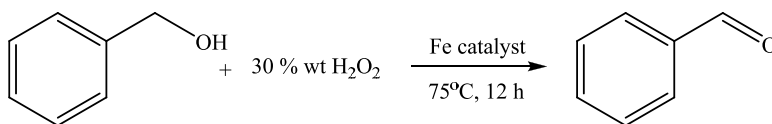
1. Introduction
2. Results and Discussion
 - 2.1. Nano γ -Fe₂O₃ in Alcohol Oxidation
 - 2.2. *H. spleen* Ferritin as Catalyst & Nano γ -Fe₂O₃ Inside *H. spleen* Apoferritin
 - 2.3. *P. furiosus* Ferritin as Catalyst & Nano γ -Fe₂O₃ Inside *P. furiosus* Apoferritin
3. Conclusion and Future Work
4. Materials and Methods
 - 4.1. Synthesis of γ -Fe₂O₃
 - 4.2. Preparation of γ -Fe₂O₃ Core in Apoferritin
 - 4.3. Benzyl Alcohol Oxidations, Typical Procedure
5. References

1. Introduction

The reactivity and selectivity of an active catalyst are controlled by the choice of metal and by the design of surrounding ligands. In comparison with other transition metals extensively used, such as palladium, platinum, rhodium and gold, iron-based catalysts are inexpensive, environmentally benign, and relatively non toxic¹. Various iron salts and iron complexes are commercially available on a large scale or readily accessible by synthesis. In the field of oxidation catalysis with iron, notable progress has been accomplished in recent years and novel iron containing systems have been developed for alcohol oxidation²⁻⁶.

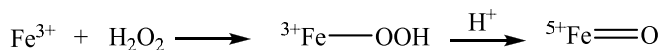
Among all iron compounds, iron oxides have often been considered to be catalytically inactive under mild reaction conditions. Iron oxides exist in a bewildering variety of polymorphs. Anhydrous ferric oxides include hematite (α -Fe₂O₃), maghemite (γ -Fe₂O₃), and the less common ϵ - and β -Fe₂O₃. Fe₃O₄ (magnetite) and Fe_{1-x}O (wüstite) contain both ferric and ferrous iron. The oxyhydroxides, nominally FeOOH, including goethite, lepidocrocite, akaganeite, and several other polymorphs, often contain excess water. More hydrated forms such as ferrihydrite, nominally Fe(OH)₃, even have a more variable water content.

Because of its two stable oxidation states that are easily interchangeable, iron can take part in redox reactions covering a wide range of potentials. However, its use in the laboratory is limited due to non-selective radical side-reactions. Although Fenton and Gif-type reactions have extensively been studied, until today, after more than a century from the first report of the so-called Fenton chemistry, the exact mechanism awaits to be resolved⁷⁻¹⁰. Recently Shi *et al.* reported a comparison between activity and selectivity of different iron oxide species in the oxidation of benzyl alcohol using hydrogen peroxide as oxidant^{11,12}.



Both with α and γ bulk iron (III) oxide good selectivities were shown (99 %), but due to their relatively small specific surface area they were not very active (conversion less than 5 % after

12h at 75°C). Not surprisingly, free Fe³⁺ is active, but the reaction exhibits a low selectivity (only 35 % towards aldehyde). A nano catalyst was believed to improve the activity, due to its coordination sites and surface vacancies. The side products in this case (benzoic acid and benzyl benzoate) are caused by overoxidation of aldehyde. The exact mechanism of iron-oxide catalyzed oxidation is not clear but one possibility is that high valent iron oxide species are present in solution as a result of oxidation with hydrogen peroxide.



Supposedly, by tuning the diameter of nano-sized iron clusters, it should be possible to reach selectivity close to bulk iron with an activity similar to free iron. For 1 equivalent of oxidant and 1 mol % nano γ -Fe₂O₃, a maximum turnover number (TON) of 32 could be achieved (increasing the catalyst amount decreased the selectivity from 97 % to 85 %). The particle size of the nanomaterial clearly effected the selectivity. In the presence of nano γ -Fe₂O₃, in which the majority of the particles is 20–50 nm in size, the conversion reached 33 % with an excellent benzaldehyde selectivity of 97 %, whereas, nano γ -Fe₂O₃, which consists of markedly smaller size of 3–5 nm, showed even higher activity (85 % conversion), with a poor selectivity of 35 %.

In our approach, we synthesized well-defined nano γ -Fe₂O₃ particles inside a protein core. Using protein cores as template and sequestering agents leads to formation of well-defined and narrow dispersed iron-oxide core¹³⁻¹⁵. The main function of ferritin is to store Fe(III) as a ferric oxide nuclear core, leading to an effective concentration of iron in living cells in the range of 10⁻³ to 10⁻⁵ M¹⁶. Ferritins have the unique characteristic of being able to control the reversible phase transition between hydrated Fe(II) in solution and Fe(III) inside its cavity. Typically, ferritins can store up to ~4500 iron ions as an inorganic complex core¹⁷⁻¹⁹ using their ferroxidase centres. Channels that connect the protein cavity with the external medium are located at the three- and four- symmetry axes of the protein²⁰. The possible suggested mechanism for aerobic oxidative uptake assumes that in a first step Fe²⁺ binds at the ferroxidase centre. Next a fast catalytic oxidation to Fe³⁺ occurs which is followed by the entry of iron into the inner core to form an oxide mineral¹⁹. In our case, instead of using the

native mineral iron-oxide inside ferritin, we incorporated γ -Fe₂O₃ directly to the core by forcing Fe²⁺ oxidation with hydrogen peroxide at alkaline pH.

Our goal was to carry out selective oxidation of primary alcohols to aldehydes using this nanocatalyst, an apoferritin reconstituted with nano γ -Fe₂O₃ core, under mild reaction conditions, with hydrogen peroxide as oxidant. We used both the commercial *Horse spleen* ferritin and the hyperthermophilic bacterioferritin from *Pyrococcus furiosus*^{21,22}.

2. Results and Discussion

Table 1: Comparison of the activity and the iron content of the catalysts being used

	Catalytic activity (benzaldehyde yield)	Iron content
Commercial nano γ -Fe ₂ O ₃	14 % (2 eq. oxidant)	61.5 % (w/w)
Synthesized nano γ -Fe ₂ O ₃	8 % (2 eq. oxidant)	63.6 % (w/w)
<i>H. spleen</i> ferritin	2 %	2.75 (mg/ml)
<i>H. spleen</i> apoferritin with nano γ -Fe ₂ O ₃	28 %	n.d.
<i>P. furiosus</i> ferritin (as isolated)	-	≤ 1 per subunit
<i>P. furiosus</i> apoferritin with nano γ -Fe ₂ O ₃	32 %	0.306 (mg/ml)

2.1. Nano γ -Fe₂O₃ in Alcohol Oxidation

Initially, we set out to prepare a nano γ -Fe₂O₃ as described in the literature²³. The synthesis route involved two steps: (i) hydrothermal synthesis of Fe₃O₄ nanocrystals and (ii) hydrothermal oxidation of the Fe₃O₄ nanocrystals to their γ -Fe₂O₃ counterpart. We selected benzyl alcohol for its simplicity and availability as a model substrate and performed oxidation reactions at different pH and temperature values in order to find the optimum conditions for this catalyst. We have also compared the results with a commercially available nano γ -Fe₂O₃ (Sigma). The oxidation of benzyl alcohol was carried out with 1 mol % catalyst, 1 equivalent

of H₂O₂ during a period of 24 hours at 45°C. Under these conditions 5 % benzaldehyde was formed (TON 5). At room temperature no product was obtained, also at higher temperatures (45-90°C) conversion did not increase. The pH of the reaction medium was an important parameter and better conversions were achieved at lower pH. When we used the two equivalents of H₂O₂, the conversion increased up to 14 %. We also tried to improve the mode of H₂O₂ addition. Neither continuous, nor addition in portions gave a significant change in the conversion. The results with the nano γ -Fe₂O₃ synthesized in the laboratory gave a TON 8 under the same conditions. Careful analysis of the material revealed that we were dealing with a mixture of γ -Fe₂O₃ and Fe₃O₄ in the case of synthesized catalyst. This could be an explanation for the lower TON observed with the synthesized catalyst compared to the commercial material.

2.2. *H. spleen* Ferritin as Catalyst and Nano γ -Fe₂O₃ Inside *H. spleen* Apoferritin

We employed both commercial *Horse spleen* ferritin as received, and apo *Horse spleen* ferritin with a γ -Fe₂O₃ core synthesized inside the protein, by following the procedure described before¹⁴. While working with *Horse spleen* ferritin, high temperatures were avoided due to possible denaturation of the protein. At 40°C the conversion was only 2 % (1 eq. oxidant) after 20 hours. Changing the reaction conditions by varying the temperature and pH did not improve the conversions obtained. This could be due to the natural structure of the protein core, which consists of a mixture of ferrihydrate (Fe₂O₃·9H₂O) and ferric phosphates instead of γ -Fe₂O₃.

When we used nano γ -Fe₂O₃ synthesized inside the apoferritin core (*Horse spleen*) the results changed dramatically. The reactions were carried out over 24 hours with 5 mmol of benzylalcohol, 1 mol % of catalyst and 1 equivalent of oxidant. The best results were achieved at 55°C, yielding 28 % aldehyde. Additionally, the catalyst could then be recycled, simply by concentrating the water phase using membrane filters followed by washing with organic solvent several times in order to remove all the residues of the previous reaction. Subsequent oxidations of benzyl alcohol yielded comparable amounts of aldehyde (22 % in the first cycle and 30 % in the second cycle). Nano- γ -Fe₂O₃ core in *Horse spleen* apoferritin in general, showed improved conversions compared to γ -Fe₂O₃ in the same conditions. This is

a strong indication that the protein core is preventing the coagulation and providing a more stable catalyst.

2.3. *P. furiosus* Ferritin as Catalyst and Nano $\gamma\text{-Fe}_2\text{O}_3$ Inside *P. furiosus* Apoferritin

Pyrococcus furiosus ferritin (as isolated) is not active in alcohol oxidation as a catalyst.

A single batch of nano $\gamma\text{-Fe}_2\text{O}_3$ inside *P. furiosus* apoferritin was prepared in order to test the behaviour of the new system. After 24 hours at 75°C and an initial pH around 3, the oxidation of 5 mmol of benzyl alcohol with 1.5 equivalents of hydrogen peroxide provided a yield of benzaldehyde of 24 % together with 5 % benzoic acid. In order to find the optimum conditions for this catalyst, a large batch of this catalyst was prepared and various reaction parameters were tested. Reactions were carried out at different pH values (pH 3, 4 and 5.5). The conditions and the final results are presented in Table 2.

Table 2: Benzyl alcohol oxidation with $\gamma\text{-Fe}_2\text{O}_3$ inside the bacterioferritin

#	pH	T [°C]	Aldehyde [%]	Acid [%]	TON	Cat/subs %*
1	3	75	32	5	95	0.33
2	4	75	32	6	95	0.33
3	5.5	75	32	4	95	0.33
4	5.5	85	30	7	90	0.33
5	5.5	85	29	9	182	0.16

24 hours, 1 eq. H_2O_2 , *mol ratio

It is clear from the table that the conversion of benzalcohol to benzaldehyde could be achieved with very low amounts of catalyst. However, conversion to aldehyde generally stalls at 30 % probably due to the decomposition of hydrogen peroxide. Temperatures above 75°C lead to an increase of benzoic acid formation.

Several reactions were made in order to analyze the conversion in time. The conditions were; 4 mmol alcohol, 1.5 eq. H_2O_2 , 75°C with 0.066 % catalyst/ substrate ratio over 0.5-12 hours (TTN 406) (Figure 1).

The conversion to benzaldehyde after 12 hours was 25 % with 0.066 % of catalyst. It is important to emphasize here that the selectivity was very high, and the final products were 96% benzaldehyde and 4 % benzoic acid.

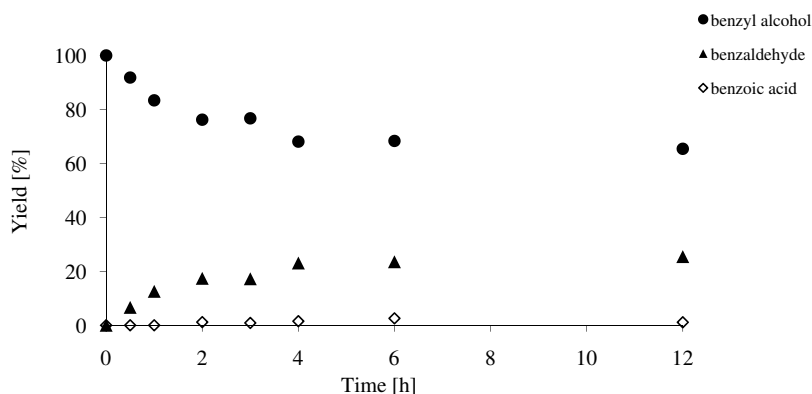


Figure 1: Relative conversion of benzyl alcohol to benzaldehyde and benzoic acid in time

Conditions; 75°C , 0.066 % catalyst/ substrate ratio, 1.5 eq. H_2O_2

Results of benzyl alcohol oxidation with different catalyst concentrations and different times are given in Table 3:

The catalyst is shown to be very active and can perform selective alcohol oxidation. The catalyst amount could be decreased below 0.1 mol %. Adding the oxidant in two portions improved the selectivity. Similarly, decreasing the amount of catalyst has decreased the formation of benzoic acid. In order to test the possible inactivation of the catalyst, an experiment in which the catalyst was added in two times was made with the same amount of oxidant present in the mixture. Comparing these two experiments showed that the catalyst was active over the course of the reaction, no significant inactivation observed.

Table 3: Benzyl alcohol oxidation with $\gamma\text{-Fe}_2\text{O}_3$ inside bacterioferritin with different catalyst/substrate ratios

#	Cat/subs % *	TON	Aldehyde [%]	Acid [%]	Time [h]
6	0.066	276	17	1	2
7	0.066	374	23	2	4
8	0.033	370	12	0	2
9 ^[a,b]	0.066	306	19	0	4
10 ^[a]	0.066	290	19	0	4
11	0.033	447	14	0	4
12	0.016	785	12	0	4

[a] oxidant added in 2 portions, [b] catalyst added in 2 portions, * mol ratio

3. Conclusions and Future Work

Materials exhibit novel and interesting properties when synthesized on the nanoscale, but these syntheses usually have been restricted to solvent based methods of synthesis because of the instability of the biological templates. The use of thermally stable biological templates adds distinct advantages to the utility of these materials in industry and medicine. As previously described, *Horse spleen* ferritin forms protein encapsulated minerals at temperatures up to 65°C, but when it is subjected to a temperature of 85°C this results in the precipitation of the protein from the solution and the formation of bulk iron oxide¹⁵. In contrast, *Pyrococcus furiosus* ferritin was able to successfully template the nanocomposites and perform the reaction at both 65°C and 85°C.

We note that the apoferritin from *Pyrococcus furiosus* can easily be loaded with $\gamma\text{-Fe}_2\text{O}_3$. The synthesized protein-iron assemblies were active as catalyst and shown to be highly selective in activating hydrogen peroxide. Turnover numbers up to 785 could be obtained in the oxidation of benzyl alcohol to benzaldehyde.

Future studies will have to elucidate its substrate scope towards other alcohols and towards other oxidation reactions, i.e. epoxidations. In addition, microscopic studies need to be

performed to establish the dispersion and stability of the iron species after reaction. This well-defined γ -Fe₂O₃ composite has potential as a catalyst for selective oxidations.

4. Materials and Methods

4.1. Synthesis of γ -Fe₂O₃

The nanocrystals of maghemite (γ -Fe₂O₃) were synthesized according to literature²³. 1.78 g of ferrous sulphate hydrate (FeSO₄·7H₂O) and 2.13 g of hydrazine hydrate (35 %) were added to 160 ml of water under vigorous magnetic stirring. After 10 minutes of stirring, the above solution was transferred into a stainless steel reactor with a teflon insert and sealed. The reactor was heated to 150°C and kept for 12 h, then left to cool down to room temperature. The black Fe₃O₄ nanocrystals were collected by centrifugation. Subsequently, Fe₃O₄ nanocrystals, 10 ml of hydrogen peroxide and 150 ml of deionized water were introduced into the reactor and sealed. Once again, the reactor was heated at 150°C for 12 h. Finally, the brown γ -Fe₂O₃ nanocrystals were collected by centrifugation, washed with water and alcohol for several times, and dried at 60°C for 24 h in vacuo.

4.2. Preparation of γ -Fe₂O₃ Core in Apoferritin

The synthesis of γ -Fe₂O₃ core in apo *Horse spleen* ferritin and bacterioferritin was made under similar conditions to those reported in the literature¹⁴. De-aerated buffer solution (EPPS pH 8.5 and 0.1 M NaCl, 15 ml) was placed in the reactor and 4.4×10^{-5} mmol of apo-protein (19.25 mg) was added to the reaction vessel under N₂ flow. For an Fe: protein cage ratio of ~400, 1.74×10^{-2} mmol of Fe²⁺ ((NH₄)₂ Fe(SO₄)₂·6H₂O) solution was prepared and made anaerobic. The reaction was started by adding 0.1 M solution of hydrogen peroxide (a total of 0.83 ml). The pH was controlled by constant addition of 50 mM NaOH solution. Mixture was stirred at 75°C for 30 minutes. Once the reaction medium had reached room temperature, it was centrifuged at 2000 rpm during 3 minutes. For the horse spleen ferritin the process was similar, but instead of 75°C, the reaction was carried out at 60°C, and the relative quantities were added to obtain 0.5 mmol of catalyst (~400 Fe per protein core).

4.3. Benzyl Alcohol Oxidations, Typical Procedure

Reactions were carried out in a closed glass reaction vessel of 30 ml capacity. 12 ml of water was added and pH was adjusted to 3.5 by using a stock solution of HCl. Addition of the given amount of catalyst and oxidant was followed by addition of 5 mmol benzyl alcohol. After the given reaction time, the reaction mixture was extracted with diethyl ether for the GC analysis. NaCl was added to the water phase and 3 x 10 ml ether was used for extractions. The water phase was brought to acidic pH by adding HCl, and extracted with 2 x 10 ml ether in order to recover possible benzoic acid formed during the reaction. The organic phases were combined and 1 ml was taken, dried over sodium sulfate, transferred to a vial and analyzed by GC using anisole as internal standard.

5. References

1. Enthaler, S.; Junge, K.; Beller, M. *Angew. Chem. Int. Edit.* **2008**, *47*, 3317-3321.
2. Martin, S. E.; Garrone, A. *Tetrahedron Lett.* **2003**, *44*, 549-552.
3. Nakanishi, M.; Bolm, C. *Adv. Synth. Catal.* **2007**, *349*, 861-864.
4. Kumar, A.; Jain, N.; Chauhan, S. M. S. *Synlett* **2007**, 411-414.
5. Shi, F.; Tse, M. K.; Li, Z. P.; Beller, M. *Chem. Eur. J.* **2008**, *14*, 8793-8797.
6. Gonzalez-Arellano, C.; Campelo, J. M.; Macquarrie, D. J.; Marinas, J. M.; Romero, A. A.; Luque, R. *ChemSusChem* **2008**, *1*, 746-750.
7. Barton, D. H. R.; Taylor, D. K. *Pure Appl. Chem.* **1996**, *68*, 497-504.
8. Sawyer, D. T.; Sobkowiak, A.; Matsushita, T. *Acc. Chem. Res.* **1996**, *29*, 409-416.
9. Walling, C. *Acc. Chem. Res.* **1998**, *31*, 155-157.
10. Goldstein, S.; Meyerstein, D. *Acc. Chem. Res.* **1999**, *32*, 547-550.
11. Shi, F.; Tse, M. K.; Pohl, M. M.; Bruckner, A.; Zhang, S. M.; Beller, M. *Angew. Chem. Int. Edit.* **2007**, *46*, 8866-8868.
12. Shi, F.; Tse, M. K.; Pohl, M. M.; Radnik, J.; Bruckner, A.; Zhang, S. M.; Beller, M. *J. Mol. Catal. A-Chem.* **2008**, *292*, 28-35.

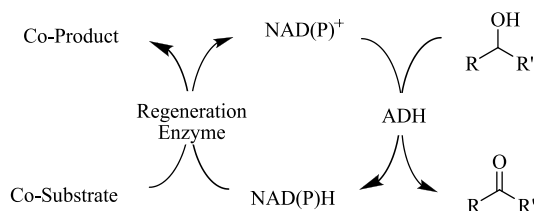
13. Wong, K. K. W.; Douglas, T.; Gider, S.; Awschalom, D. D.; Mann, S. *Chem. Mater.* **1998**, *10*, 279-285.
14. Allen, M.; Willits, D.; Mosolf, J.; Young, M.; Douglas, T. *Adv. Mater.* **2002**, *14*, 1562-1565.
15. Parker, M. J.; Allen, M. A.; Ramsey, B.; Klem, M. T.; Young, M.; Douglas, T. *Chem. Mater.* **2008**, *20*, 1541-1547.
16. Carrondo, M. A. *EMBO J.* **2003**, *22*, 1959-1968.
17. Harrison, P. M.; Arosio, P. *Biochim. Biophys. Acta-Bioenerg.* **1996**, *1275*, 161-203.
18. Chasteen, N. D.; Harrison, P. M. *J. Struct. Biol.* **1999**, *126*, 182-194.
19. Theil, E. C. *J. Nutr.* **2003**, *133*, 1549S-1553S.
20. Bou-Abdallah, F.; Zhao, G. H.; Biasiotto, G.; Poli, M.; Arosio, P.; Chasteen, N. D. *J. Am. Chem. Soc.* **2008**.
21. Matias, P. M.; Tatur, J.; Carrondo, M. A.; Hagen, W. R. *Acta Crystallogr. F* **2005**, *61*, 503-506.
22. Tatur, J.; Hagedoorn, P. L.; Overijnder, M. L.; Hagen, W. R. *Extremophiles* **2006**, *10*, 139-148.
23. Zhu, H.; Yang, D.; Zhu, L.; Yang, H.; Jin, D.; Yao, K. *J. Mater. Sci.* **2007**, *42*, 9205-9209.

A New Regeneration Method for Oxidized Nicotinamide Cofactors

1. Introduction
2. Materials and Methods
 - 2.1. Activity Assays
 - 2.2. Oxidation Reactions with the Coupled Enzyme System
3. Results and Discussion
 - 3.1. LMS-Catalyzed Oxidation of NAD(P)H
 - 3.2. The Coupled LMS-ADH System
4. Conclusions
5. References

1. Introduction

Alcohol dehydrogenases (ADHs, E.C. 1.1.1.x) are oxidoreductases catalyzing the reversible interconversion of primary and secondary alcohols to the corresponding aldehydes and ketones. To perform these reactions ADHs depend on nicotinamide cofactors to act as reductants or oxidants. Stoichiometric use of these costly and unstable cofactors is neither economically nor environmentally attractive. Regeneration of the catalytically active oxidized form is the only practical solution for the application of these enzymes in industry¹.

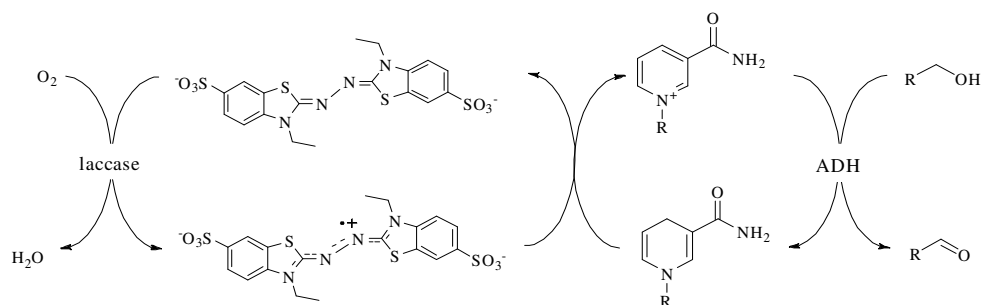


Scheme 1: NAD(P)⁺ regeneration methods with regeneration enzyme or with co-substrate

The most common method for cofactor regeneration is the use of a sacrificial co-substrate serving as terminal electron sink to drive the desired oxidation reaction. However, the need for a high molar excess of the co-substrate to shift the equilibrium to the side of the desired products can result in additional waste. Furthermore, the enzyme stability is often impaired (even though in recent times, highly solvent-tolerant ADHs have been reported)².

Recently, molecular oxygen in combination with NAD(P)H oxidases (E.C. 1.6.3.x) has acquired some interest for cofactor regeneration³⁻⁸. This approach is very practical since molecular oxygen is cheap and easy to handle. Nevertheless, some of these enzymes produce hydrogen peroxide as by product. Chemical oxidants such as quinoid structures⁹⁻¹¹ and transition metals^{12,13} are also an alternative. They are robust, inexpensive and do not distinguish between phosphorylated and non-phosphorylated nicotinamide cofactors. However, to avoid the generation of hazardous hydrogen peroxide, molecular oxygen has to be substituted by an anode as terminal electron acceptor, resulting in complicated reaction setups¹⁴. Liese and co-workers recently reported such a system, involving the combination of 2,2'-azino-bis(3-ethylbenzthiazoline-6-sulphonic acid) (ABTS) and electrochemical

regeneration, to promote ADH-catalyzed oxidation reactions¹⁵. ABTS is well-known as a spectrophotometric probe for peroxidase and laccase activity determination. Combinations of ABTS and laccases in the so-called laccase-mediator-system (LMS) have been successfully applied by Haltrich and co-workers for the oxidative regeneration of flavin-dependent oxidases^{16,17}. We became interested in the question, whether the LMS can also be used to promote ADH-catalyzed oxidation reactions. Such a system would combine the advantages of both approaches: laccase-catalyzed generation of ABTS^{•+} enables the use of O₂ from air while forming water as sole by-product and ABTS as mediator should enable regeneration of both NAD⁺ and NADP⁺ (Scheme 2).



Scheme 2: Novel LMS-based NAD(P)⁺ regeneration approach coupled to an ADH-catalyzed alcohol oxidation applied in two-phase system

Due to its supposed high thermal robustness we chose the commercial laccase from *Myceliophthora thermophila* (Novozymes) to be employed in NAD(P)H oxidation. As a model system to investigate the feasibility of the envisioned O₂-LMS-driven and ADH-catalyzed oxidation of alcohols, we chose the ADH from *Thermus sp.* (TADH)¹⁸. Especially its facile fermentation/ purification procedure, enabling production at scale within two days, make it a well-suited model system.

2. Materials and Methods

Chemicals were purchased from Sigma-Aldrich in the highest purity available and used without further purification. Laccase (Novozymes) was obtained as a 0.2 mM solution and used without further purification. TADH was produced by recombinant expression of pASZ2

(PET) in *E. coli* BL21(DE3)¹⁹ using the Overnight ExpressTM autoinduction system (Novagene). Cell lysis and TADH purification were performed simultaneously by incubating the resuspended (50 mM KPi, pH 7.5) *E. coli* cells at 80°C for 20 minutes followed by centrifugation (4000 × g, 20 minutes). The resulting light-yellow supernatant contained 1.2 mg.ml⁻¹ (29.6 μM) TADH (< 95 % purity as judged by SDS-gel electrophoresis).

2.1. Activity Assays

TADH activity and the activity of the LMS-NAD(P)⁺ regeneration system were assayed spectrophotometrically (UV-VIS Hewlett-Packard 8452A Diode Array Spectrophotometer) by following the characteristic absorbance of NAD(P)H at 340 nm (ϵ : 6.22 M⁻¹cm⁻¹). The TADH activity assay was performed in a 1 ml UV cuvette containing 10 μL purified enzyme (without further dilution), 0.1 mM NAD⁺ and 100 mM cyclohexanol in 100 mM phosphate buffer pH 8. 1 U is defined as 1 μmol NADH produced per minute. The activity of laccase is determined for NADH oxidation. 0.2 mM NADH, 5 μM ABTS and 50 μL laccase were mixed in 1 ml final volume and the characteristic NADH absorbance was followed at 340 nm. One laccase Unit is defined as 1 μmol NADH oxidized per minute. In the LMS activity measurements the reaction mixture contained 0.2 mM NADH, 20 μL laccase and 10 μM ABTS in 1 ml final volume in 50 mM phosphate buffer of the desired pH. The LMS-stability assays were performed by incubating laccase at temperatures between 30-60°C; samples were taken at intervals, supplemented with ABTS and NADH and assayed at 30°C.

2.2. Oxidation Reactions with the Coupled Enzyme System

The reactions were performed on a 1ml scale, in 50 mM potassium phosphate buffer, at pH 8, unless indicated otherwise. A typical reaction mixture contained 10 mM cyclohexanol, 50 μM ABTS, 0.1 mM NADH, 10 μM laccase (7.4 mU) and 2.96 μM (28 mU) TADH. Reactions in the two-liquid phase system were performed as above in 1:1 (v/v) mixture of buffer and octane. Samples were taken at given time intervals, extracted with diethyl ether containing 5 mM of dodecane (standard for GC) and analyzed with gas chromatography (Varian Star 3400 CX GC equipped with Varian CP-8200 autosampler and CP-Wax 52 CB column (50 m x 0.53 mm x 2.0 μm) with a FID detector).

3. Results and Discussion

3.1. LMS-Catalyzed Oxidation of NAD(P)H

Upon addition of laccase to an aerated solution of NADH and ABTS, the characteristic UV absorption band of reduced nicotinamide at 340 nm decreased (Figure 1). The characteristic ABTS^{++} peaks were only visible upon full oxidation of NADH. In the absence of either laccase, mediator, or under anoxic conditions no significant decrease was observed. Hydrogen peroxide was not detectable throughout the course of the reaction. Similar progression curves with slightly reduced rates were obtained for NADPH (approximately 90 % of the rate observed with NADH). We attribute this slightly decreased rate to the additional negative charge present in the phosphorylated NADPH and the resulting additional electrostatic repulsion with the ABTS-anion.

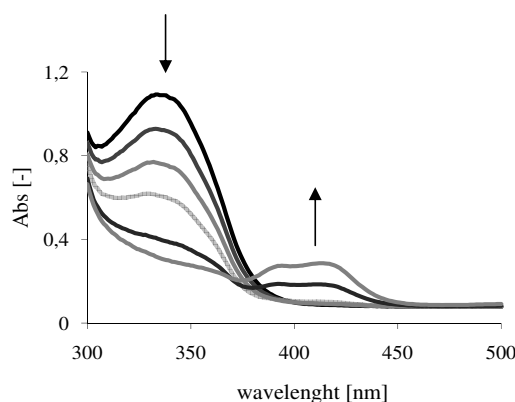


Figure 1: Decrease in absorption band of reduced nicotinamide at 340 nm

Conditions: 50 mM, pH 5 KPi buffer, 0.2 mM NADH, 6.74 μM ABTS, 10 nM laccase, 25°C, spectra were recorded at 1 min intervals.

The correlation between laccase and ABTS concentration and NAD(P)H oxidation rate was linear, as expected. The pH dependency of NAD(P)H oxidation was investigated in the pH range 5-8. The oxidation rate decreased with the increased pH value (Figure 2).

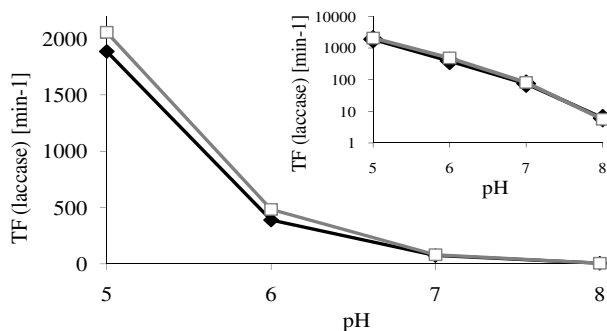


Figure 2: pH dependence of the LMS-catalyzed oxidation of NADH (closed diamonds) and NADPH (open squares)

Conditions: 50 mM KPi buffer (adjusted to the appropriate pH value); 0.2 mM NAD(P)H; 5 μ M ABTS; 10, 40, 100, and 400 nM laccase (for pH 5,6,7, and 8 respectively); 25°C. Insert: logarithmic plot.

It is known that the laccase optimum pH value often lies in the acidic range²⁰, therefore the observed decrease was not unexpected. Although at higher pH values laccase efficiency decreased dramatically, we reasoned that pH 7-8 would be a compromise, since ADHs favors the alkaline pH values for oxidation reactions. All subsequent experiments were performed at pH 8, unless indicated otherwise.

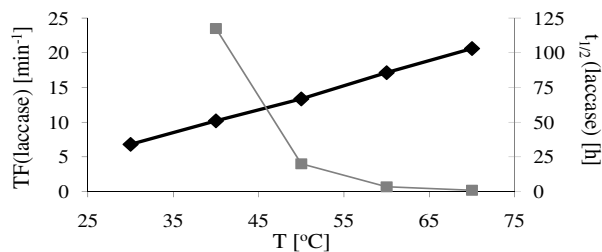


Figure 3: Temperature-dependence of the LMS-based NAD(P)⁺ regeneration system. Activity (TF (laccase), black diamonds) and stability ($t_{1/2}$, grey squares)

Conditions: 50 mM KPi pH 8, 0.4 μ M laccase, 20 μ M ABTS, 0.2 mM NADH.

The temperature dependency of the activity and stability of the LMS at pH 8 was also investigated. Interestingly, NADH oxidation activity increased linearly with temperature (Figure 3).

Currently, we are lacking a plausible explanation for the unexpected deviation from exponentiality. Nevertheless, the stability of the LMS decreased exponentially with temperature, as expected, which we entirely attribute to the thermal inactivation of the biocatalyst. The stability of laccase decreased from 125 hours to 25 hours by increasing the temperature from 40°C to 50°C. We concluded that a reaction temperature range of 30-40°C is optimum for acceptable catalytic activity and thermal stability of the biocatalyst.

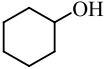
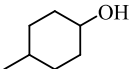
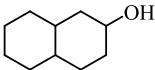
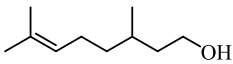
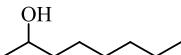
3.2. The Coupled LMS-ADH System

In a first set of experiments we compared the productivity of the coupled catalytic system with the stoichiometric addition of NAD⁺ for a representative selection of TADH substrates (Table 1).

The conversions observed in the catalytic system were always higher than when stoichiometric amounts of NAD⁺ were applied. This can be attributed to the decreased competitive inhibition of TADH by the reduced nicotinamide cofactor and shift of the equilibrium. Interestingly, there was a slight increase of enantioselectivity (*E*)²¹ when the LMS was applied. For example, *E*(TADH) for the oxidation of racemic 2-octanol increased from 5.8 to 7.1. At the moment we do not have an explanation for this observation.

We further investigated the optimum pH and temperature conditions for the coupled enzyme system in the oxidation of cyclohexanol (Figure 4). Using the conditions given in Table 1, initial productivities of up to 7.2 mM h⁻¹ were achieved. The observed pH and temperature dependence reflected the catalytic properties of TADH¹⁸. Therefore, we assume that under these conditions the TADH-catalyzed oxidation was overall rate-limiting.

Table 1: Comparison of stoichiometric administration of NAD^+ and in situ regeneration of catalytic amounts using the LMS-regeneration system

Substrate	Conv. 5h [%]		Conv. 24h [%]	
	Stoich.	LMS	Stoich.	LMS
	47.1	48.2	n.d.	62.8
	10.9	16.1	19.1	33.8
	13.2	18.0	17.6	19.6
	3.6	7.8	5.8	13.6
	n.d.	n.d.	11.4	19.3

Conditions: 100 mM KPi buffer pH 8, 10 mM substrate, 0.1 mM NADH, 50 μM ABTS, 2.96 μM TADH, 10 μM laccase, 40°C.

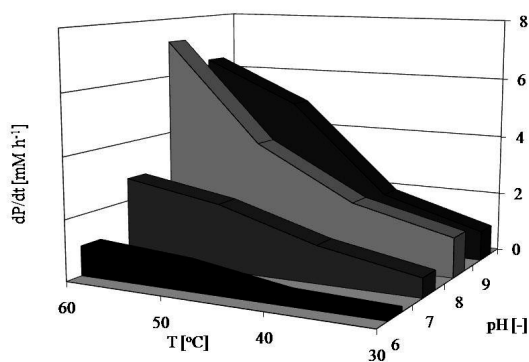


Figure 4: Temperature- and pH-dependence of the coupled system

Conditions: 10 mM cyclohexanol, 0.1 mM NADH, 50 μM ABTS, 2.96 μM TADH, 10 μM laccase.

The stability of the combined system ($t_{1/2}$ approx. 25h) was somewhat lower than expected from the stabilities of the isolated enzymes. It should be mentioned here, that the reaction mixtures exhibited the characteristic color of the oxidized ABTS radical which is in accordance with the assumption that TADH may be the overall rate-limiting factor. $\text{ABTS}^{\bullet+}$ is a known oxidant e.g. for primary alcohols and thereby may inactivate one or both enzymes.

The maximum conversion obtained with this reaction set up was in the range of 60-70 % (6-7 mM of the ketone product), also limiting the turnover number (TTN) of the catalyst. One of the possible explanations could be product inhibition. Moreover, ADHs can catalyze the reaction in both directions and accumulated product could, therefore, be a driving force to reverse the reaction, which would lead to equilibrium. Additional experiments on the NADH oxidation rate under various substrate/ product ratios showed that as the product concentration was increased, a reversible inhibition occurred and the NADH oxidation slowed down (Figure 5).

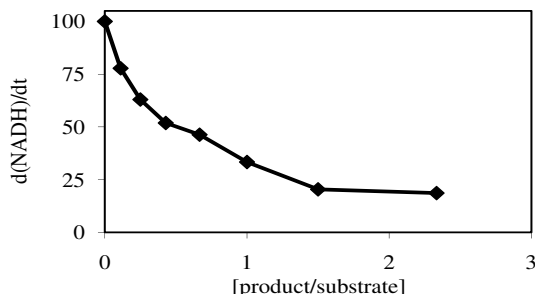


Figure 5: NADH oxidation rate with increasing product/substrate ratio

Conditions: 10-0 mM cyclohexanol, 0-10 mM cyclohexanone, (cyclohexanol + cyclohexanone: 10 mM), 0.2 mM NAD^+ , 0.6 μM TADH.

To alleviate this inhibition, we applied a two-liquid phase system comprising water and octane which would act as substrate reservoir and product sink. This improved setup resulted in a significantly prolonged reaction time and product accumulation (Figure 6).

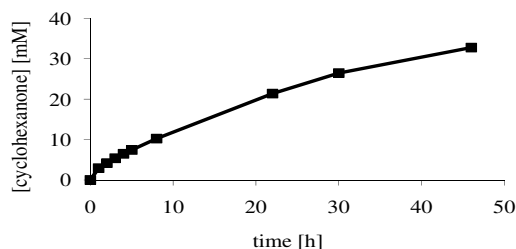


Figure 6: Time course of the two-liquid phase system for the oxidation of cyclohexanol

Conditions: buffer: octane (1:1) Organic phase: 125 mM cyclohexanol, 5 mM dodecane (internal standard); aqueous phase: 50 mM KPi buffer pH 8, 0.1 NADH mM, 2 μ M ABTS, 3.4 μ M TADH, 10 μ M laccase, 40°C.

More than 30 mM of product were obtained corresponding to a total turnover number of 325 for NAD and 16.400 for ABTS.

The catalytic mechanism of ABTS-mediated oxidation should include two sequential one electron transfer steps from the reduced nicotinamide to the ABTS radical cation. Generally, hydride acceptors are preferred to avoid the occurrence of intermediate NAD radicals which might dimerize and thereby become catalytically inactive¹⁴. Using EPR we were unable to detect a putative pyridinium radical suggesting extremely low ($< 0.1 \mu\text{M}$) concentrations of such intermediate radical species. This observation is in accordance with the published redox potentials for the first and second electron transfer steps^{22,23} indicating that the first electron transfer is overall rate limiting. The second electron transfer step is significantly easier (as expressed by a lower redox potential) which probably can also be attributed to the aromatization energy contribution.

4. Conclusions

If compared to the other established NAD(P)⁺ regeneration approaches, this novel method demonstrates high potential for practical use (Table 2).

Table 2: Comparison of the reported regeneration systems and Total Turnover Numbers (TTN) of the cofactor and mediator

Regeneration system	TTN NAD(P) ⁺	TTN mediator
Enzymatic (LDH) ²⁴	59	-
Substrate coupled (GluDH) ²⁵	800	-
Electrochemical regeneration ¹⁵	32	74
Chemical (Ru(PDon) ₃) ⁹	90	900
NADH oxidase ⁴	110	-
Our system	325	16300

First, due to the chemo-enzymatic character both NAD⁺ and NADP⁺-dependent enzymes can be applied. Second, the use of O₂ as terminal oxidant together with the exclusive formation of water as by-product enables a thermodynamically irreversible and environmentally attractive regeneration system. Furthermore, already at this early stage of developments the turnover numbers achieved in this system are amongst the highest reported.

Nevertheless, optimization of the system by balancing the activities of TADH and the LMS-NAD(P)⁺ is needed. Although the two-liquid phase system approach has solved partially the stability problems, the system is still not suitable for large scale applications. ABTS has several disadvantages as a mediator in this system. Probably, the oxidized ABTS is playing a role in the overall stability. Besides, the optimum pH and temperature values for the oxidations are not the optimum values for ABTS. The consequences of unstable ABTS should be better understood and perhaps, the mediator should be replaced with a more efficient compound under these conditions.

5. References

1. Chenault, H. K.; Whitesides, G. M. *Appl. Biochem. Biotech.* **1987**, *14*, 147-197.
2. Stampfer, W.; Kosjek, B.; Kroutil, W.; Faber, K. *Biotechnol. Bioeng.* **2003**, *81*, 865-869.
3. Riebel, B. R.; Gibbs, P. R.; Wellborn, W. B.; Bommarius, A. S. *Adv. Synth. Catal.* **2002**, *344*, 1156-1168.
4. Riebel, B. R.; Gibbs, P. R.; Wellborn, W. B.; Bommarius, A. S. *Adv. Synth. Catal.* **2003**, *345*, 707-712.
5. Geueke, B.; Riebel, B.; Hummel, W. *Enzyme Microb. Tech.* **2003**, *32*, 205-211.
6. Hirano, J.; Miyamoto, K.; Ohta, H. *Appl. Microbiol. Biotechnol.* **2008**, *80*, 71-78.
7. Hirano, J.-i.; Miyamoto, K.; Ohta, H. *Tetrahedron Lett.* **2008**, *49*, 1217-1219.
8. Findrik, Z.; Simunovic, I.; Vasic-Racki, D. *Biochem. Eng. J.* **2008**, *39*, 319-327.
9. Hilt, G.; Lewall, B.; Montero, G.; Utley, J. H. P.; Steckhan, E. *Liebigs Ann-Recl* **1997**, 2289-2296.
10. Hilt, G.; Jarbawi, T.; Heineman, W. R.; Steckhan, E. *Chem. Eur. J.* **1997**, *3*, 79-88.
11. Pival, S. L.; Klimacek, M.; Nidetzky, B. *Adv. Synth. Catal.* **2008**, *350*, 2305-2312.
12. Hollmann, F.; Witholt, B.; Schmid, A. *J. Mol. Catal. B: Enzym.* **2002**, *19-20*, 167-176.
13. Hollmann, F.; Kleeb, A.; Otto, K.; Schmid, A. *Tetrahedron-Asymmetr.* **2005**, *16*, 3512-3519.
14. Hollmann, F.; Schmid, A. *Biocatal. Biotransfor.* **2004**, *22*, 63 - 88.
15. Schröder, I.; Steckhan, E.; Liese, A. *J. Electroanal. Chem.* **2003**, *541*, 109-115.
16. Baminger, U.; Ludwig, R.; Galhaup, C.; Leitner, C.; Kulbe, K. D.; Haltrich, D. *J. Mol. Catal. B-Enzym.* **2001**, *11*, 541-550.
17. Ludwig, R.; Ozga, M.; Zamocky, M.; Peterbauer, C.; Kulbe, K. D.; Haltrich, D. *Biocatal. Biotransfor.* **2004**, *22*, 97 - 104.
18. Hollrigl, V.; Hollmann, F.; Kleeb, A. C.; Buehler, K.; Schmid, A. *Appl. Microbiol. Biot.* **2008**, *81*, 263-273.
19. Studier, F. W. *Protein Expres. Purif.* **2005**, *41*, 207-234.

20. Reinhammar, B. In *Copper Proteins Copper Enzymes*; Lonti, R. Ed.; CRC, 1984; pp. 1-35.
21. Straathof, A. J. J.; Jongejan, J. A. *Enzyme Microb. Tech.* **1997**, *21*, 559-571.
22. Hapiot, P.; Moiroux, J.; Saveant, J. M. *J. Am. Chem. Soc.* **1990**, *112*, 1337-1343.
23. Anne, A.; Fraoua, S.; Grass, V.; Moiroux, J.; Saveant, J. M. *J. Am. Chem. Soc.* **1998**, *120*, 2951-2958.
24. Bortolini, O.; Casanova, E.; Fantin, G.; Medici, A.; Poli, S.; Hanau, S. *Tetrahedron-Asymmetr.* **1998**, *9*, 647-651.
25. Wong, C.-H.; Matos, J. R. *J. Org. Chem.* **1985**, *50*, 1994-1996.

Summary

Selective oxidation reactions are important transformations for the production of fine chemicals. However, there is a need to replace current oxidation methods by more sustainable alternatives. In this respect the use of biocatalysts offers a large benefit, because they operate under mild conditions, and their use is accompanied by high chemo-, regio- and stereoselectivities in reactions of multifunctional molecules. In nature, oxidation reactions are catalyzed by so-called redox enzymes which form the class of oxidoreductases (EC 1). Despite the potential value of oxidoreductases for industrial oxidation reactions, they do not find wide application in fine chemicals industry. The reasons thereof are diverse but the crucial problems are commercial availability, operational stability, scope and, in some cases, lack of an effective method for co-factor regeneration where necessary. In order to facilitate the large scale application of enzymes as catalysts, these drawbacks need to be overcome. One approach is to design new (semi)synthetic biocatalysts with improved stability and comparable or better selectivity and activity to natural enzymes.

The focus of this thesis is on the design of oxidative enzymes that can be readily applied in fine chemical synthesis. A number of approaches were investigated that combine the advantages of biocatalysis, with the activity and versatility of chemo-catalysts. This brought us to the approach of designing protein-metal hybrids that can act as either oxidases or peroxidases.

Incorporation of vanadate in the active site of phytase which *in vivo* mediates the hydrolysis of phosphate esters, leads to the formation of a semi-synthetic peroxidase, as discussed in Chapter 2. V-Phytase has the potential to act as a peroxidase, as previously demonstrated in sulfide oxidations. Moreover, it is more stable compared to the heme-containing peroxidases that suffer from oxidative degradation. Our goal was to extend the scope of V-phytase to synthetically interesting reactions other than sulfoxidations, notably alcohol oxidations and epoxidations. However, attempts to perform oxidation reactions with V-phytase in organic media were unsuccessful. Also the successful immobilization of phytase as cross-linked-

enzyme aggregates, CLEA-V-phytase, was not able to stabilize V-phytase in such a way that oxygen transfer in organic media could be observed.

In Chapter 3, the multi-copper oxidase enzyme, laccase, was studied as template enzyme. Replacement of the Cu by Co has been previously demonstrated, and our aim was to study the redox activity of the modified laccase. A higher redox potential would endow this enzyme with the possibility to perform a wider range of oxidations, without the need for a mediator. By using a dialysis procedure and a direct incubation approach, we could observe a decrease in the copper concentration (AAS results). However, according to the EPR spectrum, the T1 copper is still present and only a 40 % decrease was estimated. Therefore, despite the high concentration of cobalt detected in the enzyme sample, it is not possible to conclude that the Cu/ Co exchange was complete.

The approach using ferritin as a catalyst template is described in Chapters 4 and 5. A novel hybrid oxidation catalyst, formed by using the apoferritin cage as a template for the formation of palladium nanoclusters, is described in Chapter 4. The nanoparticles had a diameter of ~5 nm and a narrow size distribution and are homogeneously dispersed in the solution. The palladium-ferritin nanoparticles were successfully used in the catalytic aerobic oxidation of alcohols in an aqueous medium. In Chapter 5, we report on the loading of apoferritin from *Pyrococcus furiosus* with $\gamma\text{-Fe}_2\text{O}_3$. The synthesized protein-iron assemblies were active as catalysts for oxidations with hydrogen peroxide. Turnover numbers up to 785 could be obtained in the oxidation of benzyl alcohol to benzaldehyde.

In chapter 6, we give a brief overview of the potential use of alcohol dehydrogenases as oxidation catalysts for alcohol oxidation. In this chapter we introduce a novel method for regeneration of the nicotinamide cofactor using laccase as a co-catalyst and molecular oxygen as the terminal oxidant. Compared to other established NAD(P)^+ regeneration approaches, this laccase/mediator system (LMS) shows high potential for practical application in alcohol oxidation.

Samenvatting

Selectieve oxidatiereacties zijn belangrijke transformaties voor de productie van fijnchemicaliën. Echter, er is een noodzaak om de huidige oxidatiemethoden te vervangen door meer duurzame alternatieven. In dit verband bieden biokatalysatoren een groot voordeel, omdat het gebruik ervan gepaard gaat met milde condities, en hoge chemo-, regio- en stereoselectiviteiten in reacties met multifunctionele moleculen. In de natuur worden oxidatiereacties gekatalyseerd door de zogenaamde redox-enzymen, die tezamen de klasse van oxidoreductasen (EC 1) vormen. Ondanks het potentieel van oxidoreductasen voor industriële oxidatiereacties, vinden ze geen brede toepassing in de fijnchemie. De redenen daarvoor zijn divers maar de grootste problemen zijn de commerciële beschikbaarheid, de stabiliteit, de beperkte substraat-scope en, in sommige gevallen, het ontbreken van een effectieve methode om cofactoren te regenereren waar nodig. Om grootschalige toepassing van enzymen als katalysatoren mogelijk te maken, moeten deze nadelen worden overwonnen. Een benadering is om nieuwe (semi)synthetische biokatalysatoren te ontwerpen, die een verbeterde stabiliteit, en vergelijkbare of betere selectiviteit en activiteit bezitten vergeleken met natuurlijke enzymen.

De focus van dit proefschrift ligt op het ontwerp van oxidatieve enzymen, die eenvoudig kunnen worden toegepast voor de synthese van fijnchemicaliën. Een aantal benaderingen werden onderzocht die de voordelen van biokatalyse combineren met de activiteit en veelzijdigheid van chemo-katalysatoren. Dit bracht ons tot het ontwerpen van metaal-eiwit hybriden die kunnen fungeren als oxidasen of peroxidasen.

Het actieve centrum van fytase katalyseert in vivo de hydrolyse van fosfaat esters. Opname van vanadaat in het actieve centrum leidt tot de vorming van een semi-synthetische peroxidase, en wordt besproken in Hoofdstuk 2. Zoals eerder aangetoond in sulfide oxidaties, heeft V-fytase het potentieel om te acteren als peroxidase. Bovendien is het stabielere dan heem-bevattende peroxidasen die te lijden hebben van oxidatieve degradatie. Ons doel was om de substraat-scope van V-fytase uit te breiden tot synthetisch interessante reacties, met name oxidatie van alcoholen en epoxidaties. Echter, pogingen om oxidatiereacties met V-fytase uit te voeren in organische

media waren niet succesvol. Ook de succesvolle immobilisatie van fytase als cross-linked-enzym aggregaten, CLEA-V-fytase, leidde niet tot stabilisatie van V-fytase op een zodanige wijze dat de overdracht van zuurstof in organische media kon worden waargenomen.

Hoofdstuk 3 behandelt de studies naar het multi-koper oxidase enzym laccase als “template” enzym. Vervanging van de Cu door Co was al eerder aangetoond, en ons doel was de redox-activiteit van het aldus gemodificeerde laccase te bestuderen. Een hogere redox-potentiaal zou dit enzym voorzien van de mogelijkheid om een breder scala aan substraten te oxideren, zonder dat een mediator nodig is. Door het gebruik van een dialyse procedure en directe aanpak van de incubatie, konden we een daling in de concentratie van koper waarnemen (AAS resultaten). Echter, volgens het EPR-spectrum, was Tl-koper nog steeds aanwezig en de afname ervan werd op 40 % geschat. Ondanks de hoge concentratie van het kobalt gemeten in het enzym, is het daarom niet mogelijk om te concluderen dat de Cu/ Co-uitwisseling is afgerond.

In de Hoofdstukken 4 en 5 wordt ferritine als een katalysator “template” ingezet. Een nieuwe hybride oxidatiekatalysator wordt beschreven in Hoofdstuk 4, bestaande uit een apoferritine kooi als sjabloon voor de vorming van palladium nanoclusters. De nanodeeltjes hadden een diameter van ~5 nm met een goed gedefinieerde deeltjes grootteverdeling, en waren homogeen verspreid in de oplossing. De palladium-ferritine nanodeeltjes werden met succes gebruikt in de katalytische oxidatie van alcoholen. In Hoofdstuk 5 beschrijven we het laden van apoferritin met $\gamma\text{-Fe}_2\text{O}_3$. De gesynthetiseerde eiwit-ijzer samenstellingen waren actief als katalysator en selectief in het activeren van waterstofperoxide. “Turnover” getallen tot 785 konden worden verkregen bij de oxidatie van benzylalcohol tot benzaldehyde.

In Hoofdstuk 6 geven we een kort overzicht van het potentiële gebruik van alcohol dehydrogenasen als oxidatiekatalysatoren voor alcohol oxidatie. In dit hoofdstuk introduceren we een nieuwe methode voor de regeneratie van nicotinamide cofactoren door laccase te gebruiken als cokatalysator en moleculaire zuurstof als oxidant. In vergelijking met de andere gevestigde NAD(P)⁺ regeneratie benaderingen, biedt dit “laccase/ mediator system (LMS)” goede mogelijkheden voor praktisch toepassing in de oxidatie van alcoholen.

Acknowledgements

The beginning of my PhD was also the beginning of many other things in my life and perhaps that made these 4 years even more challenging than they actually were. But the same reason makes the end more rewarding and happier. And there are quite a number of people who in one way or the other was part of this experience. I'd like to thank them all.

Roger, and Isabel thank you both for giving me the opportunity to start my PhD research in the group. Roger, thank you for all the freedom you gave me to do my own research.

Isabel, thanks for your openness and the flexibility you have shown when it came to make another turn in our direction. I would also like to thank you for your extraordinary performance during my writing period. Despite all the difficulties you had to go through, you put a special effort to keep me in track and finish almost on time. I appreciate it very much.

Frank, I am very happy to have the chance to work with you. Despite all the discussions we had every now and then, I really enjoyed the last year of my lab-life and I learned a lot from you. I also thank you for the friendly atmosphere after working hours.

Mieke, I am grateful for your time and kindness. You helped me in every matter I brought up, without questioning the relevance. I think there is no problem you cannot solve.

During these years I had the chance to work with different people. I thank Isabel Correia for the collaboration in V-phytase project and also for having me in the labs of IST in Lisbon. I would like to thank Fred Hagen, Nahid Hasan and Jana Tatur for the ferritin projects. Not only for the enzyme supply but also for their scientific input especially for Pd-ferritin work. I thank Kourosh Ebrahimi for the PyMol pictures of ferritin. I also thank Simon de Vries for his help in Co-laccase project. I would also like thank to the other colleagues in Enzymology lab, especially to Loesje and Marc; for their help in laccase purification. Valerie Butselaar and Patricia Kooyman spent long hours at TEM for me. I sincerely acknowledge their effort on

ferritin visualization. I also received help and advice from Hans-Peter de Hoog about TEM. Thanks HP!

Our industrial partners, Marcel Schreuder Goedheijt, Martin Ostendorf and Gerjan Kemperman; thank you for the close contact we had during these years and all the scientific discussions. I would like to thank Marcel also for his useful feedbacks while reading this thesis as a committee member.

I owe thanks to the two very special students I had the chance to work with, Lara Babich and Andrés Seral, for their input in this project. They both took up a PhD position after their stay in Delft, so I believe and hope they received good care, inspiration and motivation in research! Lara, you were independent since day one and very practical in the lab, which made my life easy as a supervisor. And I think I will never forget our adventures in the “cold hell”. Andrés, despite your busy schedule outside working hours (organizing trips to every corner of Holland, receiving friends almost every weekend and attending the parties every other day) you were always a hard-working student. I hope all the best for you both!

John, thank you for sharing all the B-Basic matters and the trips we had to make to Oss. When I first started in the group, you were very eager to convince me to have my defense in Dutch, dat lukt me helaas niet, maar heb ik wel Nederlands geleerd! Thanks to Andrzej, for all the fun in the lab and for sharing “the” China experience. Thanks Pedro, for the nice chats about history of Portugal and the Turkish culture. Hilda, thank you for all your help especially during my very first months in the group. Thanks to Mike, Luigi, Dani (Perez), Aurélie, Daniel, Kristina, Florian, Monica & Roberto, for the nice atmosphere and nice time spent after working hours. Aleksandra & Arek, many thanks for the good company in and outside the DCT building and for the garden parties! Sander, Inga, Linda, Aida, Hans-Peter, Jeroen, Daniela, Federico, David, Marlieke, Jin, Luuk, Silvia, Ton, Selvedin, Ulf, Fred, Leen, Joop, Maarten, Remco and all the others that I have met during my stay in the group, thank you! You all played a role in this experience, sometimes without even knowing it. I also would like to give a word of thank to the CLEA guys, to Menno and Mike, it was always possible to step in for a short question or just to trade lab stuff! It was nice to be neighbors and it is even nicer to be colleagues with you now.

I save a special thank to Maria for very useful scientific discussions, but more importantly for sharing all the other matters related to our daily life. You are irreplaceable as a friend and as a colleague! And Mapi, thanks for the cheerful atmosphere during your visits to Delft (and also during our visit to Valencia!).

Surely there are other people behind the scene, sharing laughs and tears; Vicky & Stavros, Alyona & Johan, Agnieszka & Jean-Pierre, Calista, Fevzi, Claudia & Flavio, thank you all!

I am grateful to my parents for everything they have done for me, for their unconditional love and trust, and my brother, Atakan, for always being there when I needed, for the love and fun. Their presence, even if it is over thousands of kilometers, gives me peace and comfort. I would also like to thank my parents-in-love for their love and support. Ik wil een speciale dank geven aan Arjen, voor het helpen mij om de Nederlandse taal en cultuur te ontdekken, voor al zijn interesse in mijn promotie, en voor zijn hulp bij vertalingen.

And finally, my beloved husband Suha, without your love, patience and support I would not be standing where I am now. Thank you for everything you brought in to my life. I am happy to be growing old with you.

Curriculum Vitae

Seda Kanbak-Aksu was born on January 13, 1979 in Aksaray, Turkey. She obtained her secondary school diploma in 1996 at Anatolian High School in Muğla and the same year she passed the entrance exams for university. In 1997 she moved to Ankara to start her education in Hacettepe University Faculty of Pharmacy where she obtained her university degree as Pharmacist in 2001. After graduation, she spent 2 years in the Pharmaceutical Chemistry group as research scientist and she received Master of Science degree in Pharmaceutical Chemistry in 2004 with the thesis “*Synthesis of 4(1H)-Pyridinone Derivatives and Studies on their Antimicrobial Activities*”.

In October 2004 she got married and moved to the Netherlands. In May 2005 she started her PhD research in Biocatalysis and Organic Chemistry group in TU Delft under the supervision of prof. dr. Roger Sheldon and prof. dr. Isabel Arends. The results of this research are described in this thesis. Since December 2009 she is working at CLEA Technologies as Associate Scientist.

